A Biomechanical Study of Angular Momentum and External Moments During a Ballet Turn

Coren Walters-Stewart

Thesis submitted to the
Faculty of Graduate and Postdoctoral Studies
In partial fulfillment of the requirements
For the M.A.Sc. degree in Biomedical Engineering

Department of Mechanical Engineering
Faculty of Engineering
University of Ottawa

Table of Contents

List of Figures

List of Tables

Legend

g	gravitational acceleration constant, 9.81	m/s^2
t	time	s
x, y, z	Cartesian position coordinates	
$\vec{r}$	position vector	m
$\bar{x}, \bar{y}, \bar{z}$	centre of mass	m
ρ, β, h	polar position coordinates	
η	mass fraction of the body segment	
m	mass of the dancer	kg
k	body segment index number	
$\vec{v}$	velocity	m/s
$\vec{a}$	acceleration	m/s^2
$\vec{\omega}$	angular velocity	deg/s or rad/s
$\vec{\alpha}$	angular acceleration	deg/s^2 or rad/s^2
$\vec{F}$	force	N
$\vec{M}$	moment	N·m
$\bar{\bar{I}}$	moment of inertia tensor	$kg \cdot m^2$
$\vec{L}$	angular momentum	$kg \cdot m^2/s$
$\dot{\vec{L}}$	time derivative of angular momentum	$kg \cdot m^2/s^2$ or N·m
T	kinetic energy	J
V	potential energy	J
d	distance	m
λ	direction cosine	

Glossary

anterior	in the anatomic sense, situated nearer to the front of the body
anteroposterior axis	an axis running from the back to the front of the body
distal	situated, in relation to another, further from the place of attachment
extension	increasing sagittal joint angle
flexion	decreasing sagittal joint angle
gait	manner of locomotion
inferior	in the anatomic sense, situated lower in or on the body
lateral	situated, in relation to another, further from the centre line of the body
limb	portion of the body comprised of several segments
locomotion	method of displacement from one place to another
longitudinal	the long axis of the body
medial	situated, in relation to another, closer to the body's centre of mass
mediolateral axis	an axis running from left to right
morphology	the study of the structure of an object
neurology	the study of the nervous system of the body
proximal	situated, in relation to another, closer to the place of attachment
superior	in the anatomic sense, situated higher in or on the body
vertical	perpendicular to the ground

Abstract

The following thesis applies equations of motion used in linear locomotion (gait analysis) to the analysis of the purely rotational motion of the *fouetté* or *tour à la seconde*. Modifications to the method of analysis include the creation of several MATLAB programs to compute improved estimates of the moment of inertia tensor, three-dimensional angular momentum about the dancer's centre of mass. The results of this investigation—the quantification of angular momentum and external moments—are compared to similar results from gait analysis to demonstrate how the dancer maintains balance during rotational motion. The variables calculated by the MATLAB programs are particularly relevant in the field of balance control research in the context of inputs into the body's balance control systems.

1 Introduction

The underlying mechanisms of human motion continue to be investigated by numerous researchers in multiple fields. Biomechanics research is driven by the necessity to understand human physiology, the science and mathematics that define humans and their environment, and the mechanisms which characterize their interaction. Can the ability to walk be restored to those who have lost it? Can machines be created which can replicate human motion? Interest in biomechanics is also driven by the desire to answer these questions affirmatively.

1.1 Overview

1.1.1 Organisation of the report

In the first chapter, this research study is put into context by presenting some background information about research into human motion and how balance is maintained by a group of internal control systems whose inputs are measurable.

The second chapter defines the central hypotheses of the research; angular momentum and changes in angular momentum can be use to describe the motion of the dancer as well as to shed light on how balance is maintained during the turn.

The third chapter details the procedure and theory used in this investigation. Experimental data was obtained by affixing passive optical markers to a dancer who performed a series of turns in a motion-capture laboratory. The first goal of analysis of this data set was to quantify the motion of the turn. Subsequently, the angular momentum and angular impulses were quantified to investigate characteristics of the *fouetté* such as the aesthetic illusion that the dancer is stationary for a moment in time and to elucidate which characteristics contribute to the primary motion of the *fouetté* and which characteristics contribute to how balance is maintained throughout the turn. To this end, angular momentum, energy, moment, and other relevant variables were quantified for analysis. Chapter three also presents several methods that were used for

validation. First, the results are compared to a similar study (albeit, in two dimensions) performed and published by another research group (Imura, Iino, & Kojima, 2008). Second, the analysis is applied to a scenario where a known result is expected (a simple jumping turn); therefore, can be compared to the results obtained from the angular impulse calculated at take-off.

In chapter four, results demonstrate that the period during which the heel makes contact with the ground, is an important domain of analysis in the transfer of energy and momentum during the turn. During the period when the heel makes contact, angular momentum and moments increase. In addition, significant transfers of angular momentum occur between the extended leg and the trunk as a result of the technique in which the extended leg leads the turn while the rest of the body remains stationary for a portion of the turn. When the non-supporting leg has moved laterally as much as the pelvis' morphology permits, the angular momentum of the leg is transferred to the body. While the principal motion of the turn occurs about the vertical axis, significant changes in momentum (and thus, external moments) occur in the axes parallel to the ground. Yet, the balance of the dancer is maintained using mechanisms which either transfer or dissipate extra unwanted momentum. Changes in the angular momentum about these horizontal axes must be dealt with appropriately, otherwise, external moments create torque about the ankle joint and challenge the dancer's balance, much as will occur in other human motion.

Chapter five presents a discussion of the results in the context of balance control. Variables such as torque about the ankle and hip joint, forces and moments acting about the centre of mass, limb position, velocity, and acceleration are quantities which the proprioceptive, somatosensory, and vestibular systems measure and use to maintain a person's balance. These variables are determined in this study, and in future work, can be applied to current physiological and neurological paradigms to advance the

understanding of balance modalities during human motion in the fields of gait analysis, sports pedagogy and training, and even rehabilitation.

1.1.2 Scope

In the analysis of a series of *fouettés* (or a series of *tours à la seconde*), the same variables often studied in gait analysis—for example, the position of the centre of mass, the velocity of the centre of mass, and acceleration of the centre of mass, forces and moments acting at or about the centre of mass, angular momentum and external moments—are considered. There is, however, a notable difference between gait analysis and the analysis of a series of ballet turns; while gait analysis is an analysis of a linear motion (locomotion), this study concentrates on the analysis of a rotational motion which affords the opportunity to gain insight into an important, yet overlooked component of human motion. It should be noted that many types of human motion may not be entirely one or the other but a combination of the two. The scope of this dissertation is to address the lack of research into the biomechanics of human rotational motion using variables which can also used as the input to the body's balance control systems.

1.2 Background

1.2.1 Description of the *fouetté* and *tour à la seconde*

An investigation into the biomechanics of the ballet is not only an investigation into what makes a particular ballet step possible, but also an investigation into the balance, core and limb strength, grace and agility possessed by human that is characteristic of ballet. In ballet, the aesthetic of the motion being performed is as important as the dynamic characteristics. This study primarily examines a ballet turn—a variety of whip turn appropriately called a *fouetté* and its closely related companion, a *tour à la seconde*— and applies an engineering analysis to its motion.

The *fouetté* is a two-count ballet step requiring as much strength as it does balance. On the first count, the dancer flexes the knee of his or her support leg and

begins to raise the other leg (which is flexed at the hip, extended at the knee and foot); on the second count, the raised leg whips laterally pulling the body into rotation.

Few activities in life require as much physical strength, fitness, balance, grace, and agility as that required of performers of ballet. A ballet dancer needs to be able to move his or her body in physically demanding, precisely controlled motions while outwardly projecting an air of ease and effortlessness. In addition, the aesthetic of the dancer's motion must be preserved through the fluidity and artistry of the motion. *Fouettés* and *tours à la seconde* are particularly challenging ballet steps that demands muscle strength, limb flexibility, and core rigidity as well as the ability to maintain balance in rotation. These moves are performed as described in Table 1 and shown in Figure 1-1 below.

Table 1. Steps of the *fouetté* and *tour à la seconde***(Laws, 1998)**

1, 2	usually the dancer begins in first position, arms in 1st position, the dancer then *pliés* the supporting leg while moving the other leg first, *en devant*, then raising to hip level, and finally *en dedans*, arms to 2nd then 3rd echoing leg (supporting leg: hip, knee, foot flexion; other leg: foot, knee extension, hip flexion to 90 degrees, then maximum abduction)
3, 4	-as the leading leg, head, and torso pull the rest of the body into rotation, arms close returning to 2nd, energy is added to the move when the dancer rises from *plié* into *relèvé* (supporting leg: hip, knee, foot flexion to full extension), during the second part of the motion, the dancer can either pull the leading leg into *passé* (*fouetté*) by knee flexion or keep the leg extended (*tour à la seconde*)
5	-the motion is repeated by developing the leg from *passé* to *en devant* in the case of the former, or starting anew from *en devant* to *en dedans* in the latter case.

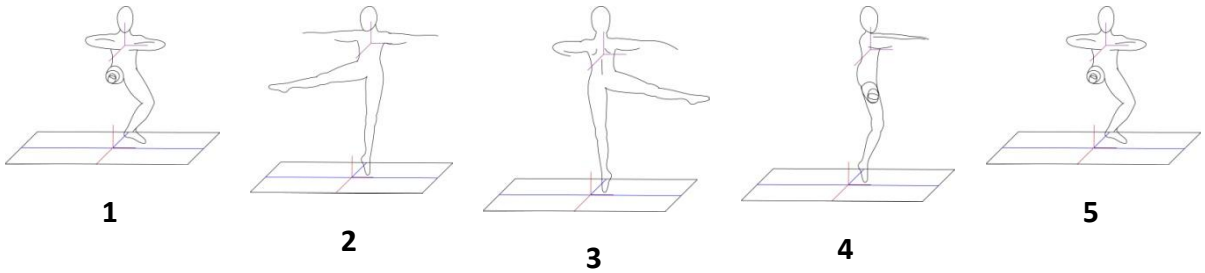

Figure 1-1. The general motion of the *tour à la seconde*

1.3 Review of literature

1.3.1 Balance control

Balance control is studied from many different aspects in diverse fields of research. Balance during stance is an example of static balance control. To maintain one's balance, one must have an accurate perception of spatial orientation (Fourre et al., 2009) Humans perceive the world as a stable environment, and define it as upright even when his or her orientation may be changing with respect to it (Daddaoua, Dicke, & Thier, 2008). An accurate perception of spatial orientation is also required to judge an object's orientation in a gravitoinertial field such as on Earth (Fourre et al., 2009). On Earth, sensory information is derived from mechanoreceptors in joints, muscles and tendon, the vestibular system, and visual input (Batson, 2009). Three sensor systems—the ankle proprioceptors, the vestibular system, and the pressure sensors of the plantar (part of the somatosensory system) contribute largely to the balance control system (Schmitt, Kuni, & Sabo, 2005). It is widely accepted that human stance is inherently unstable requiring control to maintain balance. The main task of human postural control is to counteract the effects of gravity and maintain an upright position (Cnyrim, Mergner, & Maurer, 2009; Mergner, Schweigart, Maurer, & Blumle, 2005).

To maintain an upright posture, deviations of the centre of mass must be detected and corrected. Much research has been conducted into how the body's systems detect vertical deviations and, in particular, how variables used by the body's control systems can be quantified. In some research, consideration is given to situations in which the most commonly used point of reference—the ground—is not present (Pedrocchi, Baroni, Bedotti, Masson, & Ferrigno, 2005). Microgravity environments are complicated by the inability to define vertical and the fact that human morphology not only takes gravity into account, but relies upon it in its responses (Mergner & Rosemeier, 1998).

As previously stated, several sensor control systems contribute to the body's characterization of posture and balance. The contribution of the vestibular system, somatosensory system, visual system, or proprioception to the body's integrated balance

control system depends on the type of situation as well as the information (variables) available (Cnyrim, Mergner, & Maurer, 2009). The body's motion and position, conscious or unconscious, inter-or extra-personal, static or dynamic stimuli affect the relative contribution as well (Batson, 2009).

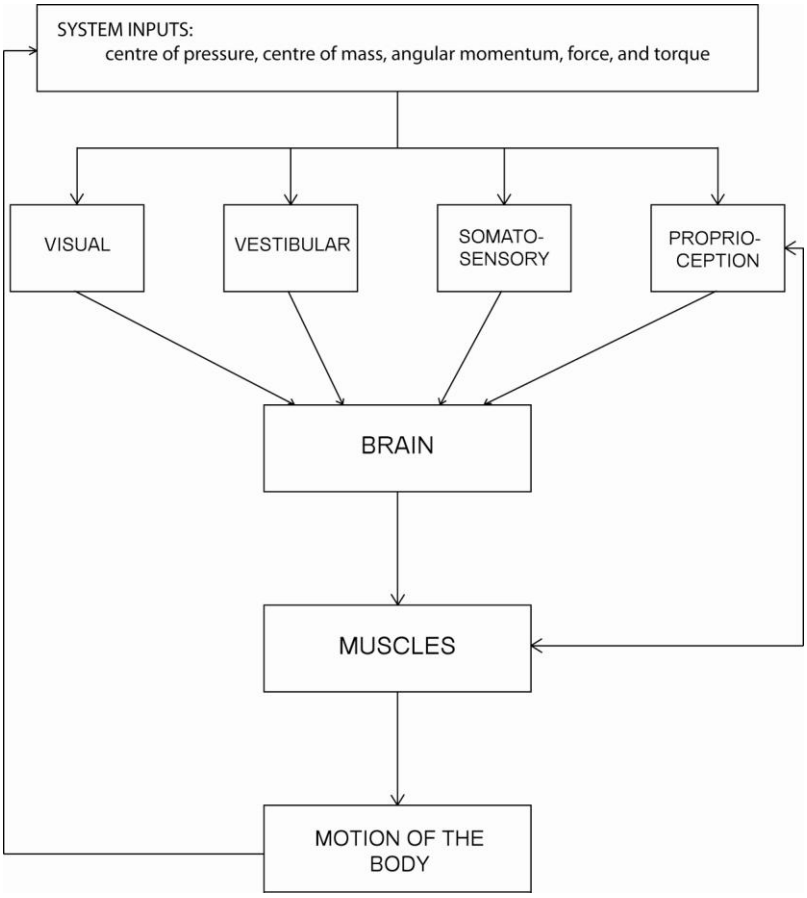

Figure 1-2. Diagram of the body's balance control system

On one hand, the mediation of balance by the vestibular system has been a well-researched topic within the field of stance control. On the other hand, a large amount of interest has recently been concentrated on ankle proprioception. To start, it is helpful to know which variables are of interest in the study of a particular system. A deviation from an upright body position creates a gravitational component in the torque about the ankle, therefore forces and torques acting on the body at proprioception sites such as the ankle are of interest (Cnyrim, Mergner, & Maurer, 2009) and important to quantify. Dynamic

measures such as rate, amplitude, and direction are important mechanical feedback while static scenarios require static measures such as orientation and position.

Proprioception

Healthy proprioception is important to a dancer because it affects his or her ability to perform techniques properly and without injury (Batson, 2009). Since deviations from the vertical result in a torque about the ankle joint, the body is further accelerated from a stable upright position. A counteracting torque from the support limb is required to arrest and reverse motion from the extra torque created by the gravitational component (acting at a distance from the centre of mass). This means a sensory system receiving force cues can automatically correct for gravitational load when the signal from the vestibular system is erroneous (Cnyrim, Mergner, & Maurer, 2009). Yet, proprioception of torques and forces at the ankle joint can be diminished when muscles are active for prolonged periods, subject to repeated maximum contractions with insufficient rest, when muscles have been injured or undergone surgery, or if there is a pathology affecting the joint (Batson, 2009). In fact, the effect of muscle exertion may even suppress afferent joint sensations (Daddaoua, Dicke, & Thier, 2008). Interpretation of any quantitative data obtained pertaining to torque and force should be tempered by these considerations.

System interactions

A variety of balance control mechanisms, which respond to numerous inputs such as body position, joint orientations, centre of mass position, centre of mass displacement, force and torque cues, visual cues, pressure and more, have been reviewed. Models which attempt to describe the balance control system can vary from simple to very complex. Human stance control can be modelled by sensory feedback mechanisms yet they need to incorporate the flexibility and robustness demonstrated by the body's ability to ignore or choose between conflicting inputs. Models which include force cues result in better estimates than models which are comprised of a vestibular system alone (Cnyrim,

Mergner, & Maurer, 2009). Feedforward mechanisms also have a place in explaining the body's ability to anticipate balance perturbations (Batson, 2009). Even so, postural responses can be described by very simple multi-sensory feedback models which model centre of mass movements with an inverted pendulum (Maurer, Mergner, & Peterka, 2006). Complications arise, however, in situations where gravity is absent and a default base of support no longer applies. In addition, the geocentric hierarchy (the ground anchors the segments in contact with it, thus external moments move the segments furthest away ground) of the body can no longer be assumed (Mergner & Rosemeier, 1998). Mergner has explained a conceptual model in which the multi-segmented body is locally controlled, but referred to global coordinates. Links between the vestibular, visual, and somatosensory systems automatically developed by gravitational and inertial reaction forces on Earth must be activated in microgravity. An example given in the paper is placing a hand on a wall is a microgravity environment such as a space station. This creates a support because the reaction force from the wall will give context to the multi-segment structure. In this study, because gravity is present, the support is the limb which is in contact with the ground.

1.3.2 Gait analysis

As in stance control, in gait analysis a fair amount of attention is paid to the mechanism which contributes to maintaining oneself upright (although in addition, the mechanisms of locomotion are also of interest) as well as the measurement of variables which contribute to the understanding of these mechanisms.

Though for decades, there have been conflicting theories to explain the mechanism of human gait, recent quantitative results support the mechanism explained by one theory. An inverted pendulum better explains the path of the centre of mass of the support leg over another well-known theory—the six determinants of gait. Furthermore, modification to the inverted pendulum analogy addresses any insufficiencies in the model (Kuo, 2007).

A dynamic walking model uses an inverted pendulum mechanism but explains the mechanical work performed at the transition between stance legs. The stance leg behaves like an inverted pendulum where the centre of mass travels a circular arc rather than a horizontal path, and work occurs when the swing leg collides with the ground. The collision redirects the velocity of the centre of mass (Herr & Popovic, 2008). The inverted pendulum model can be applied to the motion of the centre of mass and the forces and moments acting on the centre of mass with little modification. Not surprisingly, the control of stability requires energy expenditure (Kuo, 2007).

1.3.3 The biomechanics of ballet

While walking requires the transfer of linear momentum, a series of *fouettés* involves the repeated transfer of angular momentum. External torque must be exerted on the dancer's body, either through contact with the ground or by a partner. An important feature of many turns involves the extended leg's lateral motion to the maximum of its range. When the extended leg is decelerated and stopped, the angular momentum of the turn is transferred to the body by the abductor muscle group of the hip (Laws, 1998). Throughout the rotation, balance must be maintained by either the dancer, or by a partner in the case of a partnered turn.

Imura et al.'s work entitled "Biomechanics of the continuity and speed change during one revolution of the *fouetté*" proved to be an invaluable starting point (Imura, Iino, & Kojima, 2008). Imura's paper examined one revolution of the *fouetté* turn starting with the aesthetics from which the dynamics of the motion follow. As with many ballet moves—the *grand jeté*, for example—the beauty of the motion is a result of the dancer's manipulation of his or her limb's motion and its effect on the audience's perception. In a *grand jeté*, the dancer appears to float mid-jump because his or her centre of mass traces a straight line for much of the dancer's time in the air (Laws, 2002). In the *fouetté*, when facing the audience, the dancer appears stationary. Imura et al determined how the dancer creates and controls the rotational motion of the *fouetté* to create this illusion.

The authors hypothesized that an angular impulse imparted on the body by the non-supporting leg (by the torque exerted at the hip joint) controls the rotation. Imura et al.'s study will be used for comparison. It is important to note, however, that though the data are captured in three dimensions, the segment data are collapsed into two dimensions in the process of calculating angular momentum. Thus, Imura et al.'s approach must necessarily result in some loss of information; however, the study gives an accurate picture of changes in momenta that occur in the execution of a *fouetté* (and verifies earlier studies in the process) validating the assumption.

1.3.4 Angular momentum

Angular momentum of the body's limbs about the whole body's centre of mass has been described as a controlled variable (a control system definition, i.e. likely used as the input to one or more of the body's control systems) in many recent studies (Bennett, Russell, Sheth, & Abel, 2010; Bruijn, Meijer, van Dieen, Kingma, & Lamoth, 2008). The angular momentum of a particular segment of the body is calculated by summing: the angular momentum arising from the rotation of the limb about its own centre of mass with the angular momentum arising from the linear momentum of the limb acting at a distance from the body's centre of mass. Controlled angular momentum has been used to describe instances when angular momenta between limbs are cancelled, and total angular momentum is minimized. Angular momentum about the centre of mass or a particular joint of interest can be an excellent predicator of balance (Allum & Carpenter, 2005), as well as the successful execution of many activities such as the long jump (Yeadon, 1990; Ramey, 1973), or a tennis serve (Bahamonde, 2000). Angular momentum is a conserved quantity in a closed system where no external moments act about the centre of mass. In activities such as walking, whole body angular momentum can actually be quite small because of the cancellation of momentum between segments. Whole body angular momentum has been studied as it relates to changing direction, balance deficiencies in

elderly populations, and its regulation during gait (Herr & Popovic, 2008), during long jump takeoffs (Ramey, 1973) and other sports.

A particularly interesting study (Pijnappels, Bobbert, & van Dieen, 2004) describes the angular momentum generated after tripping and strategies of the subject to avoid falling. Angular momentum resulting in forward motion is created by the foot making contact with an obstacle during regular gait. During a normal walking phase, a positive external moment (essentially an increase in angular momentum) is cancelled by a negative external moment (a decrease in angular momentum) created by the heel contact of the other foot. When angular momentum resulting in forward motion is generated by tripping, moments created by joint torque of the support limb can

- stop the increasing angular momentum, or
- stop the increase as well as reduce the momentum, or
- cancel the angular momentum completely (Pijnappels, Bobbert, & van Dieen, 2004).

This mechanism of angular momentum control is similar to the mechanism used to maintain balance during a series of turns. The angular momentum generated about the mediolateral and anteroposterior axes can be compared to the angular momentum generated by tripping to gauge when the dancer may be in danger of falling.

1.3.5 Conclusions drawn from the review

Linear motion of the human body has been well researched in a number of closely related fields—motor control, balance, sports motion, injury, and rehabilitation. However, there still exists a deficit in the amount of research concerning the human body's movement and control during motion comprised largely or completely of rotation. In addition, when quantifying angular variables, analysis is often reduced to two-dimensions for simplicity, but a great deal of information is lost.

2 Problem Definition

2.1 Background

The importance of this study lies not only in its ability to characterize the rotation and balance of ballet dancer, but in the wider application to general human motion. Since, rotational motion is an important aspect of human motion and necessary to the understanding of general human motion. In addition, rotation has a unique relationship with gravity and its subtle effect on human motion.

The constant action of gravitoinertial forces on the sensory system and the body dominates our body's reactions and our understanding of these reactions (Mergner & Rosemeier, 1998). In microgravity environments, the area of support is no longer predetermined. A generalization of human motion not entirely dependent on gravitational environments is not only applicable in gravity fields but is applicable in general.

Models for gait and human motion such as the inverted pendulum have already been developed and tested for linear motion of the human body. Improvements continue to be made on control system models that explain and replicate this linear motion (Cnyrim et al, 2009; Maurer et al., 2006; Mergner et al., 2005). Yet, these models may already be well-suited to the description of rotation of the human body. Such models require the calculation of variables similar to those used in gait analysis, but these are not always as straightforward in their calculation and interpretation.

The main objectives of this study are to:

- Develop software programs to numerically calculate variables of interest,
- Adapt gait analysis for situations in which rotation dominates the motion of the human body, and

- Use these programs, model adaptations, and calculations to quantify and analyse purely rotational motion of the *fouetté* as a good example of human balance and control throughout a continuous rotation.

The analysis is used to verify hypotheses about the mechanisms which generate and transfer angular momentum, external moments or energy to contribute to the rotation of the dancer. Moreover, the mechanisms which generate and transfer angular momentum, external moments, and energy which affect the balance of the dancer are investigated. It is hypothesized that

- The main characteristics of the turn can be determined by the trends in angular momentum
- A continuous transfer of angular momentum in all three dimensions is what makes the turn possible; the axiom of conservation of angular momentum laws can be used to further the analysis of rotational motion about the centre of mass.

2.2 MATLAB programming

Mathworks' MATLAB computer program was used to calculate and process most of the data collected in this study. The calculations executed in the programs use the theoretical equations and assumptions described in the following paragraphs.

The program littledog.m, which can be found in Appendix A, is a function M-file that was written to retrieve the data stored as a large text file of column vectors. The function separates and names each type of vector so that variables such as position, velocity and acceleration can be retrieved from other MATLAB codes and be used in calculations.

The following table (Table 2) summarizes the programs that were created to numerically solve the equations described in the subsequent section. These MATLAB programs are located in Appendix A.

Table 2. MATLAB program overview

m-file name	*variable outputs*	*Description*
angularmomentum.m	$\vec{L}$, *angular momentum* *T, kinetic energy* $\dot{\vec{L}}$, *sum of external moments*	*-momentum, energy, and external moments contributing to the motion of the dancer*
balancemoments.m	*external moments*	*-external moments acting on the body (affects the balance of the dancer)*
bigdog.m		*-retrieves force and torque data, and makes it available for other programs (hence, the title's characterization of the program)*
bodyplotter.m		*-plots segment pathways during the motion of the fouetté*
energyandIcalc	*V, potential energy* $\vec{L}$, *angular momentum*	*-an alternate calculation of angular momentum is used*
fminteraction.m	*angular impulse*	*-calculates the force and moment interactions at the foot ground interface*
horizontalforce.m	$\vec{F}_H$, *horizontal force correction—force of visceral mass acting out of phase with body's motion*	*-calculates the acceleration of the visceral mass in the horizontal direction, as well as the resultant force acting out of phase*
littledog.m		*Retrieves position, velocity, and acceleration data and makes it available for use in other programs*
verticalforce.m	$\vec{F}_V$, *vertical force correction—force of visceral mass acting out of phase with body's motion*	*-calculates the acceleration of the visceral mass in the vertical direction, as well as the resultant force acting out of phase*

2.3 Theory

At each instant, the position of any point in space is given relative to a laboratory coordinate system in which the origin (0, 0, 0) is located at the corner of the force plates. This laboratory coordinate system is fixed to the force plate and therefore does not translate or rotate. In this coordinate system, a position vector, $\vec{r}$, is written in terms of the time-dependent Cartesian coordinates x, y (horizontal axes) , and z (vertical axis)

1

$$\vec{r}(t) = (x(t), y(t), z(t))$$

In the laboratory coordinate system, the centre of mass of the whole body is calculated as follows:

2

$$\vec{r}_{CG}(t) = \sum_{k=1}^{15} \vec{r}_k \eta_k,$$

where the weighting factor, η, is the mass fraction of the segment to the whole body, and the subscript k where k=1, 2, 3,..., 15 represents each of the 15 segments of the model (further explained in section 3.2). The centre of mass can also be written as

3

$$\bar{r}(t) = (\bar{x}(t), \bar{y}(t), \bar{z}(t)).$$

A new coordinate system can then be located at the body's centre of mass. While the origin of the new body-based coordinate system translates with the motion of the body, the coordinate system does not rotate. The relationship between position vectors in the body-based coordinate system and the laboratory coordinate system is shown in the figure below. The body-based coordinates are denoted by an asterisk.

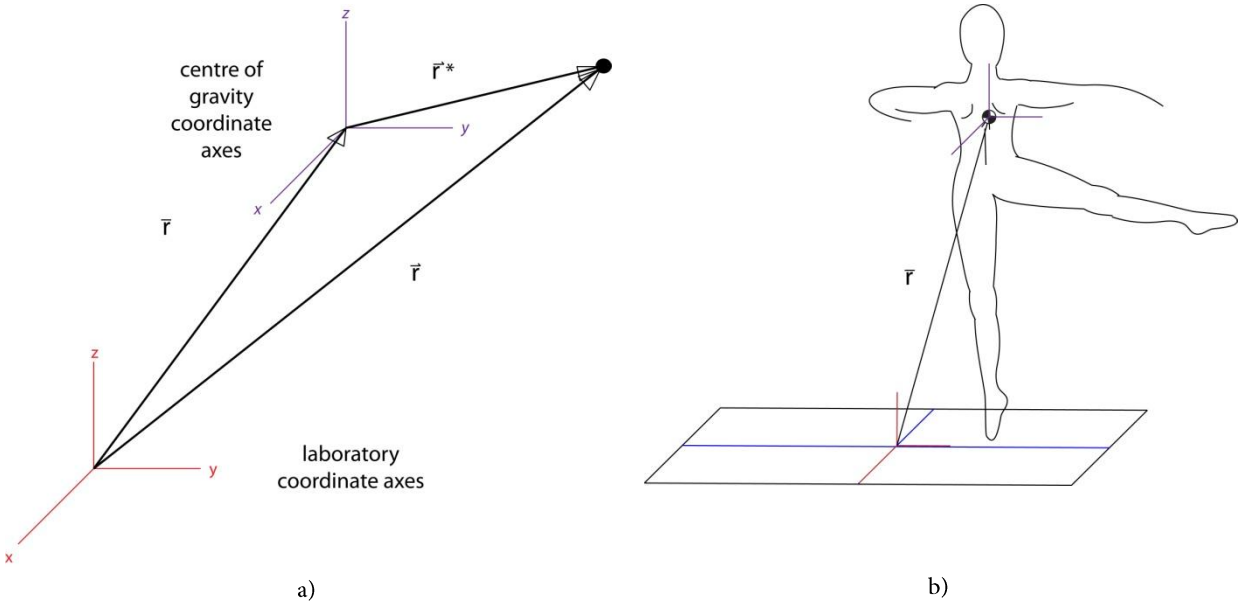

Figure 2-1. Relation between the global and local coordinate systems. The global coordinate system has an origin located at the corner of one of the force platforms on the lab floor. The local coordinate system has axes located at the dancer's centre of mass.

The transformation of any position vector, $\vec{r}$, from the laboratory coordinate system to the body-based coordinate system is performed as follows (all variables are time-dependent)

$$r^* = \vec{r} - \bar{r} \tag{4}$$

$$r^* = (x - \bar{x}, y - \bar{y}, z - \bar{z}) \tag{5}$$

$$r^* = (x^*, y^*, z^*) \tag{6}$$

Since the velocity, $\vec{v}$, is defined as the time-derivative of position, written as

$$\vec{v} = \frac{d\vec{r}}{dt} \tag{7}$$

the velocity of the centre of mass can be calculated as follows (in the laboratory coordinate system; note: η is not time dependent):

$$\begin{aligned}
\vec{v}_{\mathrm{CG}} &= \frac{d}{dt}(\vec{r}_{\mathrm{CG}}) \\
&= \frac{d}{dt}\left(\sum_{k=1}^{15} \vec{r}_k \eta_k\right) \\
&= \sum_{k=1}^{15} \frac{d}{dt}(\vec{r}_k \eta_k) \\
&= \sum_{k=1}^{15} \left(\eta_k \frac{d}{dt}\vec{r}_k + \vec{r}_k \frac{d}{dt}\eta_k\right), \\
&= \sum_{k=1}^{15} \eta_k \frac{d}{dt}\vec{r}_k
\end{aligned}$$

$$\therefore \vec{v}_{\mathrm{CG}} = \sum_{k=1}^{15} \eta_k \vec{v}_k \tag{8}$$

Likewise, since acceleration is defined as the time-derivative of velocity and the second time-derivative of position, written as

$$\vec{a} = \frac{d}{dt}\left(\frac{d\vec{r}}{dt}\right) \tag{9}$$

$$\therefore \vec{a} = \frac{d^2\vec{r}}{dt^2} \text{ or } \frac{d\vec{v}}{dt}$$

Thus, the acceleration of the body's centre of mass can be calculated in the same manner as above (in the laboratory coordinate system; note: η is not time dependent).

$$\begin{aligned}
\vec{a}_{\mathrm{CG}} &= \frac{d}{dt}(\vec{v}_{\mathrm{CG}}) \\
&= \frac{d}{dt}\left(\sum_{k=1}^{15} \vec{v}_k \eta_k\right) \\
&= \sum_{k=1}^{15} \frac{d}{dt}(\vec{v}_k \eta_k) \\
&= \sum_{k=1}^{15} \left(\eta_k \frac{d}{dt}\vec{v}_k + \vec{v}_k \frac{d}{dt}\eta_k\right), \\
&= \sum_{k=1}^{15} \eta_k \frac{d}{dt}\vec{v}_k
\end{aligned} \tag{10}$$

$$\therefore \vec{a}_{\mathrm{CG}} = \sum_{k=1}^{15} \eta_k \vec{a}_k$$

Other variables can be transformed to vectors in the new body-based coordinate system using the same principle as in equation 4—vector addition and subtraction.

$$v^* = \vec{v} - \bar{v} \tag{11}$$

$$a^* = \vec{a} - \bar{a} \tag{12}$$

$$\omega^* = \vec{\omega} - \bar{\omega} \tag{13}$$

Subject-specific information is necessary for calculations of angular momentum. In the subsequent equation, m, refers to the mass of the dancer, η_k represents each limb's mass fraction, and $\bar{\bar{I}}_k$, a diagonalized inertia tensor containing the segment's principal centroidal moments of inertia. In the initial calculations of angular momentum, values of moment of inertia used by Visual 3D software are based on the subject's anthropometric data. The mass and dimensions of each limb are based on the height and weight of the subject. Historically, anthropometric data sets have been obtained through cadaveric measurements and extended to wider populations using regression equations (Shan & Bohn, 2003). Each limb is modelled as a simple geometric solid. The details of the solid used to represent each limb in the model are detailed in Table 3 on page 26.

Each segment's moment of inertia, $\bar{\bar{I}}$, is written only in terms of the segment's principal centroidal moments of inertia, where I_{xx} is the moment of inertia about the segment's frontal axis, I_{yy} is the segment's moment of inertia about the segment's sagittal axis, and I_{zz} is the segment's moment of inertia about the segment's longitudinal axis. These coordinates are defined by the Visual 3D program and have no relation to the coordinates defined herein.

14

$$\bar{\bar{I}}_k = \begin{pmatrix} I_{xx} & 0 & 0 \\ 0 & I_{yy} & 0 \\ 0 & 0 & I_{zz} \end{pmatrix}_k$$

Because the human body is not axisymmetric and not a single, rigid body, the principal centroidal each segment's moment of inertia varies with time, consequently the body's moment of inertia varies with time. To calculate this change, each segment's moment of inertia is adjusted by the parallel axis theorem and the equations of the ellipsoid of inertia as shown below.

The parallel-axis theorem & ellipsoid of inertia (Beer & Johnston, 1999)

15

$$d^2_{(x-x)_k} = \bar{y}^2_k + \bar{z}^2_k$$

16

$$d^2_{(y-y)_k} = \bar{x}^2_k + \bar{z}^2_k$$

17

$$d^2_{(z-z)_k} = \bar{x}^2_k + \bar{y}^2_k$$

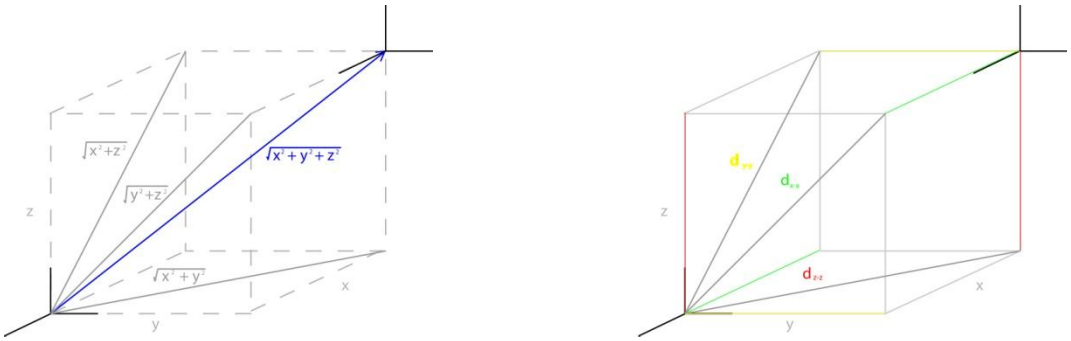

Figure 2-2. Application of the parallel axis theorem demonstrated using a projection of a cube

The components of the moment of inertia of a segment can be calculated about an alternate point by shifting each axis parallel to the original as illustrated in Figure 2-2. The distance is calculated using Equations 15 through 17.

A change in orientation of the axes can also be accounted for using equations derived from the ellipsoid of inertia. Using the moments of inertia about the principal axes of the segment, the moment of inertia about any axis at a different orientation can be calculated. Direction cosines (Eq. 18 through 20) are used to define the change in orientation.

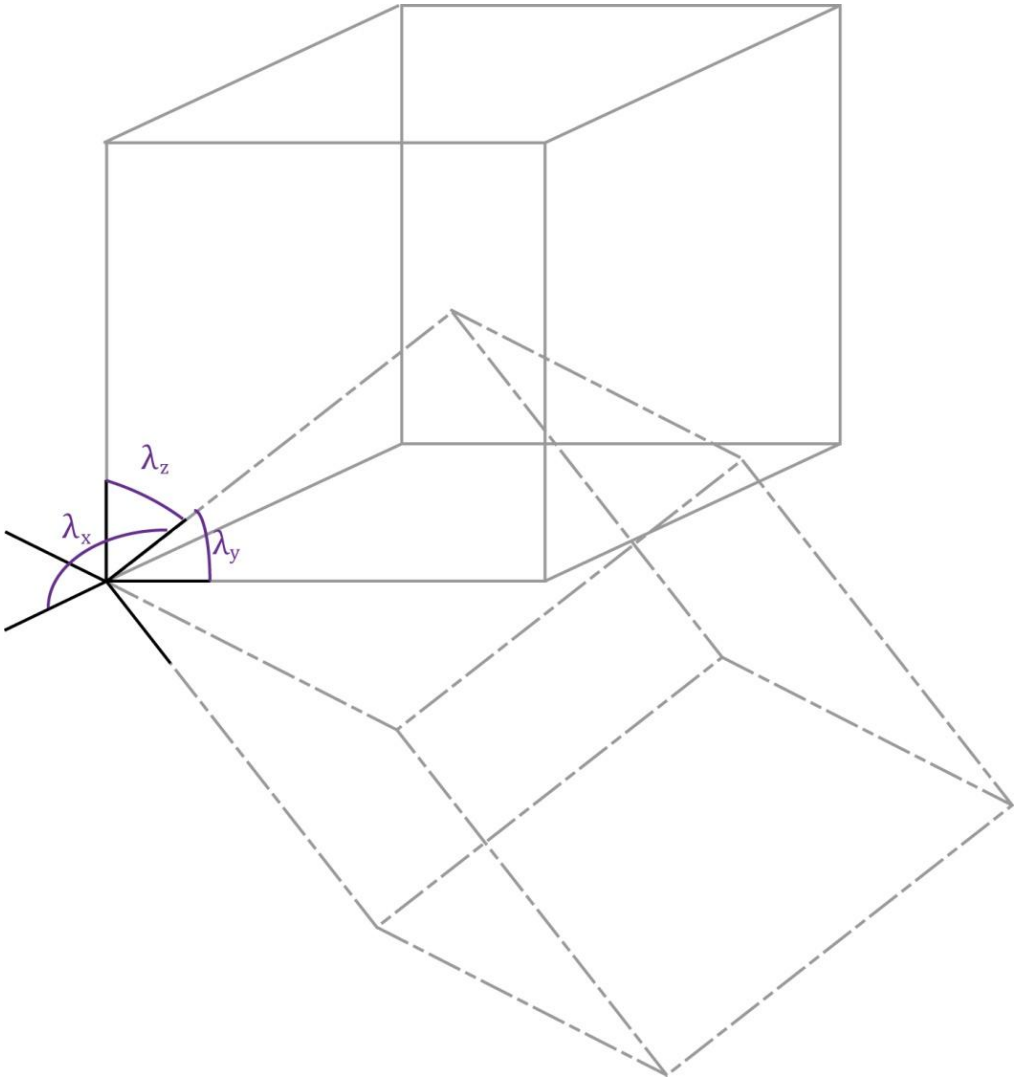

Figure 2-3. Angles used in the calculation of the direction cosines of a vector between two coordinate systems or an inclined segment

18

$$\lambda_x = \frac{(\vec{r}_D - \vec{r}_P)_x}{\|\vec{r}_D - \vec{r}_P\|}$$

19

$$\lambda_y = \frac{(\vec{r}_D - \vec{r}_P)_y}{\|\vec{r}_D - \vec{r}_P\|}$$

20

$$\lambda_z = \frac{(\vec{r}_D - \vec{r}_P)_z}{\|\vec{r}_D - \vec{r}_P\|}$$

The direction cosine of a segment is calculated from a unit vector which describes the segment. The segment is defined by a vector from the proximal to the distal joint denoted by subscripts P and D. A shift in both distance and orientation are then defined when calculating the moment of inertia at each instant (Eq. 21).

21

$$\bar{\bar{I}}_k^* = \begin{pmatrix} \left(I_{xx} + m\eta_k d^2_{(x-x)_k}\right)(\lambda_x)^2 & \left(I_{xy} + m\eta_k \bar{x}\bar{y}\right)(\lambda_x\lambda_y) & (I_{xz} + m\eta_k \bar{x}\bar{z})(\lambda_x\lambda_z) \\ \left(I_{xy} + m\eta_k \bar{x}\bar{y}\right)(\lambda_x\lambda_y) & \left(I_{yy} + m\eta_k d^2_{(y-y)_k}\right)(\lambda_y)^2 & \left(I_{yz} + m\eta_k \bar{y}\bar{z}\right)(\lambda_y\lambda_z) \\ (I_{xz} + m\eta_k \bar{x}\bar{z})(\lambda_x\lambda_z) & \left(I_{yz} + m\eta_k \bar{y}\bar{z}\right)(\lambda_y\lambda_z) & \left(I_{zz} + m\eta_k d^2_{(z-z)_k}\right)(\lambda_z)^2 \end{pmatrix}$$

To diagonalize the matrix for simplicity during MATLAB calculations, the invariants were calculated so that the final inertia tensor contains only principal moments of inertia

22

$$\bar{\bar{I}}_k^* = \begin{pmatrix} \mathbf{I} & 0 & 0 \\ 0 & \mathbf{II} & 0 \\ 0 & 0 & \mathbf{III} \end{pmatrix}$$

where **I**, **II**, and **III** are the principal moments of inertia calculated in the new body-based coordinate system:

$$\mathbf{I} = I^*_{xx}$$

$$\mathbf{II} = I^*_{yy}$$

$$\mathbf{III} = I^*_{zz}$$

The angular momentum was calculated in a series of steps in the program called angularmomentum.m (see Appendix A). First, the angular momentum was calculated for each segment about the segment's centre of mass, denoted by the subscript G. Angular momentum was then calculated about the origin at the body's centre of mass denoted by the subscript O. This angular momentum, called moment of momentum, is the angular momentum that arises from the linear momentum of each segment around an axis at some distance from the segment. The whole body angular momentum is the sum of the segments' angular momenta as seen below (adapted from Beer & Johnston, 1999).

23

$$\vec{L}^*_{G_k} = \bar{\bar{I}}^*_k \vec{\omega}^*_k$$

24

$$\vec{L}^*_{O_k} = \vec{r}^*_k \times m\eta_k \vec{v}^*_k + \vec{L}^*_{G_k}$$

25

$$\vec{L}^*_{O_k} = \sum_{k=1}^{15} \vec{L}^*_{O_k}$$

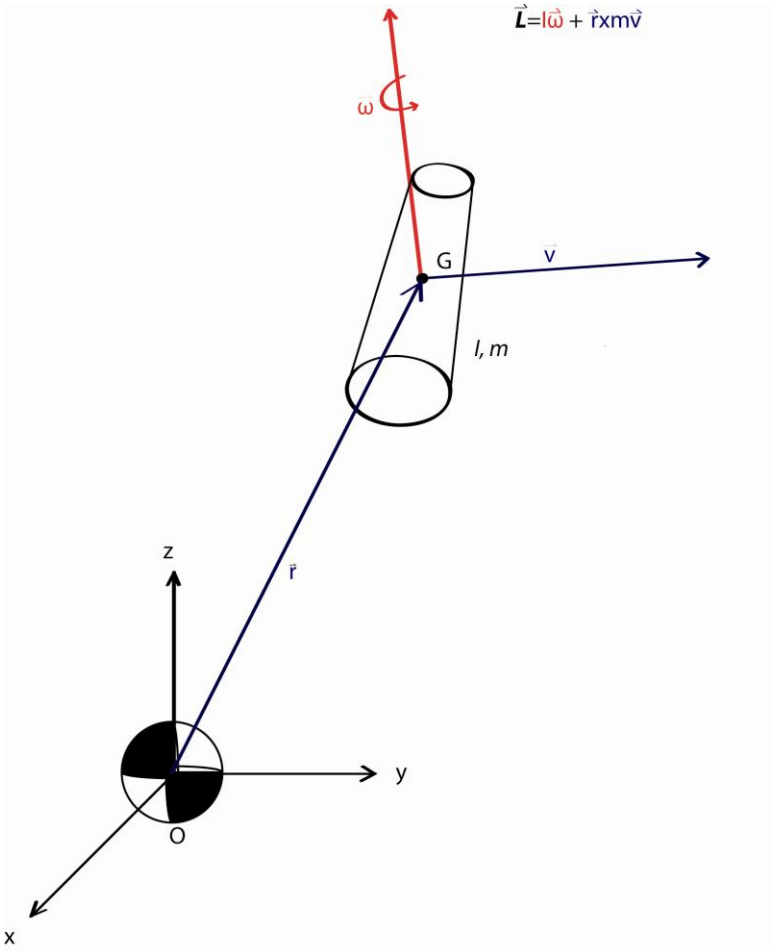

Figure 2-4. Method of angular momentum calculation. O denotes the centre of mass of the body

The principle of impulse and momentum is especially useful in this biomechanical analysis for the transition from one turn to the next. The angular momentum of the dancer is related to any external angular impulses by the following equation

26

$$\vec{L}^*_O(t_1) + \int_{t_1}^{t_2} \vec{M}^*_O dt = \vec{L}^*_O(t_2)$$

The angular impulse and moment can be found by rearranging the previous equation.

27

$$\int_{t_1}^{t_2} \vec{M}_O^* dt = \vec{L}_O^*(t_2) - \vec{L}_O^*(t_1)$$

Since, the body-based coordinate system does not rotate with the dancer as the dancer turns, reference vectors are created to describe the direction the dancer is facing. Shoulder and hip reference unit vectors are created as demonstrated:

28

$$\hat{r}_{shoulder,hip}^* = \frac{\vec{r}_{right}^* - \vec{r}_{left}^*}{\left\|\vec{r}_{right}^* - \vec{r}_{left}^*\right\|}$$

As the direction of the shoulder and hip vectors may not always be parallel, they are averaged and projected onto a horizontal plane located at the body's centre of mass to define the mediolateral axis. The unit vector perpendicular to the mediolateral axis and pointing in the direction that the dancer is facing is then defined as the anteroposterior axis.

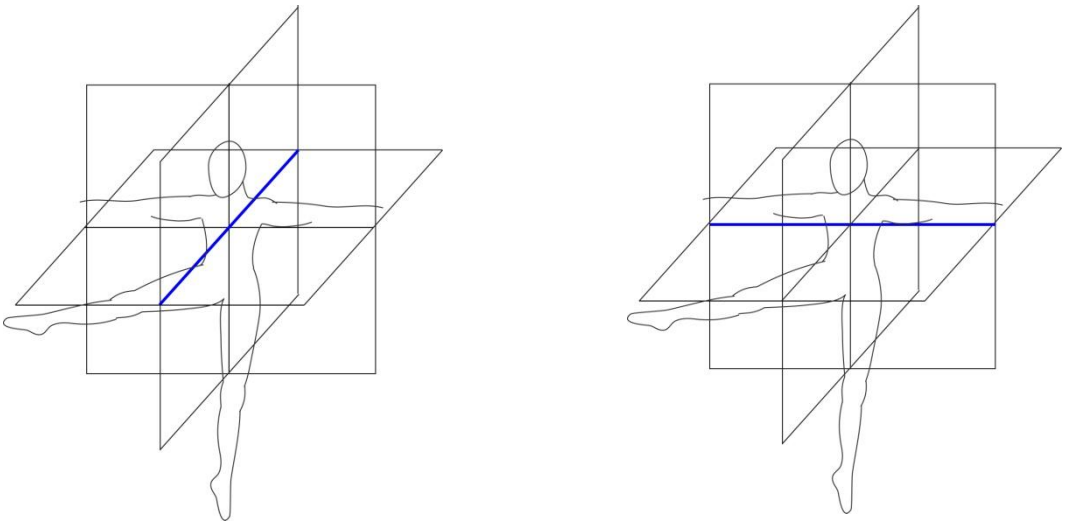

Anteroposterior axis in blue
positive=right, negative=left

Mediolateral axis in blue
positive=forward, negative=backward

Figure 2-5. Axes parallel to the ground.

The angular momentum can be disassembled into components which correspond to the body's anatomic axes which are shown in Figure 2-5.

The sum of moments can also be calculated in a rotating frame of reference to yield values which correspond to the body's anatomic axes. The sum of moments must then take into account the rotation of the frame of reference (Beer & Johnston, 1999).

29

$$\sum \vec{M}_O^* = \dot{\vec{L}}_O^* + \vec{\omega}_{CG} \times \vec{L}_O^*$$

Energy

The principle of conservation of energy is also an important tool for analysis in energy transfer. The kinetic energy, *T*, of the dancer is calculated from the following relation.

30

$$T = \frac{1}{2}\sum_{k=1}^{15} m\eta_k \vec{v}_k^* \cdot \vec{v}_k^* + \frac{1}{2}\sum_{k=1}^{15} (\bar{\bar{I}}_k^* \cdot \vec{\omega}_k^*) \cdot \vec{\omega}_k^*$$

When the moment of inertia can be written as a diagonalized tensor, the equation for kinetic energy can be expressed as follows(Merriam, 1978):

31

$$T = \frac{1}{2} m\bar{v}^2 + \sum_{k=1}^{15} \left(\frac{1}{2} I_{xx}\omega_x^2 + \frac{1}{2} I_{yy}\omega_y^2 + \frac{1}{2} I_{zz}\omega_z^2 \right)$$

The potential energy, *V*, due to gravity is an important consideration as well.

32

$$V = mg\bar{z},$$

Note: Because the potential energy depends on the motion of the centre of mass, it must be calculated in the original coordinate system or will yield a value of zero.

where z is the vertical coordinate of the centre of mass.

The total mechanical energy of dancer, the sum of the potential and kinetic energy, can determine whether the dancer can be characterized as an idealized mechanical system (Pfau, Witte, & Wilson, 2006).

3 Methods

3.1 Motion Lab

The data set was collected at the University of Ottawa's Biomechanics Lab using a Vicon MX motion capture system and two ground-level force platforms (Kistler). The cameras were arranged in a 5-camera configuration. The markers were affixed to the subject according to the University of Ottawa marker set (Robertson, 2009). All subjects wore free-moving, form-fitting clothes in order to avoid restricting the subject's movement and in order to minimize relative marker motion. The data set was collected at a frequency of 200 Hz for a series of turns for as many turns as the dancer was capable of performing. The best series of turns was decided based on the number of turns as well as staying on the force plate for the entire duration.

3.2 Data collection and processing

The data set was then digitized and processed using Visual 3D software. A fourth-order, zero-lag, Butterworth filter with a cut-off frequency of 6 Hz was used to smooth the data by reducing noise and removing artifacts not associated with the body's actual motion. For the purposes of this research project, the body is modelled as a multi-link system shown in Figure 3-1.

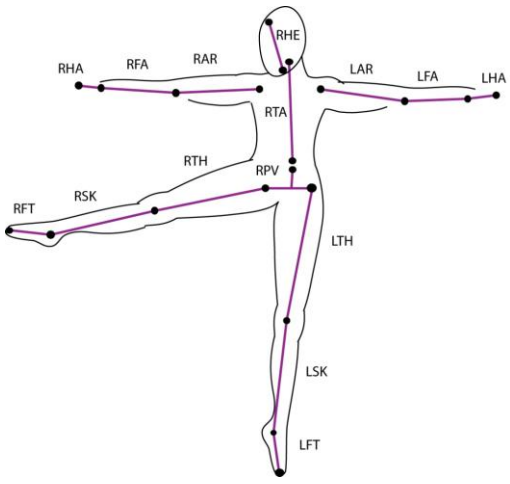

Figure 3-1. Diagram of labelled segments

Table 3. Segments of the body

k	*Geometric shape*	*Label*	*Segment name*
1	*cone*	*LAR*	*left upper arm*
2	*cone*	*LFA*	*left forearm*
3	*cone*	*LFT*	*left foot*
4	*sphere*	*LHA*	*left hand*
5	*cone*	*LSK*	*left shank (lower leg)*
6	*cone*	*LTH*	*left thigh*
7	*cone*	*RAR*	*right upper arm*
8	*cone*	*RFA*	*right forearm*
9	*cone*	*RFT*	*right foot*
10	*sphere*	*RHA*	*right hand*
11	*ellipsoid*	*RHE*	*head*
12	*cylinder*	*RPV*	*pelvis*
13	*cone*	*RSK*	*right shank (lower leg)*
14	*cylinder*	*RTA*	*thorax*
15	*cone*	*RTH*	*right thigh*

The body is divided into 15 segments. The segments are the head, thorax, pelvis, left upper arm, right upper arm, left forearm, right forearm, left hand, right hand, left thigh, right thigh, left lower leg, right lower leg, left foot, and right foot. Each of the 15 segments of the body and their associated variables are denoted by the subscript, k, where k=1, 2, 3,..., 15. In addition, certain quantities are assumed to be known. The mass, *m*, of the subject is used along with anthropometric and geometrical relationships. The model is shown in Figure 3-2 below.

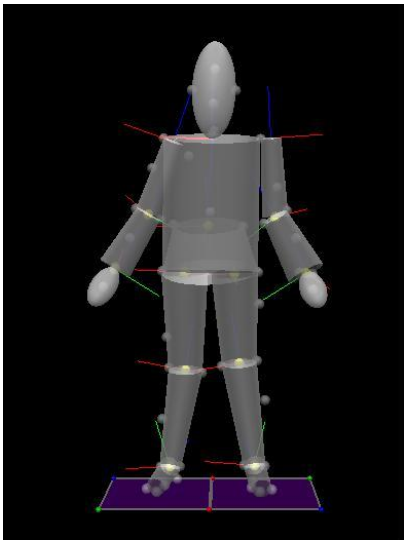

Figure 3-2. Geometric representation of the body (screenshot Visual3D, Colorado, USA)

Each segment is a rigid body represented by a line element having two endpoints, the distal, D, and proximal, P, ends, and one point denoting the segment's centre of mass. Each segment has the following variables associated with the definition of its motion. Position vectors are drawn from the origin of the coordinate system to the proximal, centre of mass, and distal points of the segment.

$\vec{r}_D$, distal segment position
$\vec{r}$, segment's centre of mass
$\vec{r}_P$, proximal segment position
$\vec{v}$, velocity of the segment's centre of mass
$\vec{v}_P$, velocity measured at the proximal position of the segment
$\vec{a}$, acceleration of the segment's centre of mass
$\vec{\omega}$, angular velocity of the segment
$\vec{\alpha}$, angular acceleration of the segment
$\vec{f}$, $\vec{f}_T$, force and torque

The segments representing the right and left foot have additional variables associated with them: centre of pressure (subscript COP), free moment, and ground force reaction. The free moment is the reaction to the force couple exerted by the foot or feet on the ground, which acts about a vertical axis at the centre of pressure (Almosnino, Kajaks, & Costigan, 2009). It is the moment caused by friction between the feet and the ground.

3.3 Validation

Three separate methods are used to validate the programs that were written and their results. In the first section of this validation, the results obtained are compared to a similar study. Imura et al.'s research group, as described in the literature review, studied the rotational speed changes and the angular momentum of several dancers as they performed the *fouetté*. However, Imura et al.'s study (2008) calculates the angular momentum in a horizontal plane, assuming any momentum in vertical planes to be negligible, and the dancer in our study performs a slightly modified version of the *fouetté* (sometimes called a *tour à la seconde*.) The main difference between these two turns is the technique of the acting leg. In the *fouetté*, the leg is only extended for a brief moment before being pulled into and held in *passé* (the acting leg is bent at the knee, the

foot near the calf of the support leg) for the remainder of the turn, during a *tour à la seconde* the acting leg remains extended throughout the turn. Nonetheless, the data can be compared because the rest of the body uses the same technique and goes through the same motions when either turn is being performed.

In the second section of this validation, the method of calculation of angular momentum is compared to Visual 3D's method of calculating angular momentum for each segment. Visual 3D is the same software that was used to process and smooth the original motion capture data in this study, but has additional calculation functions in its beta version that need to be tested.

The third section of this validation tests the overall procedure and any assumptions made in the calculations using the principle of conservation of angular momentum. A jumping turn was performed for this purpose. The calculation programs are applied to this turn, a situation where loss of energy due to friction is minimized since the subject's turn occurs in the air and thus, angular momentum throughout the turn should be conserved. The accuracy of this calculation will give the results obtained in the rest of the study some context.

3.4.1 Comparison with a 2D study

To compare the results obtained by Imura et al.'s study and the results obtained by this study, several important considerations must be taken into account.

- Imura et el.'s calculation of angular momentum is only considered about a vertical axis.
- The dancers turn in the clockwise direction in Imura et al.'s study, and counter-clockwise in this study (i.e., in opposite directions)
- Angular momentum is shown on a graph in which the time scale is normalized by the average duration of a turn, expressed as a percent (of a single turn) and are graphed starting at -25% of the turn

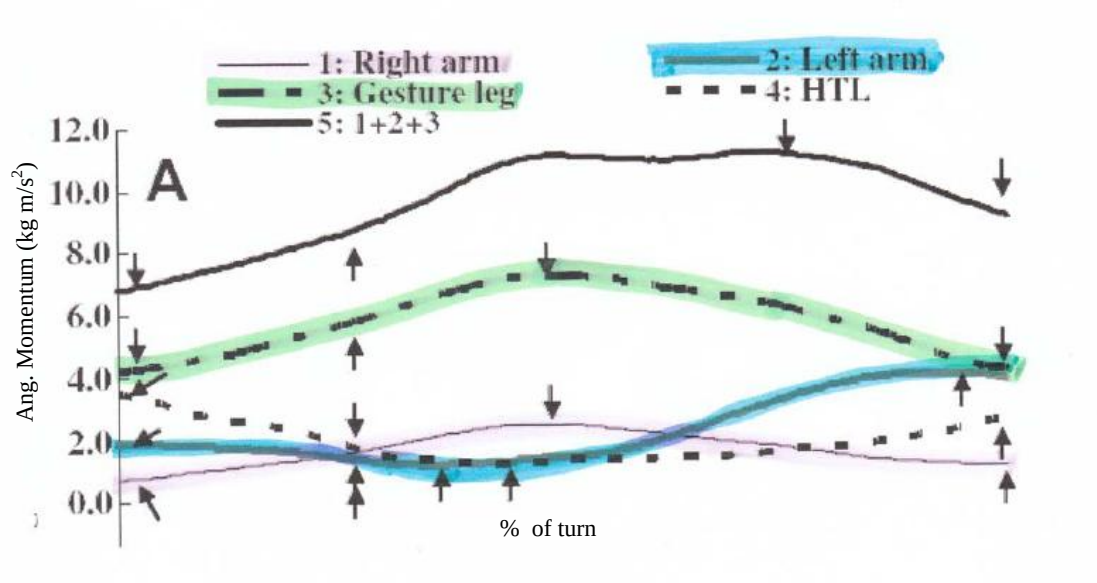

Figure 3-3. Imura et al.'s results showing angular momentum

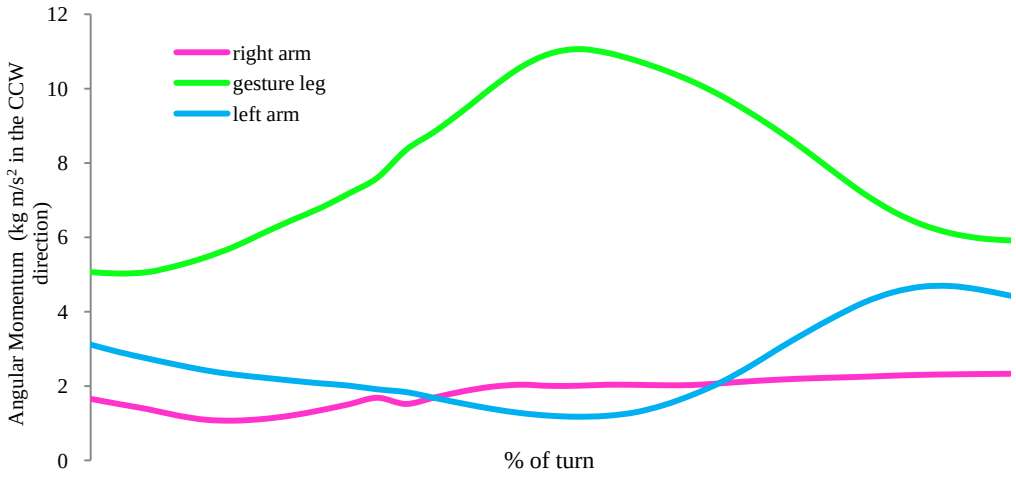

Figure 3-4. Results showing angular momentum with axes corresponding to Imura et al.'s study

Angular momentum of the right arm, left arm, and gesture leg are labelled as 1, 2, and 3 in the graph in Figure 3-3 showing Imura et al.'s results. Similarly, the angular momenta of the same three segment groups are shown in Figure 3-4, using the results of this study. Both graphs show the same general trend over the course of a single turn, as well as a similar range in values. Table 4 shows the difference in the range of results. While the results from both arms correspond quite well between the two studies, the range of values for the acting leg differ a significant amount between both studies. This is because

a greater amount of momentum is generated in the leg by virtue of it being extended throughout the entire turn in a *tour à la seconde*. When the dancer's leg is extended, its centre of mass is further away from the axis of rotation resulting in a greater moment of inertia and consequently a greater angular momentum (assuming no change to the angular velocity of the leg).

Table 4. Approximate ranges in value

	Imura et al.	***This study***
Right arm	*0 to 2*	*1 to 2*
Gesture or acting leg	*4 to 7*	*5 to 11*
Left arm	*1 to 4*	*1 to 5*

3.4.2 Verification of Visual 3D's calculations

As previously discussed, a segment's angular momentum is comprised of two parts: the angular momentum which results from the segment's angular velocity and the distribution of its mass, described by Equation 23, and the angular momentum which arises from the linear velocity of the segment acting at a distance from the axis of rotation, the first term in Equation 24. The total angular momentum is the sum of these two terms. Visual 3D's beta program calculates and displays graphs of angular momentum for each individual segment, but does not specify an equation. To determine which equation is used to obtain the values given by the program, three different equations for determining angular momentum were used to obtain three sets of graphs for comparison. An example, using the right thigh segment is given below.

Table 5. Comparison between calculation method of angular momentum of the right thigh (acting leg). The results from the unknown method of calculation on the left is compared to the known methods of calculation on the right. Angular momentum about the *x*-axis are shown in blue, angular momentum about the *y-axis* is shown in green, and angular momentum about the *z-axis* is shown in red. Since there are four turn in the series, four curves are shown for each.

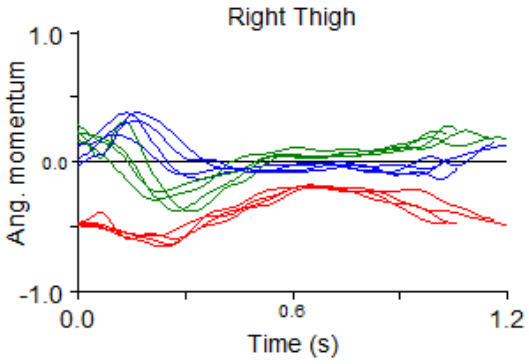

Figure 3-5. Visual 3D results

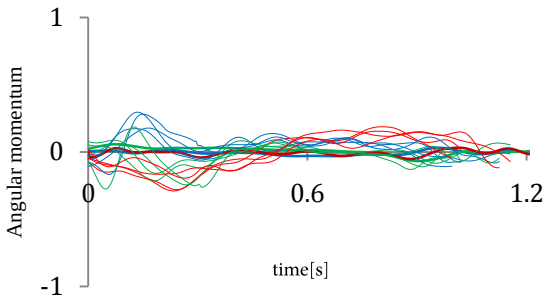

Figure 3-6. Case 1

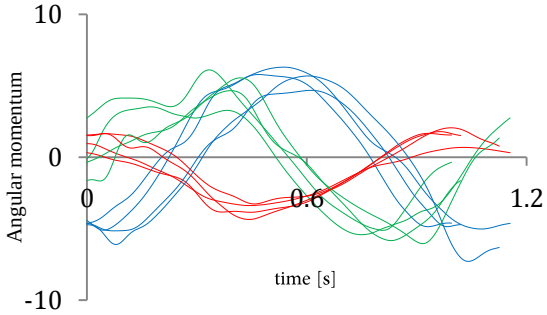

Figure 3-7. Case 2

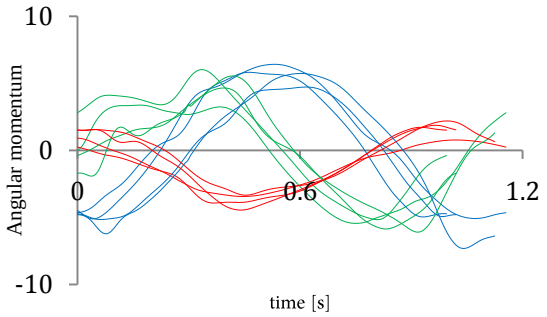

Figure 3-8. Case 3

The results show in case 1 are calculated from equation 23, the results shown from case 2 are calculated from the first term of equation 24, the moment of momentum, while the

results shown in case 3 are calculated using the entirety of equation 24 (i.e., the sum of cases 1 and 2). From this example, it can be determined that the equation used in case 1 (in Figure 3-6) most closely matches the method of calculation used by Visual 3D (in Figure 3-5) though there is an obvious bias in the curves representing angular momentum about the *z*-axis. This bias is representative of the vertical axis being located at two different distances for each calculation. It should also be noted that the ordinates of case 2 (Figure 3-7) and case 3 (Figure 3-8) are ten times as great as the ordinates of case 1 and on the left. Case 2 and case 3 graphs appear to be identical because of the relatively small magnitude of the results shown in case 1.

To confirm, the graphs of the rest of the segments are examined (included in Appendix E.) The individual graphs of each separate term in the equation for angular momentum can be examined to determine if the results make sense.

3.4.3 Conservation of Angular Momentum

The programs and equations were applied to a scenario in which a minimal amount of force would act on the body during its turn thus allowing angular momentum to be conserved. In a closed system without friction, air resistance, or any other forces acting on the body, all rotations would have a constant angular momentum. In a numerical biomechanical estimation, however, it is simply not possible to accurately calculate many of the variables which are used to determine angular momentum. Nonetheless, by examining a turn in the air, we can reduce the amount of work done on the system (by eliminating friction) and use a situation in which a constant angular momentum, dependant only on the forces exerted on the body at take-off, is theoretically expected. Three different turns were performed by two subjects to gauge the capacity of this study's procedures and calculation programs. The subject performed either a full or half turn, in the air, jumping and landing on the force plate.

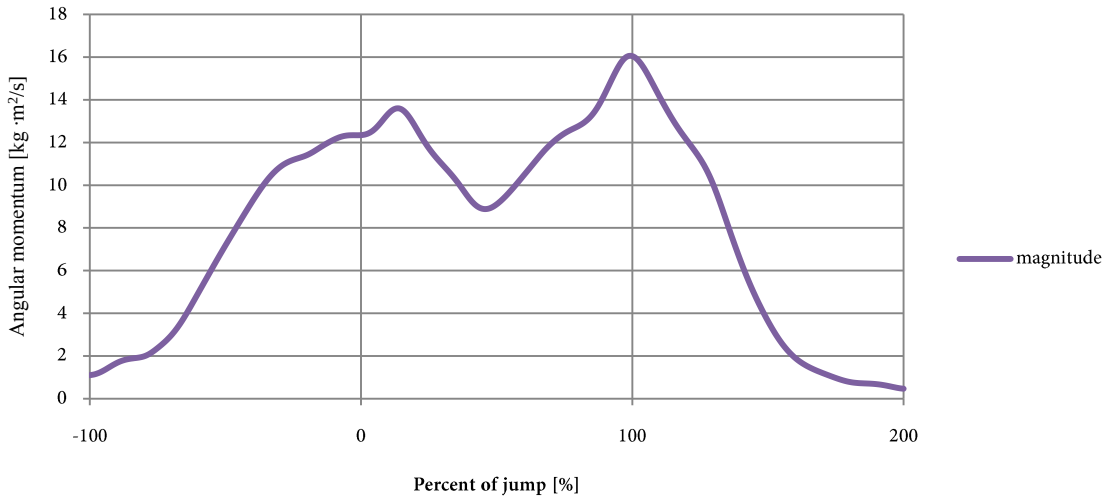

Figure 3-9. The magnitude of angular momentum during the jump is not constant; however, the curve oscillates periodically about a constant value

The mean magnitude of angular momentum that is present during the airborne phase of the jump is 12.09 kg·m^2/s. The angular momentum of each individual component is -8.53 kg·m^2/s, 1.01 kg·m^2/s, and -8.08 kg·m^2/s, respectively, for the momentum about the *x*, *y*, and *z*-axes. The desired motion of the jump occurs around the *z*-axis as the subject turns in the clockwise (negative) direction; therefore, a large amount of angular momentum is present about this axis. A significant angular momentum is also generated about the *x*-axis (parallel to the ground lying in the medial-lateral plane). Only a small amount of angular momentum is maintained about the *y*-axis (the anteroposterior axis.) It is clear that the magnitude of the angular momentum is not constant during the airborne phase, yet according to the laws of conservation of angular momentum if angular momentum is not constant, there must be external moments acting about the centre of mass.

In actual fact, the apparent moment acting about the calculated centre of mass is the true centre of mass. Gravity acting on the body will always act through the true centre of mass and the body necessarily moves according to this rule. If the centre of mass is assumed to be in a position other than the correct position, it will appear as if

external forces are acting on the body at a distance from the centre of mass (creating apparent external moments).

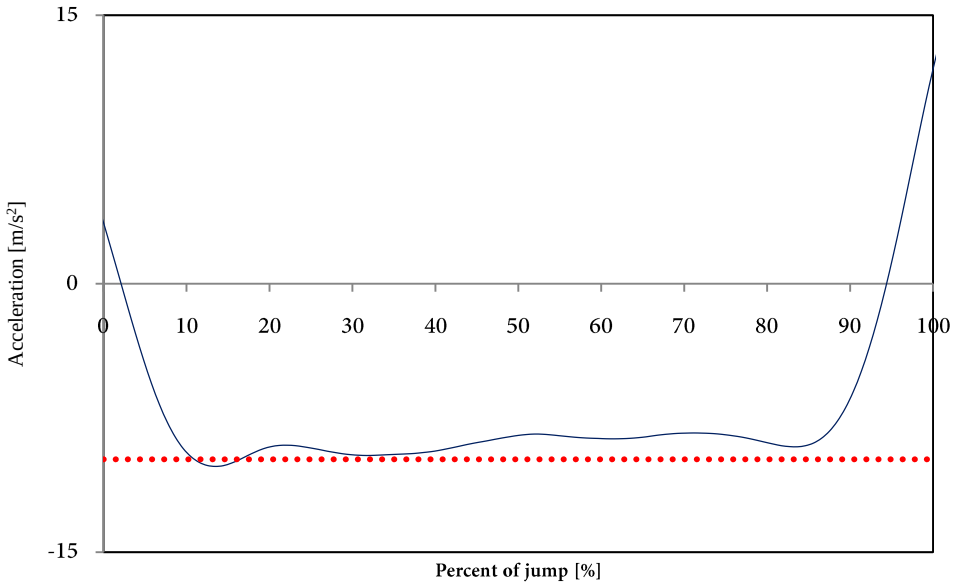

Figure 3-10. The acceleration of the centre of mass of the subject during the jump. The broken red line denotes the gravitational constant -9.81 m/s^2.

The acceleration (calculated according to equation 10) of the centre of mass of the subject is shown in Figure 3-10. If the centre of mass's position were calculated accurately, the acceleration of the centre of mass should be a constant of 9.81 m/s^2 downward when the subject is airborne. Figure 3-10 shows that the acceleration of the subject is not a constant -9.81 m/s^2; therefore, the position of our model's centre of mass, though reasonable, is not accurate.

3.4.4 Validation Conclusions

Comparison with Imura et al.'s study demonstrates that angular momentum is being calculated reasonably by our MATLAB programs, since the equations stated within Imura et al.'s paper are the same equations presented in the theoretical section (these are commonly used equations). A comparison of Figure 3-3 and Figure 3-4 show similar results (values and trends) for angular momentum about a dancer's centre of mass.

Special attention must be paid when using software which calculates angular momentum, because though the calculation of angular momentum might be correct (see Table 5), the reference (the point and axes about which the calculations are made) needs to be made clear in order to put the results into context.

Finally, in the absence of a microgravity environment, it is difficult to obtain an agreement between angular impulses produced at take-off during a jump and angular momentum. Non-conservative forces such as friction and wind resistance, as well as erroneous estimates in the location of action of conservative forces such as gravity will prevent the calculated angular momentum from remaining constant. However, constant angular momentum has been found in studies conducted in a microgravity environment (Pedrocchi, Baroni, Bedotti, Masson, & Ferrigno, 2005).

4 Results

4.1 General

The results of the three-dimensional biomechanical analysis of a series of *tours à la seconde* are presented in this chapter. To put the following results into proper context, certain time points are required from the 3D motion capture video. Important characteristics of the dance step that were noted during analysis of the motion capture video included:

- the heel position of the dancer,
- the motion of the extended leg in relation to the rest of the body, and
- the instant when the dancer is presenting.

Presenting should occur in the same direction of each turn; presumably while facing the audience, the dancer's arms are held open and the acting leg is extended laterally (as depicted in step 2 of Figure 1-1).

The timing of some of the general features of the turn is shown in Figure 4-1 and Figure 4-2. Figure 4-1 shows that the start of the turn is defined by heel contact of the dancer's support leg with the ground lasting approximately 22% of the turn. The raising and lowering of the heel comprises another 19% of the turn. The dancer is fully on her toes for the majority of the turn—59% of the turn. In Figure 4-2, the period in which the acting leg moves laterally while the rest of the body appears stationary is denoted by the light-coloured region of the pie chart. This period lasts approximately 18% of the turn. It can then be concluded that the dancer is presenting at the end of this period.

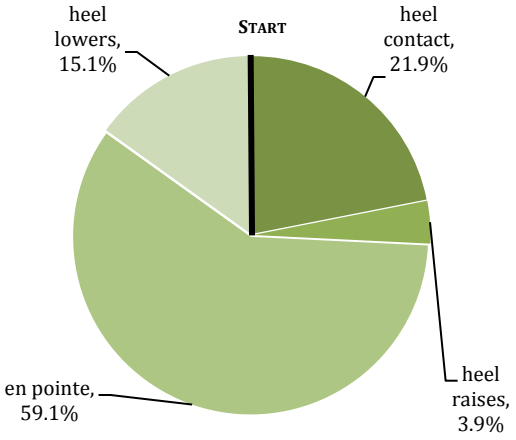

Figure 4-1. Percent of cycle features, defined by 0% at start

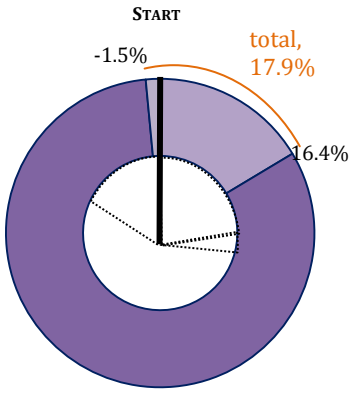

Figure 4-2. Percent of cycle during which extended leg rotates (depicted by the light purple section) while torso appears stationary—the inner part of the chart shows the cycle breakdown from Figure 4-1

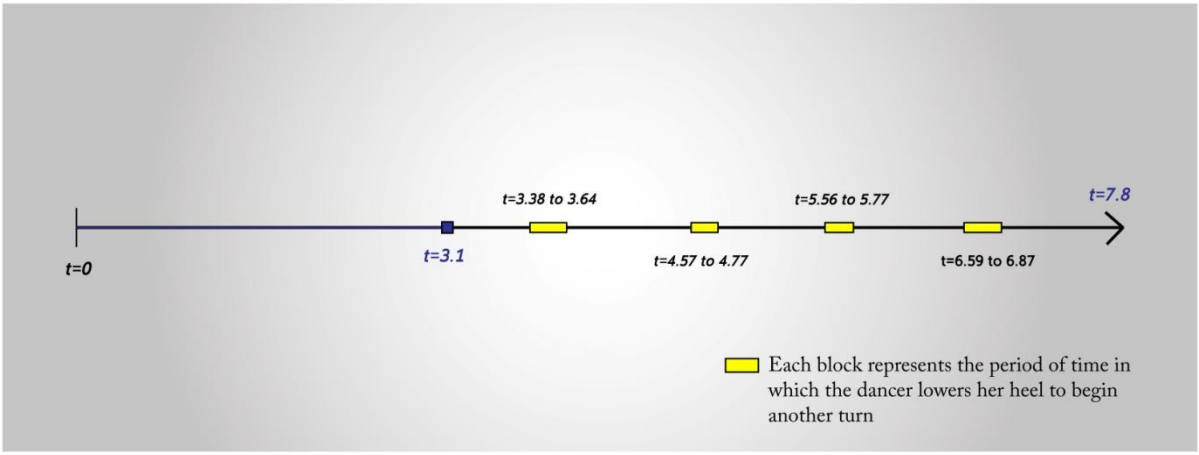

Figure 4-3. Timeline of the series of turns. During the initial phase from t=0s to approximately t=3.1s, the dancer is balancing herself, shifting her weight back and forth until she feels ready to begin. The dancer pushes off at t=3.1s.

The average period of a complete turn for this particular dancer is approximately 1.05s. This period is a characteristic of all of the graphical results. The position of each of the 15 segments was graphed individually. The position of each segment of the dancer's limbs is a variable which not only describes the important features of the turn, but is also an important input into the balance control system. However, the position of the dancer within the laboratory coordinate system is of limited use. The location of the laboratory coordinate system is an arbitrary choice. Motion relative to an arbitrary location does not have as much meaning in this analysis as motion relative to the dancer. As an input

to the body's sensory system, it is more informative to know the dancer's movement with respect to herself. Figure 4-4 shows the movement of the dancer's centre of mass in the laboratory coordinate system. This movement is also reflected in any other plots drawn using the laboratory coordinate system. Though Figure 4-4 only shows movement in two dimensions, the centre of mass does move in all three dimensions. In fact, the motion of the dancer is not entirely rotational since the centre of mass drifts in the transverse plane. Because we are most concerned with the dancer's movement with respect to herself (for example, how a dancer positions her arm relative to his or her torso rather than how it is positioned relative to a wall), this general movement with respect to the lab can be removed. By using a body-based coordinate system located at the dancer's centre of mass, we are able to perceive the same type of data that the body perceives and thus can draw more useful conclusions.

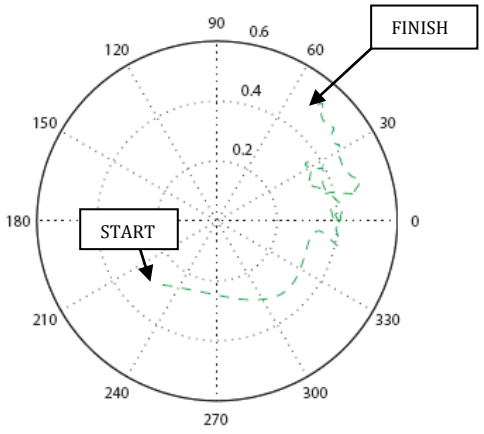

Figure 4-4. Planar movement (in the transverse plane) of the dancer's centre of mass

Additional figures below show how the change in coordinate system from the lab coordinate system to a body-based coordinate system allows for data to be presented with the translation of the body's centre of mass removed. Figure 4-5 through Figure 4-8 are plots showing the position of the left (top) and right feet (bottom) before (Figure 4-5, Figure 4-7) and after (Figure 4-6, Figure 4-8) the motion of the dancer's centre of mass is subtracted from each limb's motion to filter the dancer's general movement from the

coordinate system (refer to equation 4). When this adjustment is made, as shown in Figure 4-6 and Figure 4-8, it is easier to see how the position of the foot changes as the body rotates. The left foot essentially stays stationary underneath the centre of mass, while the right foot traces a circle around the centre of mass as the dancer rotates.

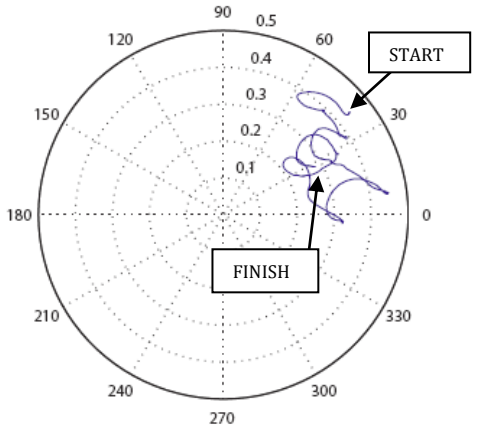

Figure 4-5. Motion of the left (support leg) foot in the lab coordinate system (radial direction is in metres, angular direction is in degrees)

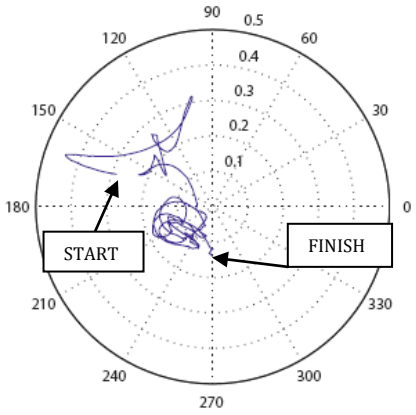

Figure 4-6. Motion of the left (support leg) foot with respect to the dancer's centre of mass (radial direction is in metres, angular direction is in degrees)

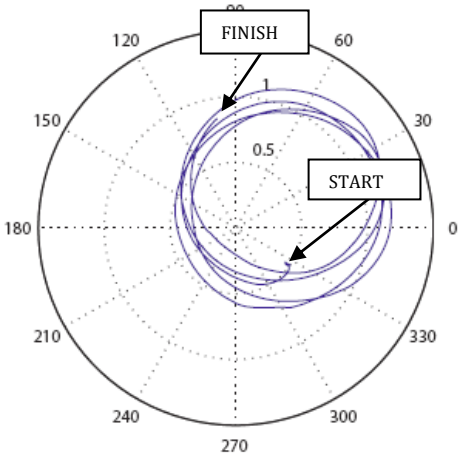

Figure 4-7. Motion of the right (acting leg) foot in the lab coordinate system (radial direction is in metres, angular direction is in degrees)

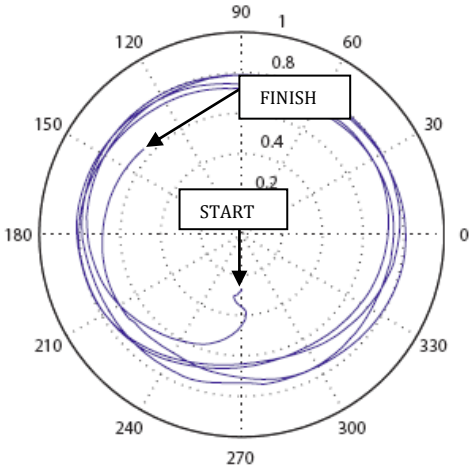

Figure 4-8. Motion of the right (acting leg) foot with respect to the dancer's centre of mass (radial direction is in metres, angular direction is in degrees)

Both the radial path and the angular position of the limbs reveal information about the nature of the turn. In an example of a perfect turn, a figure showing the position of the

left foot in a transverse plane would display a point. The foot would not translate in order to minimize friction forces that result from contact with the ground. The dancer would rotate about the contact point between her toe and the ground much as a spinning top rotates. This is not possible because the position of the foot shifts as a result of the changing balance of the dancer, factors such as the unevenness of the ground, non-homogeneous surface properties, and the footwear of the dancer. Because of these factors, the dancer does not stay in one location. The translation of the dancer can be estimated by the movement of her centre of mass within the lab coordinate system.

The position of the dancer's left foot with respect to her own centre of mass in Figure 4-6 is more localized and closer to being directly below her centre of mass. Similarly, while Figure 4-7 shows that the dancer's right foot moves in a circular path, Figure 4-8 gives the additional information that the circular path is centred at the dancer's centre of mass.

Polar plots around the centre of mass' axis are shown in three dimensions below in Figure 4-9. A complete set of polar plots is available in Appendix D. A three-dimensional representation of the polar plots gives an accurate picture of the turn.

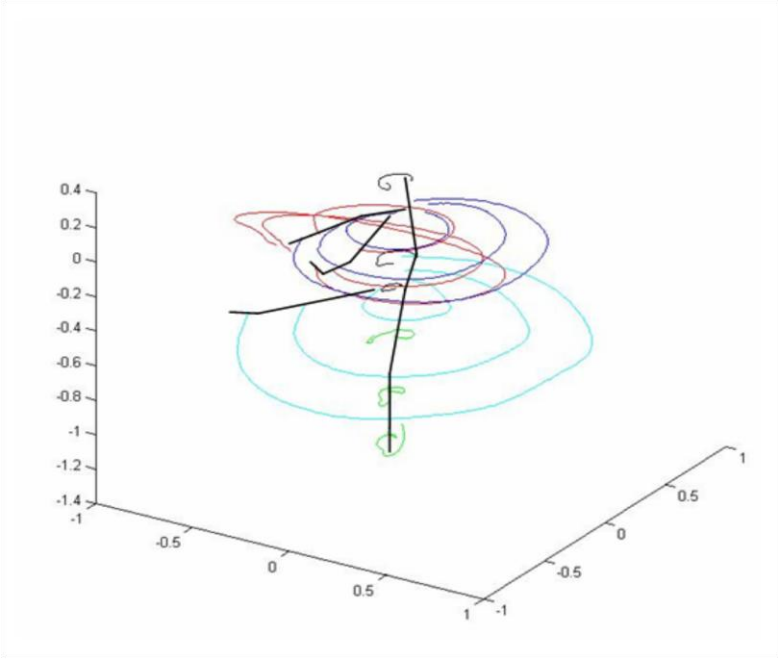

Figure 4-9. Segment pathways during one revolution of the turn [units are metres]

In Figure 4-9 above, each limb's set of data is represented by a different colour as shown in the legend in Table 6. A description of each segment group is also provided in Table 6. Since the dancer rotates clockwise, the black stick-figure represents the dancer's position at the end of the revolution.

Table 6. Segment Descriptions

Segment group	Colour
Right leg *comprised of right thigh, right lower leg, right foot*	Cyan
Left leg *Comprised of left thigh, left lower leg, left foot*	Green
Right arm *Comprised of right upper arm, right forearm, right hand*	Red
Left arm *Comprised of left upper arm, left forearm, left hand*	Blue
Central region *Comprised of head, thorax, pelvis*	Black

Figure 4-10 shows the phase difference between the right hand and left hand while the turn is being performed. As previously mentioned, the right hand moves in and out of phase with the right foot while a turn is being performed. The right hand moves in and out to join the left hand which stays motionless with respect to the body (i.e., the sinusoidal nature of the curve denoting the left hand shows the almost perfect circular motion of the arm). The repeated touching and separation of the curves demonstrates that the angle between the hands increases to a maximum and diminishes to zero periodically. These are the instants in which the hands are brought together in front of the body. It is important to note that figures show unwrapped data—successive rotations are modified by adding 2π in order to avoid discontinuous jumps in the curve.

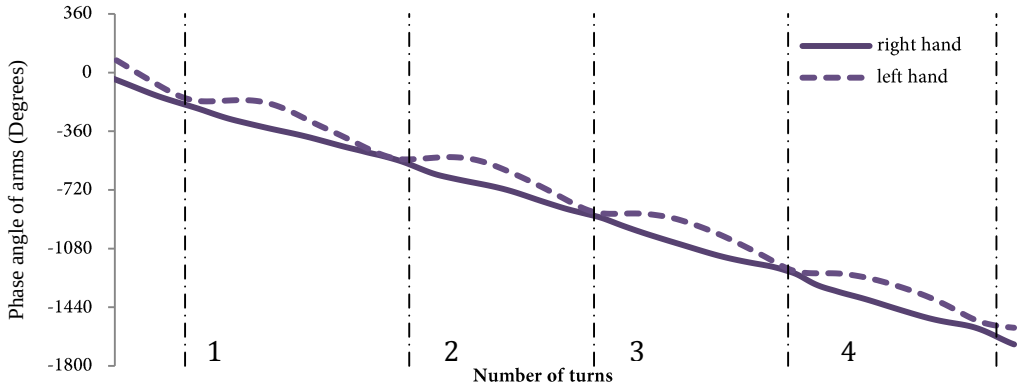

Figure 4-10. The phase angle of the left and right hand for the series

Figure 4-11 shows the difference in phase angle between the right and left hands. The hands are together when the difference is a minimum, approximately 30°, and are separated when the difference is a maximum, approximately 145°. This angle is illustrated in Figure 4-12.

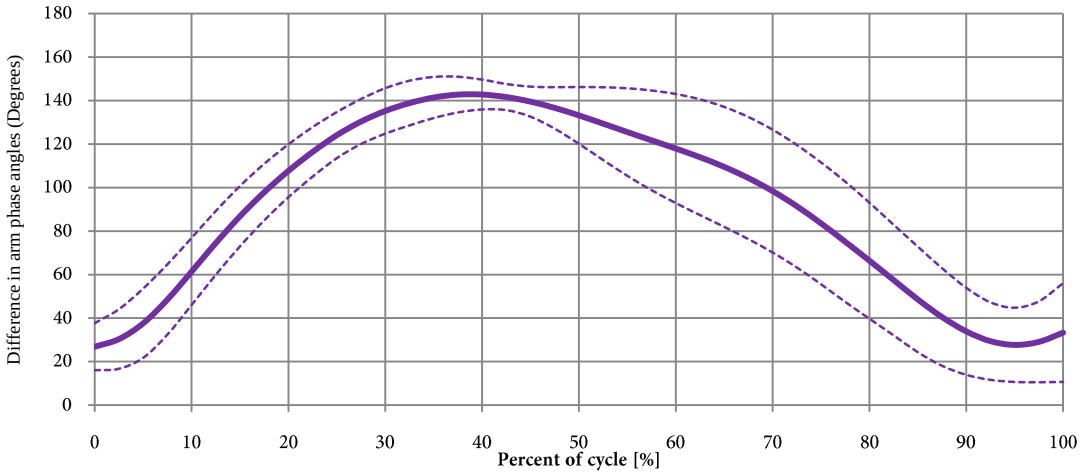

Figure 4-11. The phase angle of the left and right hand for one turn

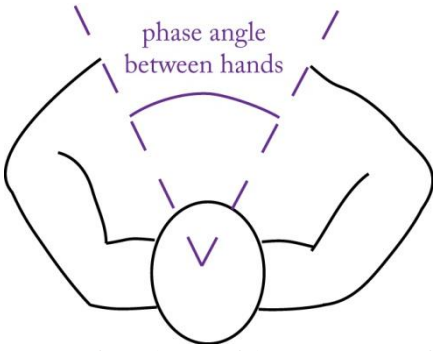

Figure 4-12. A view from the top of the arm position of the dancer

The results demonstrate periodicity and other characteristics of circular motion as is expected.

4.2 Angular momentum of the dancer

This section provides results that quantify the angular momentum of the *tour à la seconde*. No such results currently exist in the literature and our results can be useful for producing simulations of the turn. The angular momentum of the dancer was calculated according to equations 23 through 25. Of primary interest is the angular momentum of the dancer in the direction of the turn (about the longitudinal axis) because it is the main goal of the turn. Figure 4-13 shows the average trends in angular momentum about the longitudinal axis for the turns in the series of *tours à la seconde*. In Figure 4-13 and Figure 4-14, broken lines following the curve represent the standard deviation while vertical broken lines in black represent the different phases of the cycle as explained in Figure 1-1. Since 0% represents the start of the phase in which the heel is in contact with the ground (lasting approximately 22% of the initial part of the cycle), it can be seen that angular momentum increases during the time in which the heel is in contact or transitioning from or to contact with the ground. The angular momentum continues to increase to an average value of 15.52 kg·m^2/s when the dancer is fully *en pointe* (on her toe). The angular momentum of the dancer decreases between 38% and 80% of the cycle to reach an average minimum of 11.50 kg·m^2/s when the heel begins to lower in preparation for the next turn.

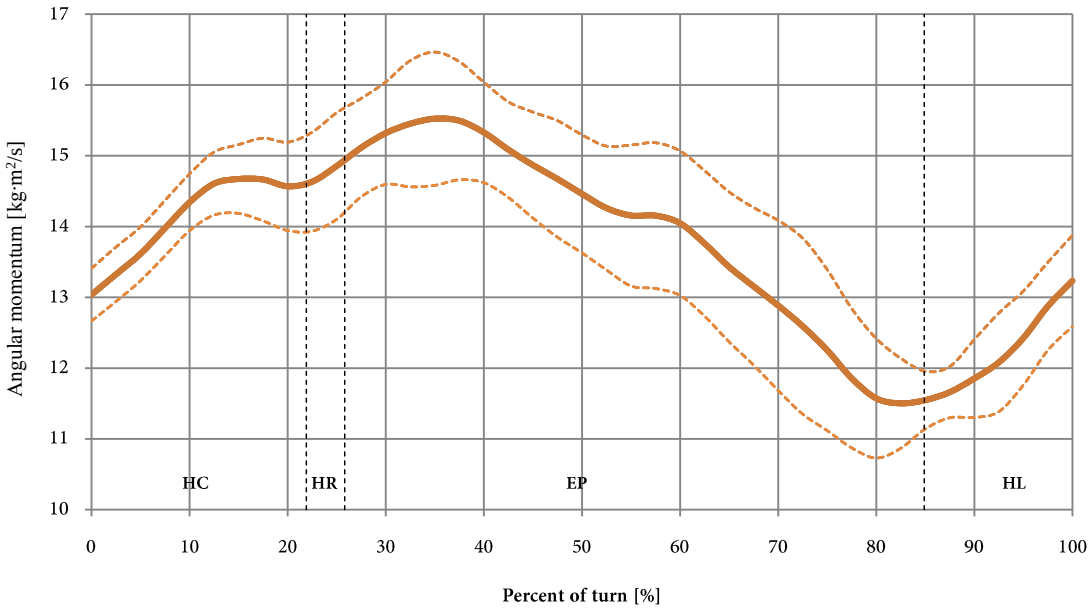

Figure 4-13. Angular momentum about the longitudinal axis throughout one revolution

The angular impulse is shown as calculated using equation 27 in Figure 4-14. The angular impulse curve shows that the maximum impulses or changes in angular momentum about the longitudinal axis occur when the heel is lowering or on the ground. Thus, as is expected, the peaks in the angular impulse correspond with the increases in the angular momentum. These impulses—occurring about the vertical axis—contribute to the desired rotation of the turn.

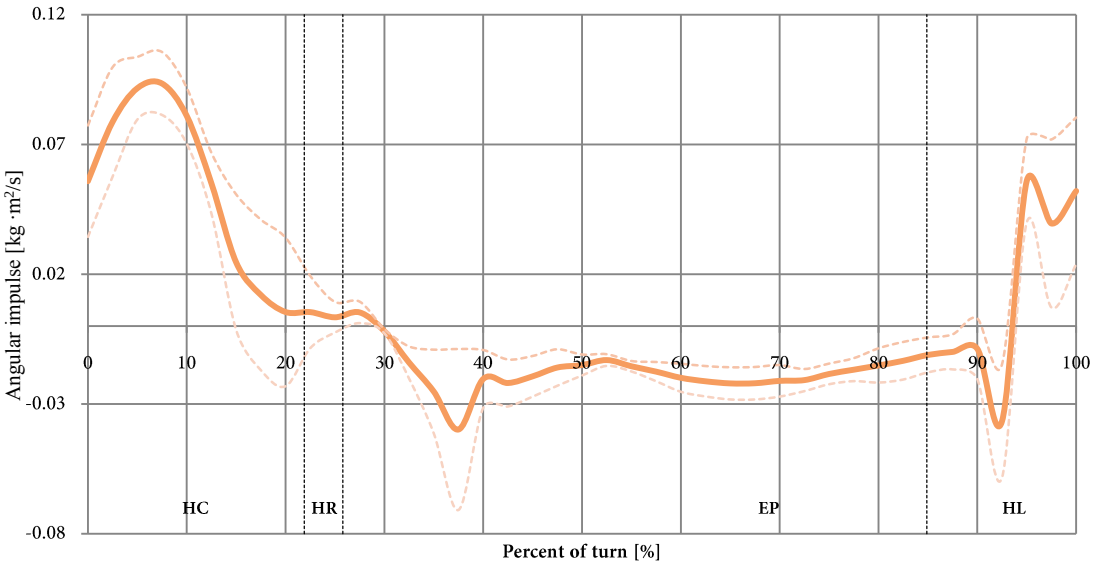

Figure 4-14. Angular impulse about the longitudinal axis of rotation

Since the results in Figure 4-13 and Figure 4-14 were calculated from the resulting motion of the body, it was important to confirm the results using an alternate method of calculation. Therefore, using equation 36, the angular impulse about the vertical axis of rotation was calculated. This method measures the forces and moments directly as opposed to determining them from the resulting motion of the body.

Figure 4-15 shows the difference between the two methods of calculation for a series of turns.

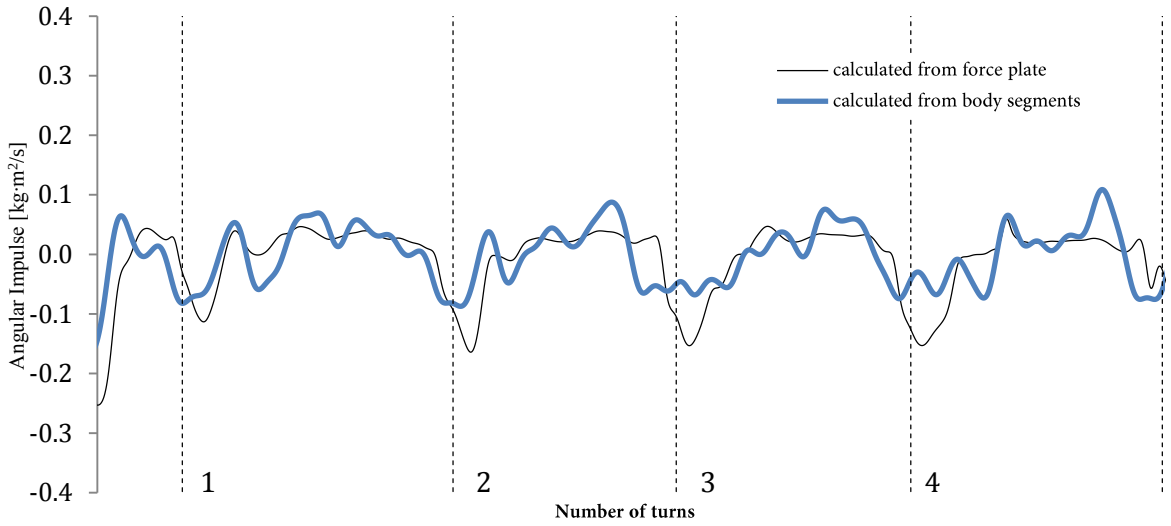

Figure 4-15. Angular impulse about the vertical axis calculated by two separate methods for a series of turns. Angular impulse calculated from the force plate and from the motion of the body segments.

Discrepancies between the two curves exist because of modelling errors. The model assumes segments are rigid bodies where most are not, and does not take into account relative motion of visceral masses (Minetti, 1994). The curve obtained from the motion of the body's segments is based on a rigid body estimation that does not take into account motion of the dancer's visceral mass.

Though angular momentum about the axes parallel to the ground will not contribute to the desired motion of the turn, it will have an effect on the outcome of the turn. Figure 4-16 shows angular momentum calculated about the horizontal axes. A constant value between 4 and 5 $kg \cdot m^2/s$ is highlighted in yellow in Figure 4-16 during the

part of the turn when the dancer is *en pointe*. When the dancer is not *en pointe*, two distinct peaks in the curve can be seen. It is speculated that the cause of these peaks is from the support leg's heel contact with the ground and the acting leg reaching its maximum range of lateral motion. Axes defined as parallel to the shoulder and hip vectors, the mediolateral axis, and an axis perpendicular to the mediolateral and longitudinal axis, the anteroposterior axis, are shown in Figure 4-17. Angular momentum components about these axes are shown in Figure 4-18 and Figure 4-19.

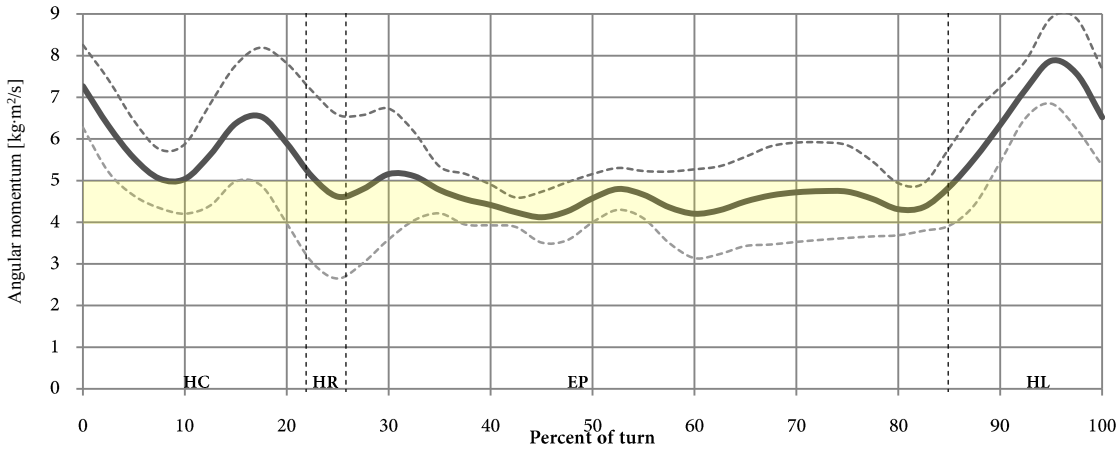

Figure 4-16. Angular momentum about horizontal axes

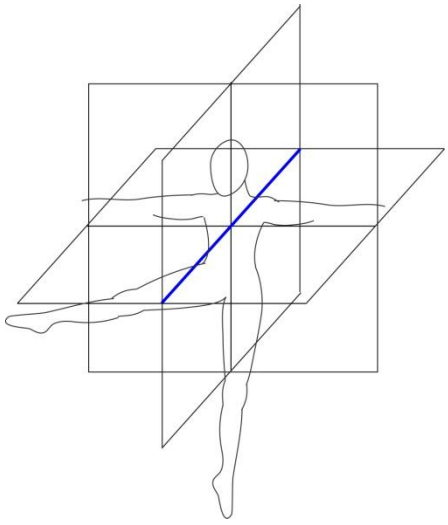

Anteroposterior axis in blue
positive=right, negative=left

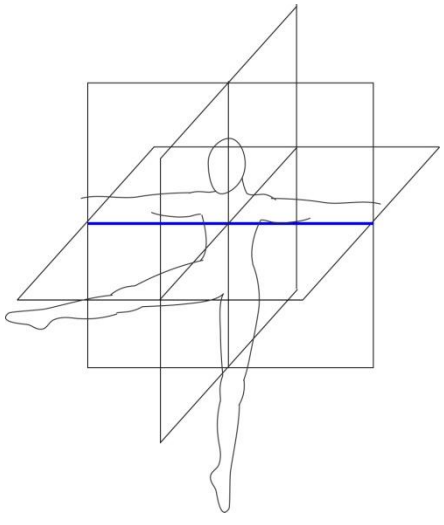

Mediolateral axis in blue
positive=forward, negative=backward

Figure 4-17. Axes parallel to the ground.

Angular momentum about the mediolateral axis will cause the dancer to rotate forward or backward depending on the polarity while angular momentum about the anteroposterior axis will cause the dancer to tip left or right, again depending on the polarity. In Figure 4-18 and Figure 4-19, it can be seen that significant amounts of angular momentum exist about these axes. Though the momenta about the axes vary significantly throughout each cycle, they average to relatively small values of 1.92 kg·m²/s and 2.49 kg·m²/s, respectively. On the other hand, the angular momentum about the longitudinal has an average value of 13.70 kg·m²/s.

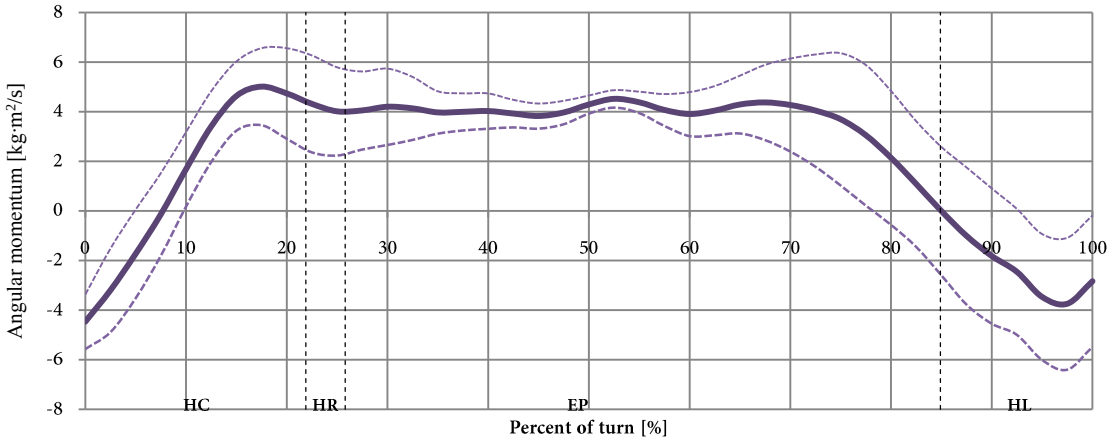

Figure 4-18. Angular momentum about the mediolateral axis (a positive momentum indicates the tendency to tip forward)

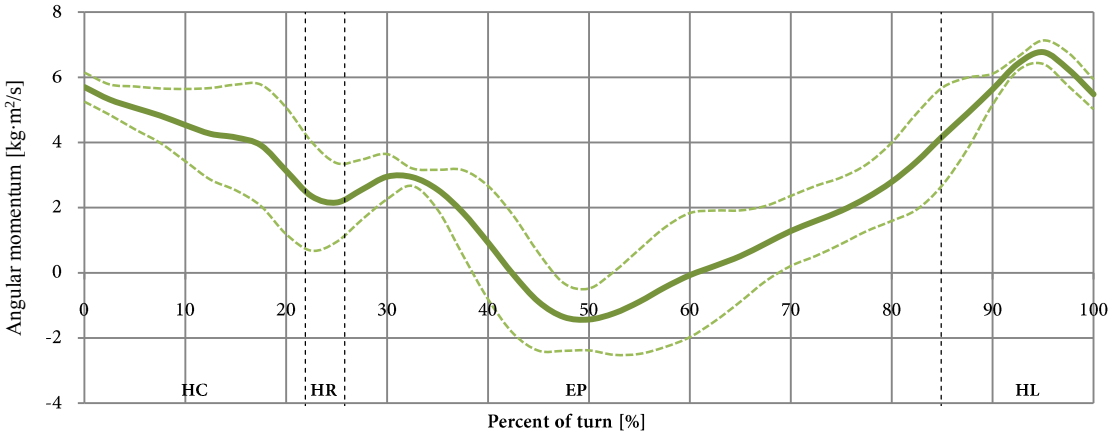

Figure 4-19. Angular momentum about the anteroposterior axis (a positive momentum indicates a tendency to tip to the right)

Figure 4-18 shows that the momentum about the mediolateral axis is highest during the middle portion of the turn (between 20% and 75%) while it can be seen in

Figure 4-19 that momentum about the anteroposterior axis is lowest during this same period. When angular momentum about the anteroposterior axis is highest during the initial 20% and final 25% of the turn, the momentum about the mediolateral axis is lowest. This trade-off, showing a transfer of angular momentum, is also shown quite clearly in Figure 4-20. The trend in angular momentum about the mediolateral and anteroposterior axis is the same throughout the series, but out-of-phase with one another.

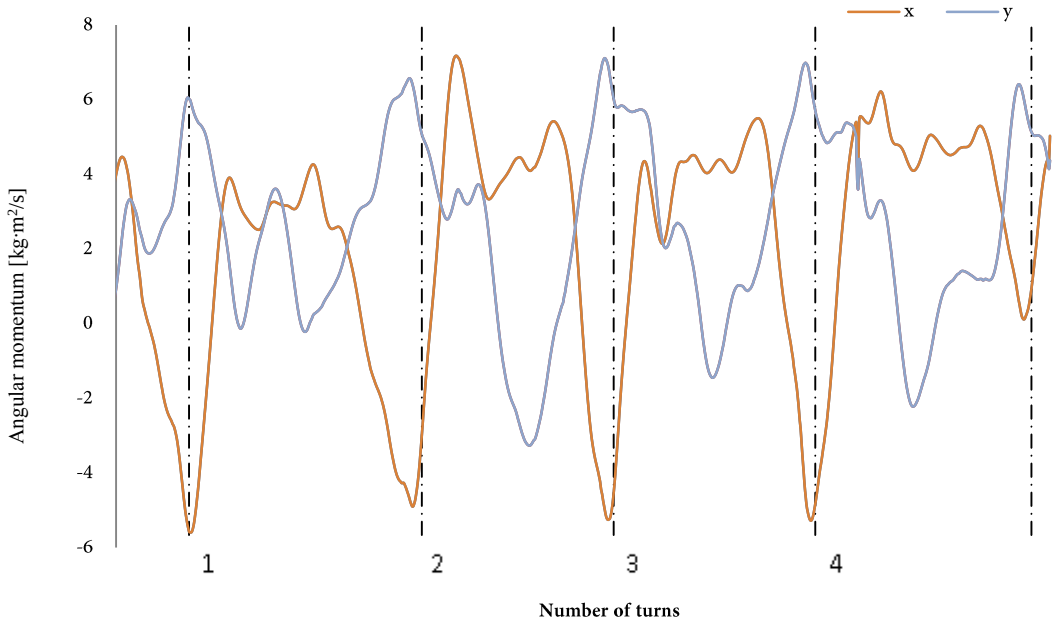

Figure 4-20. Angular momentum about the mediolateral axis (x) and the anteroposterior axis (y) throughout the series of turns. A transfer between axes is clearly demonstrated by the out-of-phase undulations of the curves

The total angular momentum about the centre of mass of the dancer is largely dependent on the angular momentum about the longitudinal axis of rotation because it is so much larger than the angular momenta about the other axes. Figure 4-21 and Figure 4-22 show both the magnitude of the angular momentum about the centre of mass and the direction of the angular momentum vector (angle from vertical), respectively. The magnitude follows the same trends as the momentum about the vertical axis. Figure 4-22 shows the direction of the angular momentum vector; the combination of momenta about the three axes is such that the direction of angular momentum, and likewise, the

angle of the dancer with the ground is close to 90 degrees, but never reaches 90 degrees. If the angular momentum vector is used as an estimate of the dancer's lean, it can be seen that the dancer's axis of rotation is closest to being perpendicular to the ground when she has a maximum amount of angular momentum, and conversely she leans the most when she has the least amount of angular momentum.

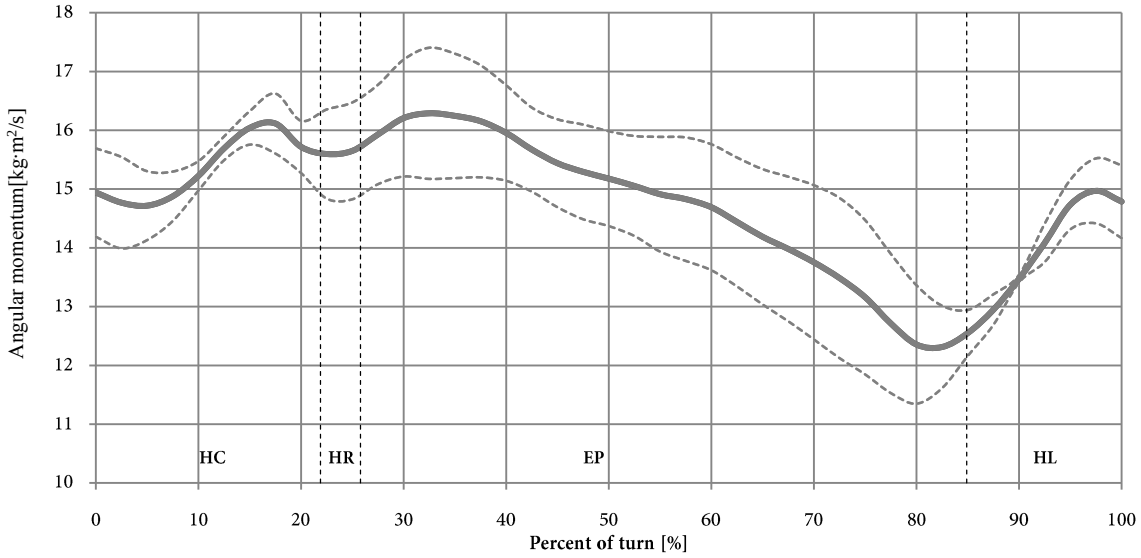

Figure 4-21. The magnitude of angular momentum about the dancer's centre of mass

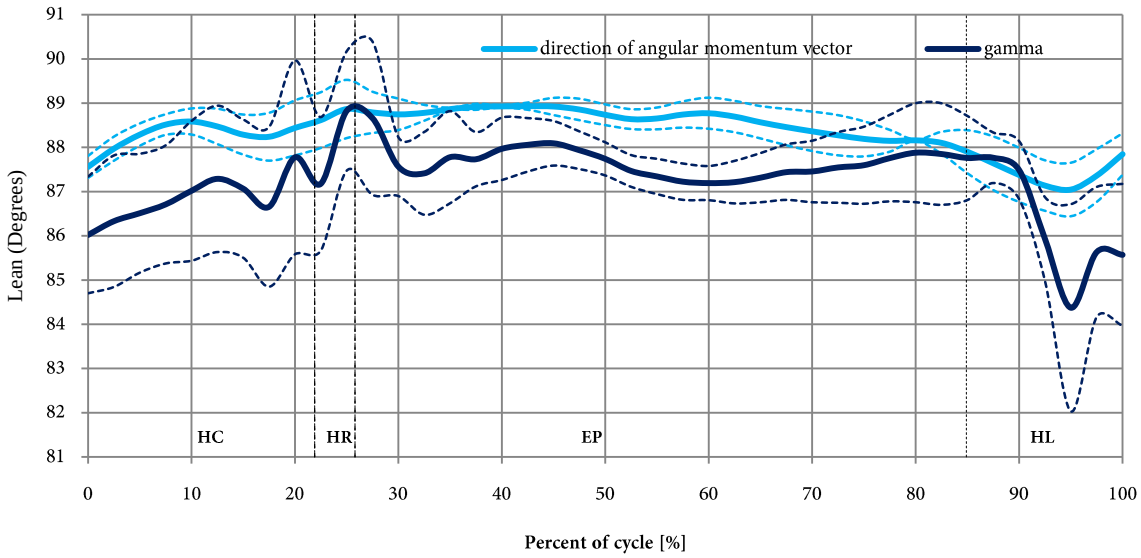

Figure 4-22. Estimates of the lean of the dancer

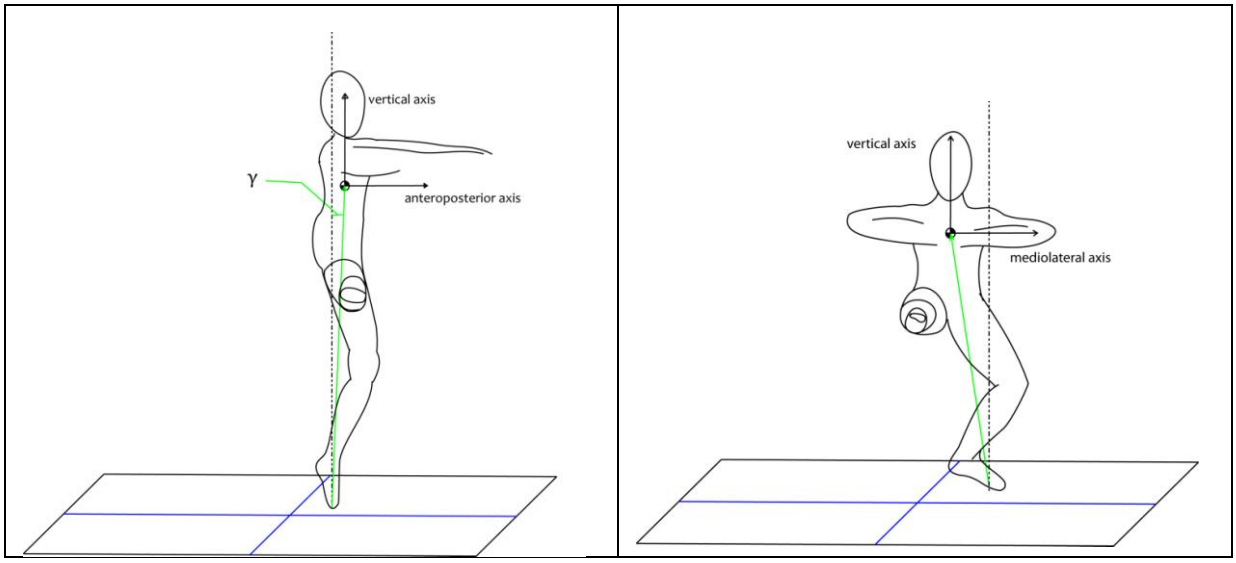

Figure 4-23. Angle of lean calculated by the vector from the centre of mass to the centre of pressure, shown from two different views

Figure 4-22 also shows the angle of lean calculated from the vector depicted in Figure 4-23. Figure 4-23 demonstrates the angle of lean as calculated from a vector drawn from the centre of pressure to the centre of mass of the dancer. The lean of the dancer is an estimate of the dancer's balance, but will also affect her ability to maintain balance. The angle of lean will also affect how the torque acts about the pivot point. These results are presented later in the chapter.

4.3 Transfers of angular momentum between the dancer's limbs

The body of the dancer is not a rigid object. Unlike a spinning top, which is a single rigid body, the dancer is composed of several parts which move relative to one another. Because the dancer's limbs move relative to one another, it is possible to transfer angular momentum between them. The following section shows results which show transfers of angular momentum between different parts of the dancer's body during the turn. Table 7 shows the general trend of an individual segment's angular momentum (magnitude) in comparison to the body, as well as in comparison to adjoining segments. Each row in the table represents a group of segments sharing a common motion (a limb). The left arm and right arm both have significant angular momenta during the same periods of the turn though the segments of the left arm have greater amounts of

momenta than their corresponding right arm segments. During different parts of the turn, the amount of momentum each segment contributes to the total angular momentum may not be apparent in the outward production of the motion of the dancer. For example, in the first two rows of Table 7, it is shown that the upper limbs can produce a significant amount of angular momentum when compared to the whole body's angular momentum. The left upper arm's momentum can have a magnitude of up to 60% of the total body's angular momentum. This is possible because the angular momentum of another segment can have a significant amount of momentum that can, at times, act in the opposite direction. Figure 4-10 shows the relative motion of the right and left arm during the series of turns. The right arm moves in the direction of the turn, while the left arm moves opposite to the turn when the hands are brought together in first position (a crucial feature of the turn) which, because the momentum components are in opposing directions, results in only a very small contribution to the whole body's angular momentum. The right arm can have an angular momentum of up to 40% of the turn. This means that the actual contribution of the left arm to the whole body angular momentum is reduced. Another feature of the turn, the motion of the right leg about the pivot point of the left leg, is reflected in the results. The angular momentum of a segment is largely affected by its distance from the centre of mass and its relative motion. The left foot is a considerable distance from the body's centre of mass, but since it is the pivot point of the motion there is very little relative motion. In Table 7, the right leg has a significant amount of momentum while the left leg has almost no angular momentum. This characteristic of the central region in comparison to the right leg is shown in greater detail in Figure 4-24 and Figure 4-25.

Table 7. Magnitudes of segments' angular momenta about the dancer's centre of mass as a percent of the total angular momentum. The abscissae represents the percentage of the turn. The ordinates represents the percentages of the whole body angular momenta. Because these are magnitudes only, and directions may in fact be opposite to one another, it should be noted that the momenta will not add to 100%.

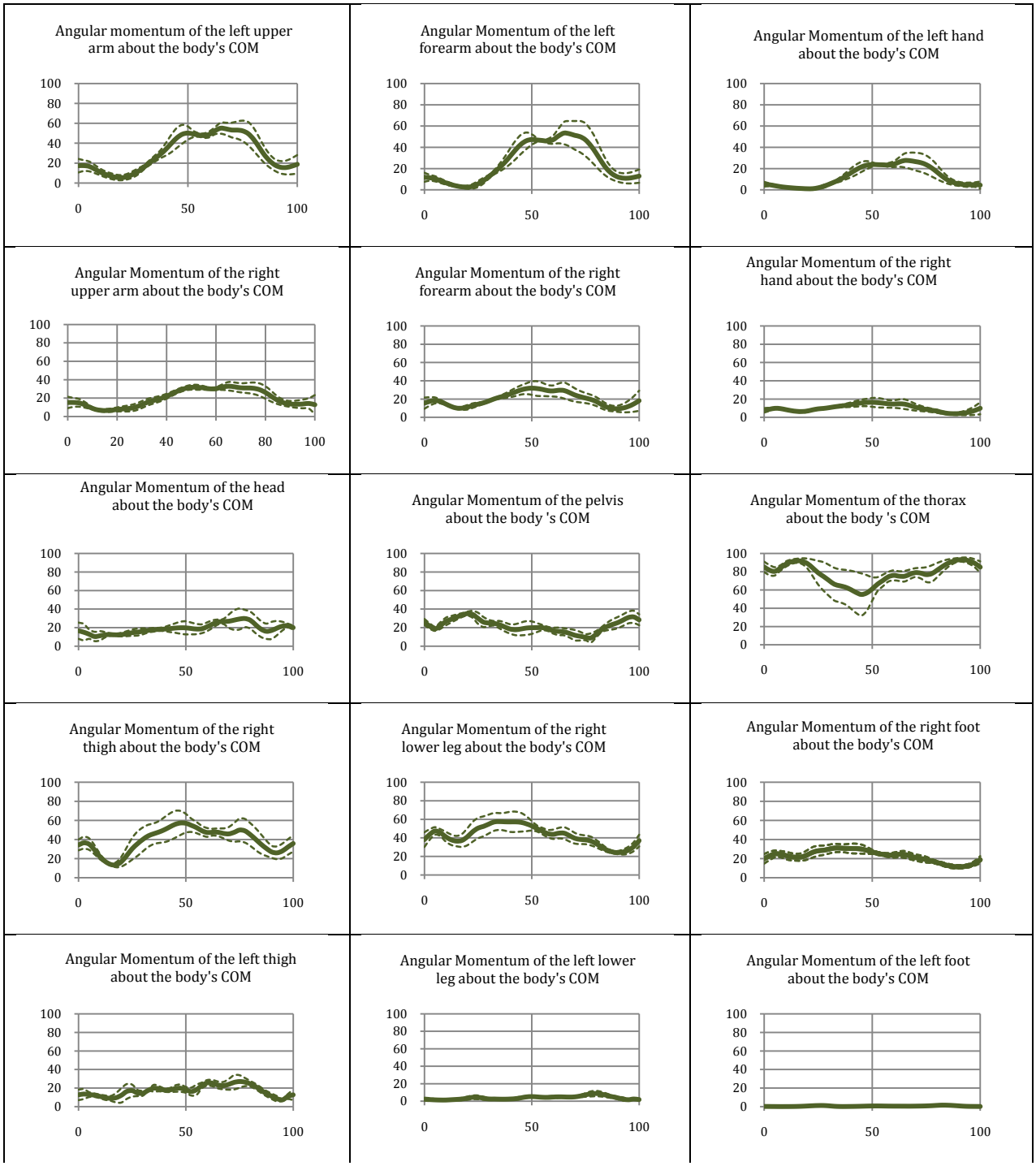

Figure 4-24 shows that transfers in angular momentum occur between the segments as well. The right thigh has its maximum amount of momentum when the

thorax's momentum is at a minimum and vice versa. The same is true for any right leg segment in comparison to the thorax or pelvis. A transfer between two angular momentum curves demonstrates a transfer in angular momentum between the two.

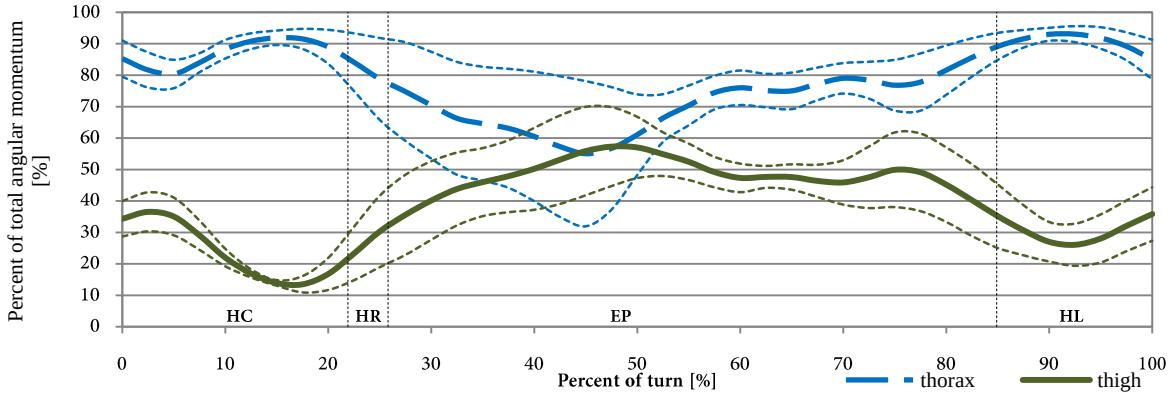

Figure 4-24. Angular momentum of the right thigh and thorax about the body's centre of mass

All of the segments of the central region and right leg are compared in Figure 4-25. Smaller segments such as the foot, head, and pelvis possess smaller magnitudes of momenta. Angular momenta of the head, pelvis, and thorax are higher in the beginning and end of the turn, while angular momenta of the right thigh, lower leg, and foot are higher in the middle portion of the turn. The transfer between the smaller segments is not as pronounced as the transfer between the thigh and thorax; however, it is present, nonetheless.

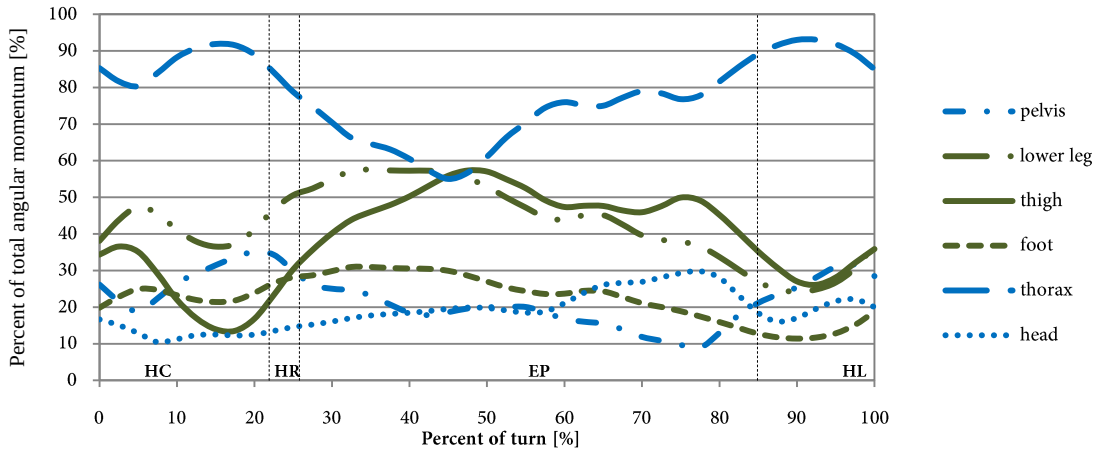

Figure 4-25. Angular momentum of the central region (head, pelvis, and thorax) in blue and the right leg (thigh, lower leg, and foot) in green

The transfer between the right leg and the central region suggests momentum is being transferred between the acting leg and the body.

4.4 Energy

The energy trends of the dancer during the turn allow the mechanical system of dancer to be characterized. When considering which models (such as those based on an inverted pendulum analogy) can be applied for analysis of a dancer during a turn, it is necessary to know the behaviour of the dancer as a mechanical system. The results in this section characterize the mechanical energy of the dancer.

The average kinetic energy during a cycle of the turn is shown in Figure 4-26 and the average potential energy during a turn is shown Figure 4-27. Just prior to the period when the heel makes contact with the ground, significant variations occur in kinetic energy. The kinetic energy of the dancer reaches its maximum of 69 J in the middle of the heel contact period as the heel pushes off from the ground. During contact, the kinetic energy of the dancer drops sharply until it reaches its minimum of 39 J as the dancer begins to raise her heel to transition to being *en pointe*. Throughout the remainder of the turn, the kinetic energy increases gradually. The sharp decrease in kinetic energy is seen because the lowering of the heel and push off from the ground functions as a brake to slow the motion of the turn.

Conversely, the gravitational potential energy of the dancer is at its lowest when the heel is in contact with the ground, but increases sharply as the foot is raised onto its toe before again decreasing throughout the turn. Shown in Figure 4-27, the gravitational potential energy increases to an average maximum of 625 J, 87 J above the dancer's starting potential energy. As expected, the peaks in the graph correspond to the instants in which the dancer is raised on her toes (*en relevé*) and the troughs correspond to the times when the dancer is lowered in *plié* and has lowered her heel. This is contrast to the trend seen in the kinetic energy of the dancer.

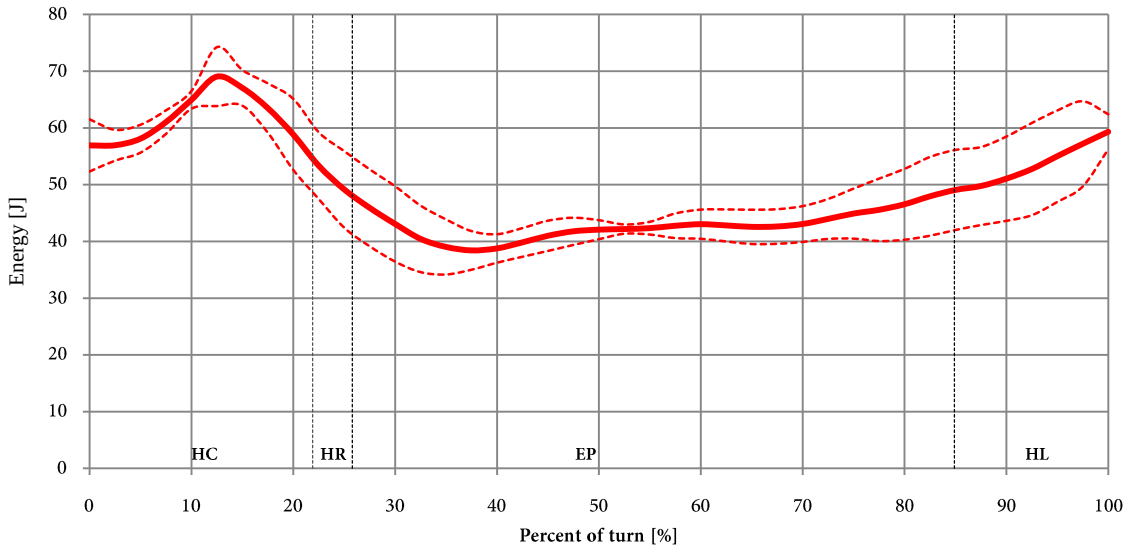

Figure 4-26. Kinetic Energy of the dancer during the turn

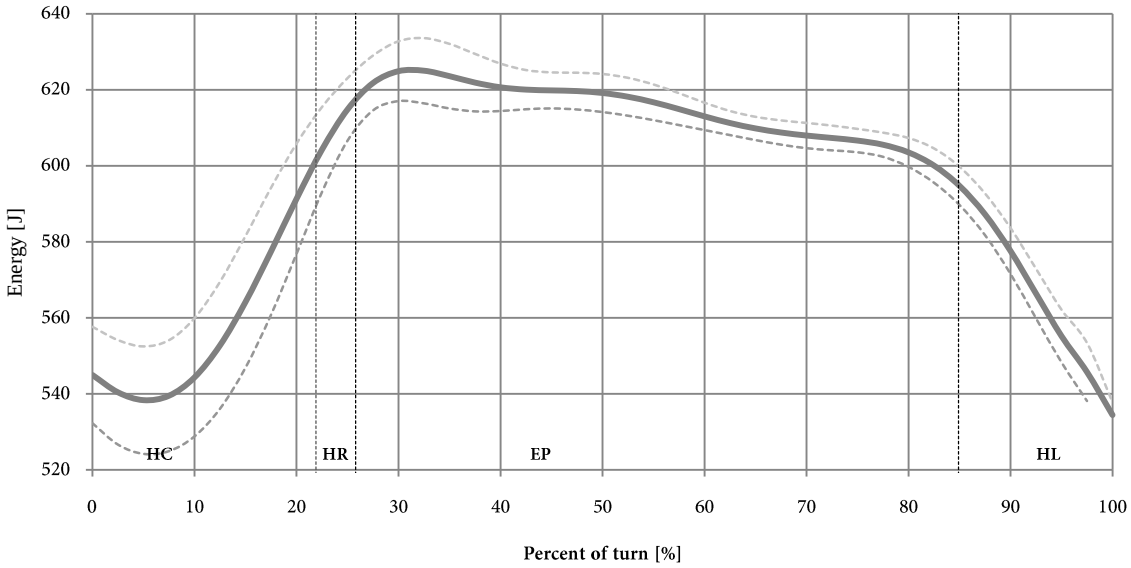

Figure 4-27. Potential Energy of the dancer during the turn

Figure 4-28 shows the total change in the mechanical energy of the dancer calculated by summing the amount of kinetic energy of the dancer and the change potential energy of the dancer. The kinetic energy and the change in potential energy of the dancer are also included to facilitate comparison. The maximum total energy of the dancer is 145 J attained 30% into the turn when the dancer is *en pointe*. At the end of the *en pointe* phase, the total energy of the dancer has been reduced to 121 J, 83% of the maximum amount of mechanical energy. When the dancer is no longer *en pointe*, her

total energy reduces drastically to 49 J, only 33% of the maximum total energy. It is important to note, in Figure 4-28, that a large amount of energy is lost when the heel lowers to make contact with the ground. During the period when the dancer is *en pointe*, the dancer's potential energy and kinetic energy vary inversely, so that the total energy of the dancer remains relatively constant.

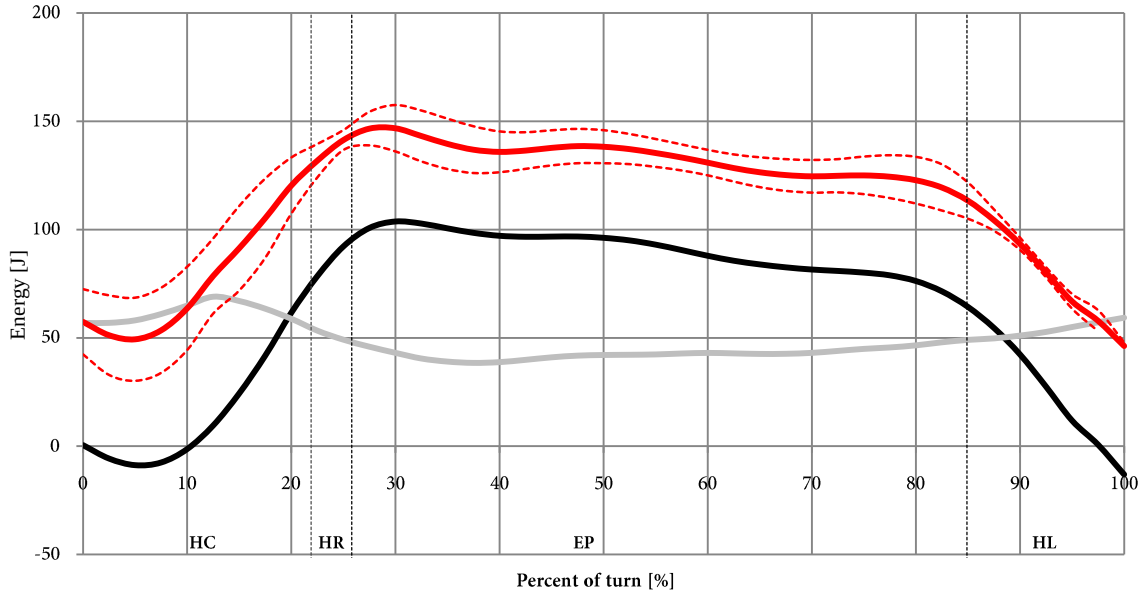

Figure 4-28. The total change in energy of the dancer is shown in red. Kinetic energy and change in potential energy are also shown for comparison

4.5 External moments

The moments shown in Figure 4-29, Figure 4-30, and Figure 4-31 are calculated from equation 29 as the time derivative of angular momentum. Figure 4-29 presents the moments acting about the longitudinal axis of the body. To cause a change in angular momentum, an external force or external moment must act on the dancer. The only part of the dancer's body which can produce an external force or moment is the support foot; therefore, muscles acting across the ankle joint must play a role in making the dancer turn. Figure 4-29 shows that the greatest magnitude of external moment acts on the body when the heel is being lowered or in contact with the ground. When the dancer is *en pointe*, the external moments acting on the dancer are lesser in magnitude.

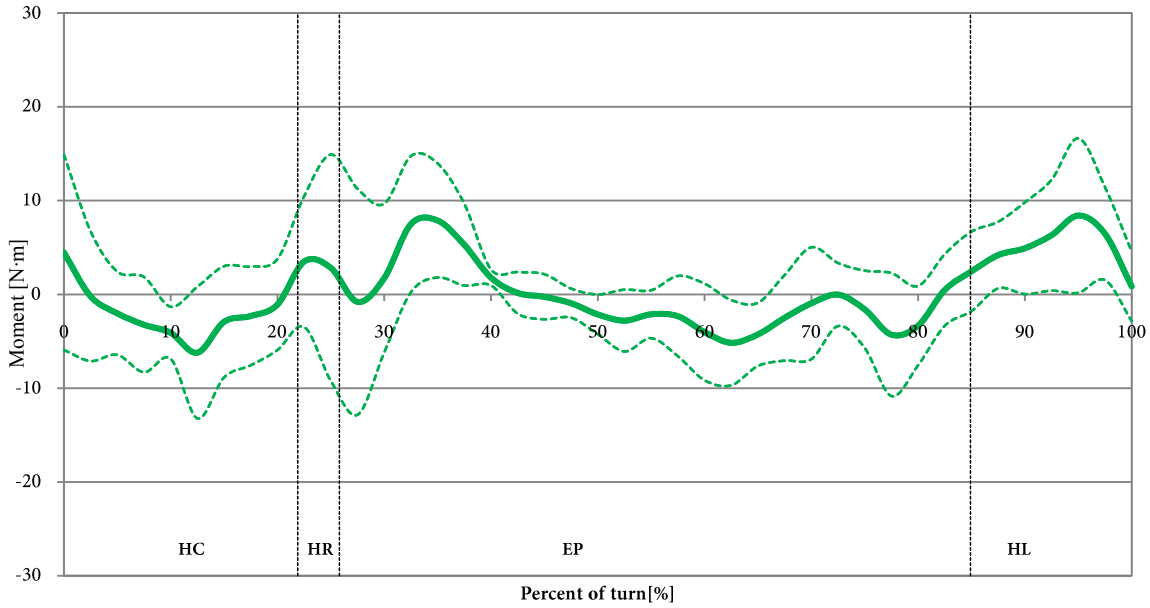

Figure 4-29. External moments about the longitudinal axis

Figure 4-30 demonstrates the time derivative of the angular momentum (Figure 4-18) about the mediolateral axis. Moments about the dancer's mediolateral axis are close to zero for the period from approximately 25% to 70% of the turn highlighted in yellow in Figure 4-30. This corresponds with the constant amount of angular momentum shown in Figure 4-18 for the same time period. When angular momentum is constant, there are no external moments acting on the dancer. Figure 4-31 shows the time derivative of the angular momentum about the anteroposterior axis (Figure 4-19). Angular momentum in Figure 4-19 is never constant, thus, correspondingly Figure 4-31 does not show any period during the turn where moments about the anteroposterior axis are zero.

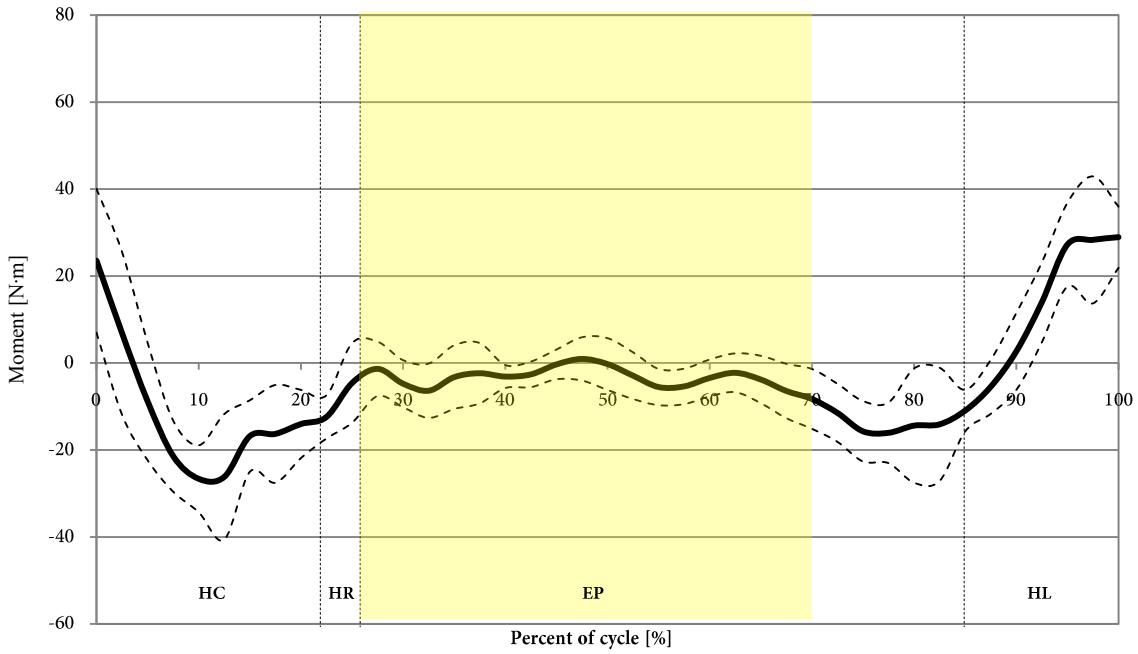

Figure 4-30. Moments about the dancer's mediolateral axis

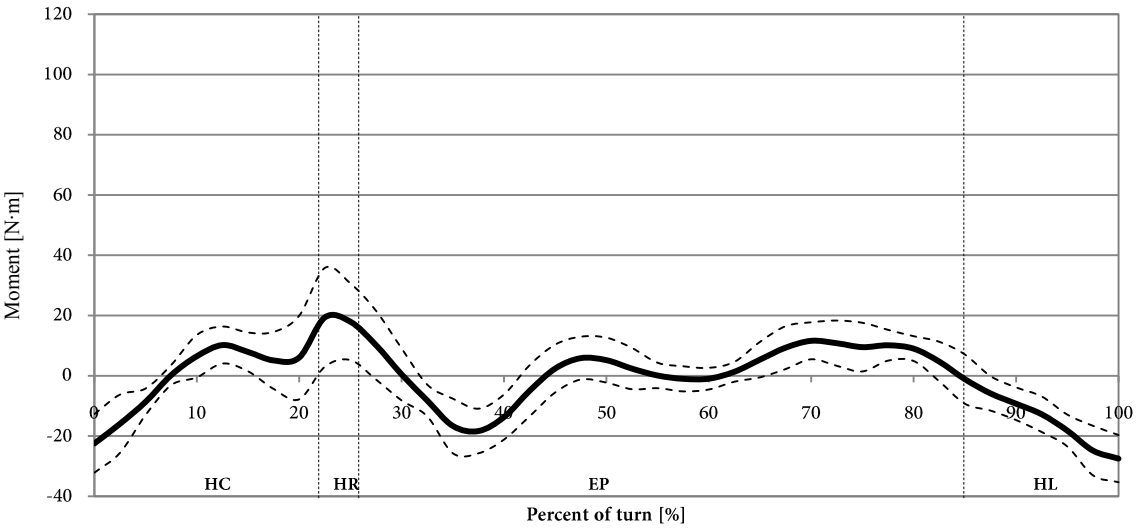

Figure 4-31. Moments about the dancer's anteroposterior axis

5 Discussion

5.1 Summary of the results

The results from chapter four presented several interesting findings. Section 4.1 described the motion of the dancer using polar plots. Figure 4-6 and Figure 4-8 showed that once the linear motion of the dancer is removed the remaining motion is referenced to the dancer's centre of mass, thus, the information obtained is similar to what the dancer perceives. Limb motion which is referenced to the centre of mass rather than an arbitrary laboratory coordinate system is summarized in a three-dimensional plot (see Figure 4-9). The dancer's form can be critiqued from Figure 4-9 making this presentation of limb position a useful tool in dance pedagogy. Section 4.1 also describes how other techniques of the *fouetté* such as hand position, and the direction of presentation can be quantified for use in improving a dancer's form.

In section 4.2, the angular momentum of the dancer was presented. The dancer's angular momentum about the longitudinal axis is examined to shed light on how the motion of the turn is produced. Figure 4-13 and Figure 4-14 demonstrated that the angular momentum and the angular impulse of the dancer result from the heel-contact phase. Angular momentum generated during heel contact must be carried through the remainder of the turn. During heel contact, angular momentum is not only produced about the vertical axis, but about the horizontal axes as well (see Figure 4-17). These angular momenta, shown in Figure 4-18 and Figure 4-19, will be transferred continuously during the turn to prevent excessive angular momentum from developing about one axis.

However, section 4.3 demonstrated that angular momentum is not only transferred about axes, but between segments as well. During the turn, the extended leg transfers angular momentum to the body (shown in Figure 4-24). This transfer of momentum is a crucial component in the technique of the turn. While the extended leg

is moving, central region of the body is able to stay relatively still and the angular momentum of the turn is maintained. This gives the appearance that the dancer pausing mid-turn when facing the audience. It is an aesthetic illusion that contributes greatly to the beauty of the turn.

Section 4.4 revealed that, similar to locomotion, the mechanical energy of the dancer is out-of-phase. Kinetic energy and potential energy (shown in Figure 4-28) are exchanged during the turn to maintain a relatively constant amount of total energy during the *en pointe* phase of the turn.

Moments calculated about the dancer's centre of mass were presented in section 4.5. External moments are directly related to changes in the angular momentum of the dancer.

5.2 Form and motion of the dancer

One revolution of *fouetté* is performed in approximately 1.05 s. All segments of the body accomplish one complete revolution, albeit at different angular velocities. The dancer moves the segments at different velocities to achieve the motions distinctive to a *fouetté*. During the *fouetté*, the dancer appears to be stationary for a moment in time. This is achieved because while segments such as the right arm, the left arm, and the right leg move continuously, the central trunk and head region do not. The transfer of angular momentum, angular impulse, and energy are important factors during the turn that allow this motion to be possible. The same is true for any complex three-dimensional motion achieved by the body.

It is inevitable that when performing a series of *fouettés*, the dancer is not always able to execute each technical step perfectly. To study a dancer's motion and to compare his or her technique to later trials, other dancers, or performances, the data must be independent of the dancer's surroundings—in this case—the laboratory. Figure 4-4 in the results section shows that the motion can be expressed independently of a laboratory coordinate system if the each data point is transformed to be expressed in terms of a

body-based coordinate system. Each graph now describes the motion about the dancer's centre of mass. Additional polar plots, included in Appendix D, fully define this dancer's form. Knowledge of the angular position and motion of the body segments allows the technical aspects of the *fouetté* to be analyzed.

There are several important motions in the execution of a *fouetté*. If the right leg is selected as the moving leg and the left leg is selected as the pivot point, the right leg must lead the body during the turn. At some point, however, the angular momentum of the leg must be transferred to the rest of the body. This transfer of momentum is clearly shown in Figure 4-24 and Figure 4-26. The trade-off in angular momentum that occurs is the transfer of momentum between the extended leg and the rest of the body.

During push off, angular momentum is not only produced in the desired direction (about the vertical axis of rotation), but in other directions as well (about horizontal axes) (see Figure 4-18 and Figure 4-19). To put the results obtained into context, one can make comparisons with angular momentum developed about a horizontal axis when a person trips. Pijnappels' study (2004) demonstrates that during a trip, a subject must rely on the support leg to counteract angular momentum of the body. Our study demonstrates that, likewise, the support leg must manage angular momentum developed about the horizontal axes, in addition to producing the angular momentum in the vertical axis to drive the turn. It is known that excessive angular momentum about an axis parallel to the ground (the mediolateral and anteroposterior axes) will result in a fall (Pijnappels, Bobbert, & van Dieen, 2004), or at the very least, the end of the series of turns since the dancer will be forced to step out. In Pijnappels et al.'s study (2004), it is demonstrated that a typical value for angular momentum generated after tripping is 11.4 $kg \cdot m^2/s$ (about the mediolateral axis). During the turns, our results of angular momentum about the axes parallel to the ground, a maximum of 5.01 $kg \cdot m^2/s$ about the mediolateral axis and 6.63 $kg \cdot m^2/s$ about the anteroposterior axis are well below the value measured in Pijnappels' study. Figure 5-1 demonstrates that the sum of the angular momentum about the axes

parallel to the ground remains roughly constant (between 4 and 5 kg·m²/s) when the heel is not in contact with the ground. When the heel is raised, there are negligible external moments acting on the dancer to change the angular momentum.

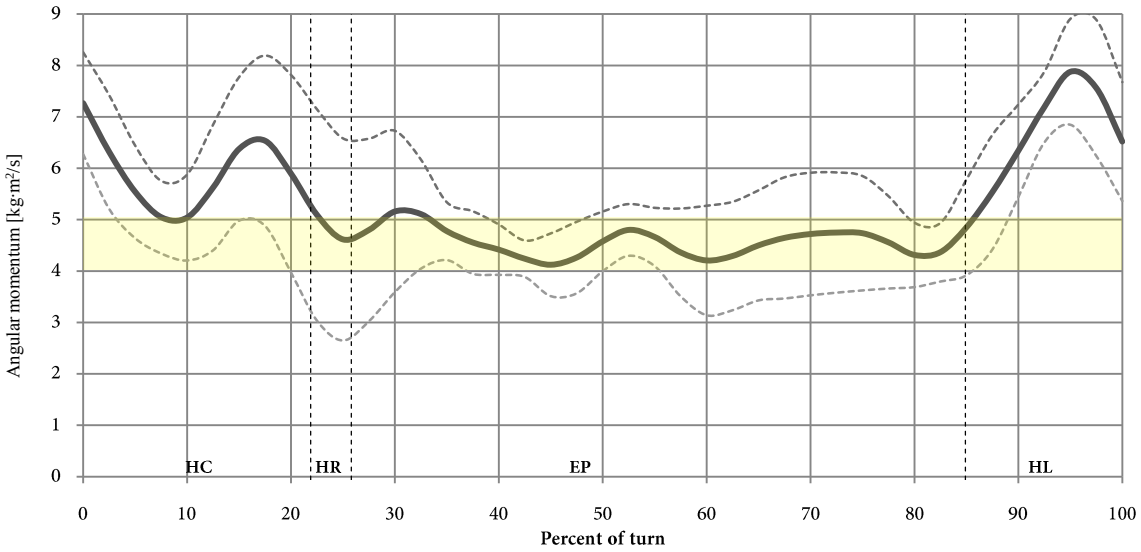

Figure 5-1. Angular momentum about axes parallel to the ground (Figure 4-16, repeated)

It makes sense that the angular momentum during the dancer's turns is less than the angular momentum calculated when a person trips, otherwise it would be expected that the dancer would be unable to continue and would be forced to step out of the turn. The regulation of angular momentum during the *fouetté*'s turn can be also contrasted to the trend in angular momentum during walking. During walking, when increasing angular momentum is generated by one foot, it is subsequently redirected by the heel strike of the opposite foot (Herr & Popovic, 2008). During the turns, the regulation of angular momentum is similar to the regulation of angular momentum during tripping because angular momentum is controlled largely by the support limb. Torque is generated at the ankle joint to counteract the external moments on the body.

The results demonstrated are a foundation for the investigation of balance control during a ballet turn, using the same tools of analysis used in gait analysis. The trends in angular momentum shown in Figure 4-18 and Figure 4-19 are indicative of the external moments acting on the body during the turn at the foot-ground interface. A deviation

from an upright body position creates a gravitational component in the torque about the ankle, therefore forces and torques (demonstrated by changes in angular momentum) acting on the body at proprioception sites such as the ankle (Cnyrim, Mergner, & Maurer, 2009) are of interest and important to quantify. The quantification of angular momentum during the turn identifies what level of angular momentum must be dealt with by the ankle joint of the support leg. Since deviations from the vertical direction result in a torque (which can be measured by changes in angular momentum) about the ankle joint, the body is further accelerated from a stable upright position.

5.3 Conservative and non-conservative energy transfer

The total energy of the dancer can be used to characterize the system as a conservative or non-conservative system. If the total energy is constant, then the system can be characterized as conservative. However, when non conservative forces, such as friction, do work, energy from the system is dissipated. The dancer and the ground are a non-conservative system because there is friction between the dancer's foot and the ground. Nonetheless, a conservative system such as an inverted pendulum can be used to model the dancer during the *fouetté*.

Kinetic energy and potential energy of the series of *fouettés* proves to be a very descriptive variable of the technical performance of a *fouetté*. The kinetic energy is an ideal descriptor of the dancer's angular rotation, while potential energy is an ideal descriptor of the dancer's vertical motion. Furthermore, since energy obeys well defined conservation laws, when appropriate assumptions are made, the transfer of energy during the turns can be compared to transfer in momentum.

The kinetic energy, potential energy, and total energy of the dancer shown in Figure 5-2 show that when the dancer is *en pointe* the total energy decreases only 17%. This decrease can be attributed to non-conservative forces such as friction and wind resistance doing work on the dancer. During the *en pointe* phase, the kinetic energy and potential energy are out of phase. An out-of-phase relationship demonstrates a

"pendulum-like" exchange as an energy-saving mechanism (Pfau, Witte, & Wilson, 2006).

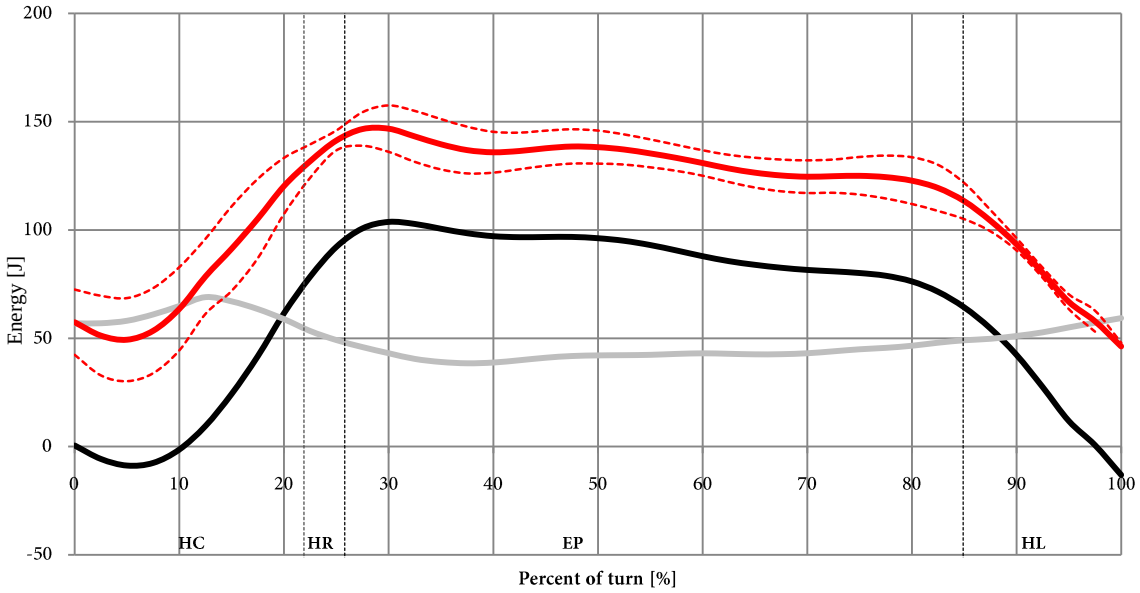

Figure 5-2. Total mechanical energy of the dancer is shown in red. Kinetic energy (grey) and potential energy (black) are also shown (Figure 4-28, repeated)

Human and animal locomotion are often modelled as mechanical models exhibiting energy saving mechanisms (Pfau, Witte, & Wilson, 2006). Out-of-phase potential and kinetic energy curves are often demonstrative of systems that show some degree of conservation of energy. Though there will always be a metabolic cost associated with human motion since negative work cannot replace energy used during motion (Kuo, 2007), nonetheless, conservative systems (those that can be described by springs, or inverted pendulums) represent physiological attempts to minimize energy costs during motion.

5.4 Modelling the pivot point

An instant of turn during the rotation can be examined where one leg acts as the support and there are no moments or forces acting about the vertical axis to alter the dancer's rotation. To simplify, the determination of forces and moments acting about the pivot point of the dancer, the mass of the dancer can be concentrated at the centre of mass to approximate an inverted pendulum. The reaction forces maintain contact

between the ground and the dancer but they do not contribute to any moments since the line of action runs directly through the pivot point. An inequality can be approximated where the sum restoring moment of the dancer and the leaning moment of the dancer is less than or equal to the torque, τ, produced by the muscle action of the support ankle.

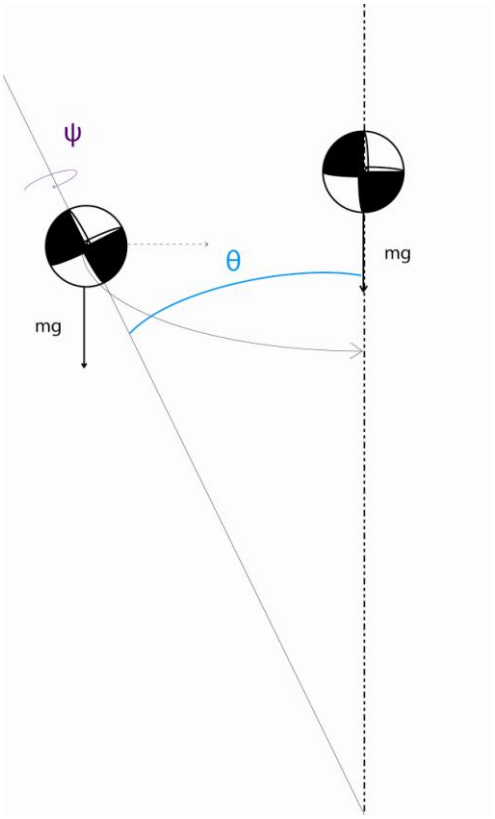

Figure 5-3. Diagram of the dancer as an inverted pendulum aproximation

33

$$\boldsymbol{M_{restoring} - M_{falling} \leq \tau_{ankle}}$$

Figure 5-4, Figure 5-5, and Figure 5-6 are based on the inequality (33). How well these moments balance will be dependent on how close to perpendicular the dancer is (demonstrated by Figure 4-22) at that given instant because the distance of the forces from the pivot ankle changes with the angle of body lean. Too much lean and the dancer will have a large moment causing her to fall, however some lean will allow a restoring force calculated from the centripetal force or her rotation about the vertical axis.

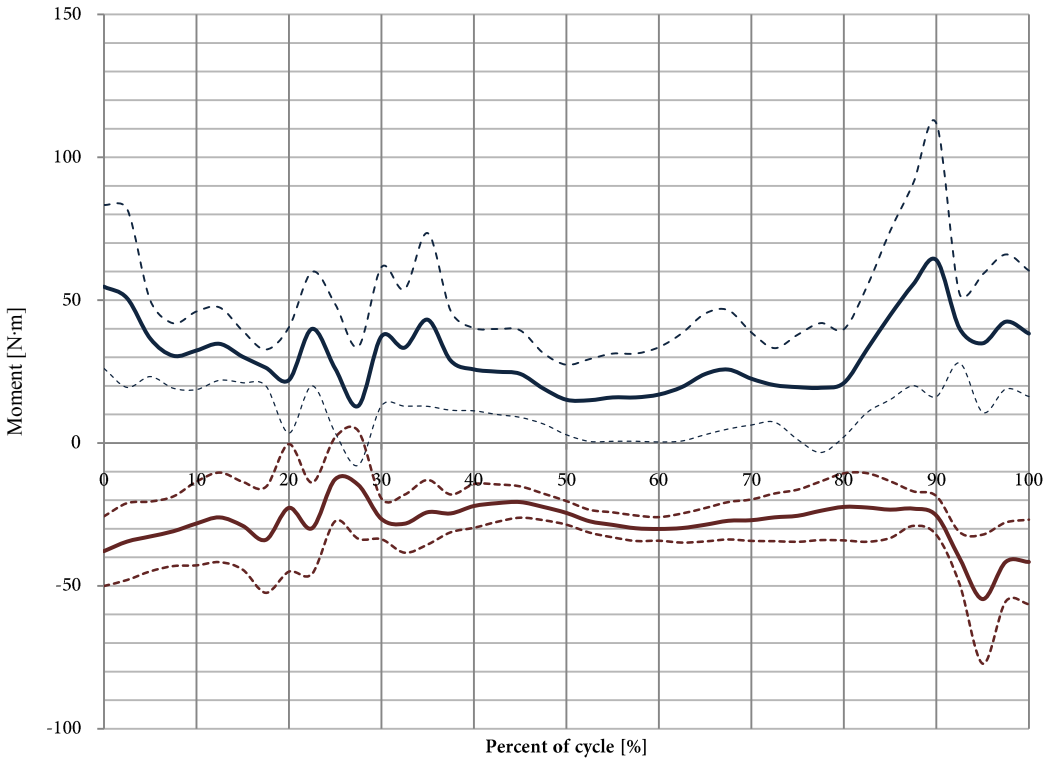

Figure 5-4. The moments at a distance from the pivot ankle to create a falling moment (below the axis), the centripetal force causing a restoring moment (above the axis)

Figure 5-5 displays the difference between the moments about the pivot ankle resulting from the forces in Figure 5-4. The difference in moments is a good representative of the external moment about the ankle that is felt by the dancer as she rotates and attempts to maintain her balance.

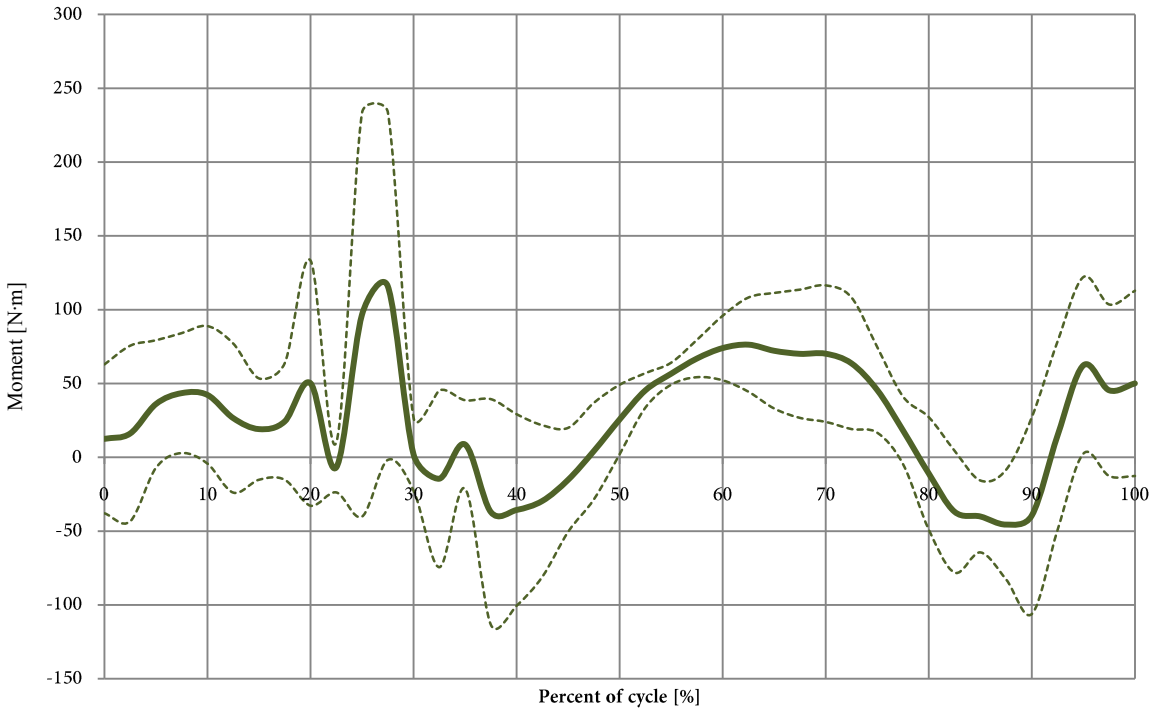

Figure 5-5. The difference in moment about the pivot ankle created by the forces in Figure 5-4, the ankle must create a torque to counteract this moment

34

$$Power = M\omega$$ (Beer & Johnston, 1999)

To counteract any external moments, the dancer's ankle must be capable of producing a torque at the correct rate. Figure 5-6 shows how much power would be required from the dancer's ankle to produce the moments in Figure 5-5. Schmitt et al conducted a study of male and female professional dancers and the joint power the ankle is capable of producing. Joint power maximums are dependent on the speed at which the maximum torque is generated (Schmitt, Kuni, & Sabo, 2005) therefore a single maximum value cannot be assumed. Rather a maximum range can be estimated by taking the joint powers produced at a range of different speeds. Figure 5-6 includes two sets of broken lines to indicate the range of maximum power a female dancer's ankle is capable of producing. In one instant, at approximately 35% of the cycle's completion the power required from the joint is in its maximum range.

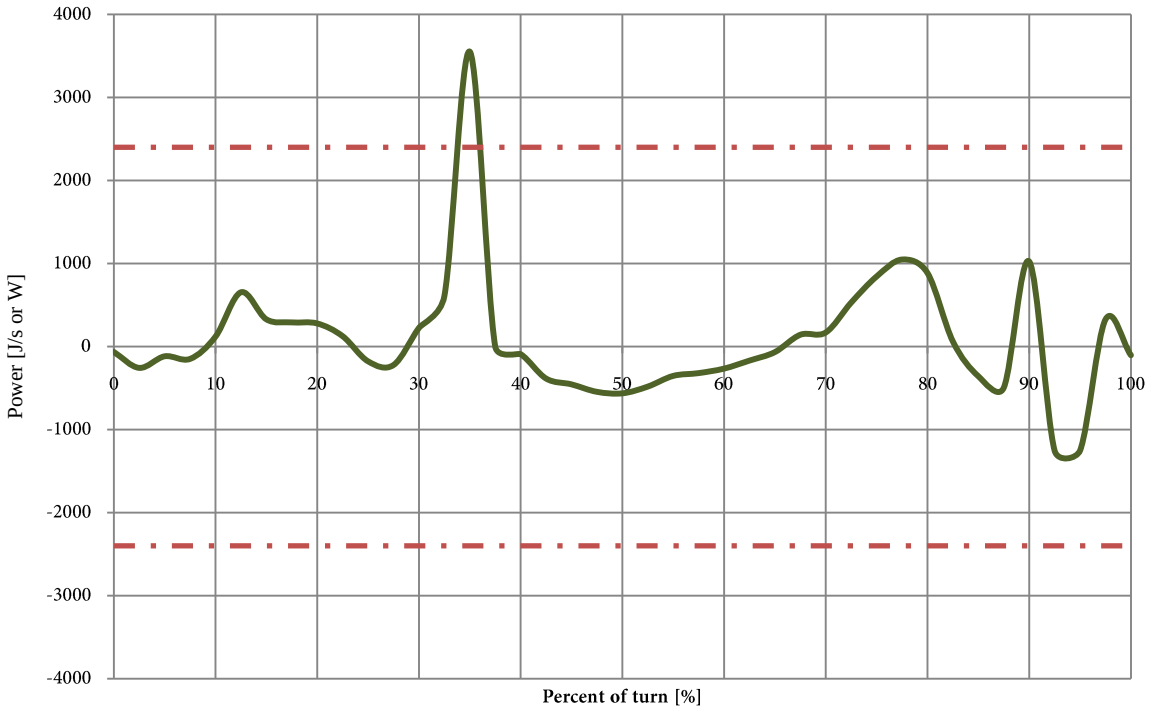

Figure 5-6. Power required from the ankle estimated from the difference in moments acting on the pivot ankle. Above and below the red dashed lines represents maximum range of joint power that the ankle is capable of producing (estimated from **(Schmitt, Kuni, & Sabo, 2005)**)

5.5 Concluding Summary

The results of this study confirm the main premises of the hypothesis, in particular, our results demonstrate that:

- Characteristics of the turn are evident in angular momentum curves (see Figure 4-13) —angular momentum is generated about all three axes when the heel is lowered—and in angular impulse curves (see Figure 4-14).
- During the remaining portion of the turn, momentum is transferred between segments and between axes. No additional external forces or moments act on the dancer to further the motion of the turn though friction will act against the motion of the turn. Similar to locomotion, angular momentum is a controlled by the body during the turn.

Our validation demonstrated that though angular momentum is being calculated reasonably by our MATLAB programs, it is difficult to obtain results showing a constant

angular momentum where there should theoretically be a constant angular momentum because non-conservative forces, such as wind resistance and friction, as well as modelling errors are not negligible. These are characteristics, however, that are present to some degree in every study.

In contrast to walking, during which angular momentum is ultimately used for linear locomotion, in ballet, when performing a *fouetté* or a *tour à la seconde,* angular momentum is used to accomplish a purely rotational motion. The purpose of this study was to characterize the mechanisms used by a dancer to generate and control his or her angular momentum and to quantify the transfer of angular momentum throughout a turn. Our results demonstrate that the period during which the heel makes contact with the ground, the initial portion of the turn, is an important domain of analysis in considering the dancer's ability to develop angular momentum. In addition, significant transfers of angular momentum occur between the extended leg and the trunk as a result of the technique in which the extended leg leads the turn. While the principal motion of the turn occurs about the vertical axis, significant changes in momentum (and thus, external moments) occur in the axes parallel to the ground. Yet, the balance of the dancer is maintained by continuously transferring momentum between the mediolateral axis and the anteroposterior axis. If changes in the angular momentum about these horizontal axes are not dealt with appropriately, external moments create torque about the ankle joint and can cause the dancer to lose balance.

These external moments acting on the body during a turn can be calculated from changes in angular momentum. In addition to these desired external moments, external moments also act on the dancer in a manner which destabilizes his or her balance. Moments can tip the dancer if an opposing torque is not generated by a joint of the support limb. If sufficient torque is generated, the dancer will be able to maintain an upright position.

5.6 Future Directions

While the information gathered herein sheds light on the most important aspects of performing the *fouetté*, thereby specifying variables of interest (angular impulse, angular momentum, moments at the support), simulation of these parameters is needed to quantify specific parameter contribution to the performance of a technically correct *fouetté*.

Models that approximate a human body as an inverted pendulum already exist. The MATLAB programs created during this study can be used as inputs in future balance control model to further examine angular momentum and moment during human rotational motion.

References

Allum, J. H., & Carpenter, M. G. (2005). A speedy solution for balance and gait analysis: angular velocity measured at the centre of body mass. *Current Opinion in Neurology*, 15-21.

Almosnino, S., Kajaks, T., & Costigan, P. (2009). The free moment in walking and its change with foot rotation angle. *Sport Medecine, Arthroscopy, Rehabilitation, Therapy, & Technology*.

Bahamonde, R. E. (2000). Changes in angular momentum during the tennis serve. *Journal of Sports Sciences*, 579-592.

Batson, G. (2009). Update on Proprioception Considerations for Dance Education. *Journal of Dance Medicine & Science*, 35-41.

Beer, F., & Johnston, E. R. (1999). *Vector Mechanics for Engineers Dynamics 3rd SI metric edition.* Toronto: McGraw Hill Ryerson.

Bennett, B. C., Russell, S. D., Sheth, P., & Abel, M. F. (2010). Angular momentum of walking at different speeds. *Human Movement Science*, 114-124.

Bruijn, S., Meijer, O., van Dieen, J., Kingma, I., & Lamoth, C. (2008). Coordination of leg swing, thorax rotations,and pelvis rotations during gait: The organisation of total body angular momentum. *Gait & Posture*, 455-462.

Campbell, N. (2002). *Biology 6th edition.* San Francisco: Benjamin Cummings.

Cnyrim, C., Mergner, T., & Maurer, C. (2009). Potential roles of force cues in human stance control. *Experimental Brain Research*, n/a.

Daddaoua, N., Dicke, P., & Thier, P. (2008). The subjective visual vertical in a nonhuman primate. *Journal of Vision*, 1-8.

Fourre, B., Isableu, B., Bernardin, D., Gueguen, M., Giraudet, G., Vuillerme, N., et al. (2009). The role of body center of mass on haptic subjective vertical. *Neuroscience Letters*, n/a.

Gray, H. (1918). *Anatomy of the human body.* Philadelphia: Lea & Febiger.

Herr, H., & Popovic, M. (2008). Angular momentum in human walking. *The Journal of Experimental Biology*, 467-481.

Imura, A., Iino, Y., & Kojima, T. (2008). Biomechanics of the continuity and speed change during one revolution of the fouette turn. *Human Movement Science*, 903-913.

Kuo, A. D. (2007). The six determinants of gait and the inverted pendulum analogy: A dynamic walking perspective. *Human Movement Science*, 617-656.

Laws, K. (1998). Momentum Transfer in Dance Movement. *Medical Problems of Performing Artist* , 136-145.

Laws, K. (2002). *Physics and the Art of Dance.* Oxford Univerity Press.

Maurer, C., Mergner, T., & Peterka, R. J. (2006). Multisensory control of human upright stance. *Experimental Brain Research*, 231-250.

Mergner, T., & Rosemeier, T. (1998). Interaction of vestibular, somatosensory and visual signals for postural control and motion perception under terrestrial and microgravity conditions--a conceptual model. *Brain Research Reviews*, 118-135.

Mergner, T., Schweigart, G., Maurer, C., & Blumle, A. (2005). Human postural responses to motion of real and virtual visual environments under different support base conditions. *Experimental Brain Research*, 535-556.

Merriam, J. (1978). *Engineering Mechanics: Statics and Dynamics.* New York: Wiley & Sons.

Minetti, A. (1994). A model for the estimation of visceral mass displacement. *Journal of Biomechanics*, 97-101.

O'Brien, T., Reeves, N. D., Baltzopoulos, V., Jones, D., & Maganaris, C. N. (2009). Strong relationships exist between muscle volume, joint power, and whole-body external mechanical power in adults and children. *Physiology in Press*, n/a.

Pedrocchi, A., Baroni, G., Bedotti, A., Masson, J., & Ferrigno, G. (2005). Inverse dynamic investigation of voluntary leg lateral movements in weightlessness: a new microgravity-specific strategy. *The Journal of Biomechanics*, 769-777.

Pfau, T., Witte, T. H., & Wilson, A. M. (2006). Centre of mass movement and mechancal energy fluctuation durig gallop locomotion in the thoroughbred racehorse. *The Journal of Experimental Biology*, 3742-3757.

Pijnappels, M., Bobbert, M., & van Dieen, J. (2004). Contribution of the support limb in control of angular momentum. *Journal of Biomechanics*, 1811-1818.

Ramey, M. (1973). Significance of angular momentum. *The Research Quarterly*, 488-497.

Robertson, G. E. (2009). *Vicon Workstation Quick Refernce Guide.* Ottawa: School of Human Kinetics, University of Ottawa.

Schmitt, H., Kuni, B., & Sabo, D. (2005). Influence of professional dance training on peak torque and proprioception at the ankle. *Clinical Journal of Sports Medecine*, 331-339.

Shan, G., & Bohn, C. (2003). Anthropometrical data and coefficients of regression related to gender and race. *Applied Ergonomics, 34*, 327-37.

Tong, K., & Granat, M. (1999). A practical gait analysis system using gyroscopes. *Medical Engineering & Physics*, 87-94.

Wyon, M., Deighan, M. A., Nevill, A. M., Doherty, M., Morrison, S. L., Allen, N., et al. (2007). The cardiorespiratory, anthropometric, and performance characteristics of an international/national touring ballet company. *Journal of Strength an Conditioning Research,* 389-393.

Yeadon, M. R. (1990). The simulation of aerial movement-iii. The determination of the angular momentum of the human body. *Journal of Biomechanics*, 75-83.

Appendix A

MATLAB PROGRAMS

angularmomentum.m

```
clear all
close all

%subject specific data

nn=1568; %number of frames
n=nn-9;
time = [0:0.005:n*0.005]; %[seconds]
m = fiona(1); %mass [kg]
w=fiona(3);%limb weighting
inertia=fiona(4);%moments of inertia for each limb


g = 9.81; %gravitational acceleration [m/s^2]
bcgp=littledog(8); %centre of mass of the body position [m] output of --
eq.13--
og=littledog(1); %angular velocity omega [radians/s]
ogflip=og';
al=littledog(2); %angular acceleration alpha
cgpn=littledog(3); %position centre of mass (segments) [m] output of --
eq. 3--
CGVn=littledog(4); %velocity of the centre of mass (segments) [m] output
of --eq. 18--
CGAn=littledog(5); %acceleration of the centre of mass (segments) [m]
output of --eq. 19--


c=1;
k=1;
T=0;
vv=0;
icctotal=0;

DEP=littledog(6); %distal end position [m]
PEP=littledog(7); %proximal end position [m]
limb=DEP-PEP; %vector representing the limb

shoulderreference=PEP(:,19:21)-PEP(:,1:3); %right-left
hipreference=PEP(:,43:45)-PEP(:,16:18);%right-left
vref=[shoulderreference hipreference];

for c=1:15

    xbar=cgpn(:,k)-(PEP(:,k)-bcgp(:,1)); %(PEP(:,k)-bcgp(:,1)) --eq.23--
not performed by littledog
    ybar=cgpn(:,k+1)-(PEP(:,k+1)-bcgp(:,2));
    zbar=cgpn(:,k+2)-(PEP(:,k+2)-bcgp(:,3));

    vx=w(c)*CGVn(:,k);
    vy=w(c)*CGVn(:,k+1);
    vz=w(c)*CGVn(:,k+2);

    vtot=[vx vy vz];
    vv=vv+vtot;%linear momentum
```

```
    %lambdax,y,z are the direction cosines of the limb
    %reminder--((column),(row),(page))
    lambdax(1,1,:)=limb(:,k)./mag(limb(:,k:k+2)); %--eq.38--
    lambday(1,1,:)=limb(:,k+1)./mag(limb(:,k:k+2)); %--eq.39--
    lambdaz(1,1,:)=limb(:,k+2)./mag(limb(:,k:k+2)); %--eq.40--

    Im = inertia;

    Ic=Im(c,:); %--eq.33--

    Ix(1,1,:)=Ic(:,1) + m*w(c).*(ybar.^2+zbar.^2); % (ybar.^2+zbar.^2)
%--eq.35-7--
    Iy(1,1,:)=Ic(:,2) + m*w(c).*(xbar.^2+zbar.^2);
    Iz(1,1,:)=Ic(:,3) + m*w(c).*(ybar.^2+xbar.^2);

    Ixy(1,1,:)=m*w(c).*xbar.*ybar;
    Iyz(1,1,:)=m*w(c).*ybar.*zbar;
    Ixz(1,1,:)=m*w(c).*xbar.*zbar;

    %--eq.41--
    Is=[Ix(1,1,:).*lambdax(1,1,:).^2 -
Ixy(1,1,:).*lambdax(1,1,:).*lambday(1,1,:) -
Ixz(1,1,:).*lambdax(1,1,:).*lambdaz(1,1,:);
                    -Ixy(1,1,:).*lambdax(1,1,:).*lambday(1,1,:)
Iy(1,1,:).*lambday(1,1,:).^2 -
Iyz(1,1,:).*lambday(1,1,:).*lambdaz(1,1,:);
                    -Ixz(1,1,:).*lambdax(1,1,:).*lambdaz(1,1,:) -
Iyz(1,1,:).*lambday(1,1,:).*lambdaz(1,1,:)
Iz(1,1,:).*lambdaz(1,1,:).^2;];


invI=Is(1,1,:)+Is(2,2,:)+Is(3,3,:);

invII=(Is(2,3,:).*Is(3,2,:)-Is(2,2,:).*Is(3,3,:))+(Is(1,3,:).*Is(3,1,:)-
Is(1,1,:).*Is(3,3,:))+(Is(1,2,:).*Is(2,1,:)-Is(1,1,:).*Is(2,2,:));

invIII=0; %note:initializes determinant calculations in for loop below

    for q=1:n+10
        invIII(q)=det(Is(3,3,q));
        q=q+1;
    end

Icc = [reshape(invI,[n+10 1]) reshape(invII,[n+10 1])
reshape(invIII,[n+10 1])];
icctotal=Icc+icctotal;

%--eq.43--
Iss =[Icc(1) 0 0;
      0 Icc(2) 0;
      0 0 Icc(3)];

ogs = og(k:k+2,:);
als = al(k:k+2,:);
```

```
Ts1 = CGVn(:,k:k+2).^2;
Ts2 = (Iss*(ogs.^2))';
Ts = 0.5*w(c)*m*sum(Ts1,2) + 0.5*sum(Ts2,2);%segment kinetic energy [J]

q=1;
for q = 1:n+10
    Hg(:,q) = Iss*ogs(:,q); %--eq. 27--
    hdot(:,q) = Iss*als(:,q);
    q=q+1;
end

Hgmatrix(:,k:k+2)= Hg';
hdotmatrix(:,k:k+2)=hdot';
T=T+Ts;%kinetic energy [J]

c=c+1;
k=k+3;
end

Hb=0;
Hd=0;
vel=0;

for v=1:3:43
   H = cross(cgpn(1:n,v:v+2),m*w((v+2)/3)*CGVn(1:n,v:v+2)) +
Hgmatrix(1:n,v:v+2); %--eq. 28--
   h1(:,v:v+2)=cross(cgpn(1:n,v:v+2),m*w((v+2)/3)*CGVn(1:n,v:v+2));
   h2(:,v:v+2)=Hgmatrix(1:n,v:v+2);
   h(:,v:v+2)=cross(cgpn(1:n,v:v+2),m*w((v+2)/3)*CGVn(1:n,v:v+2)) +
Hgmatrix(1:n,v:v+2);

   hd1(:,v:v+2)=hdotmatrix(1:n,v:v+2) +
cross(ogflip(1:n,v:v+2),h(:,v:v+2));
   Hd=Hd+hd1(:,v:v+2);

   Hb=Hb+H; %--eq. 29--
end

%Write the data to excel files for graphing
xlswrite('impulsedata.xlsx',Hb,2)%outputs angular momentum of the body
xlswrite('impulsedata.xlsx',T,3)%outputs kinetic energy
xlswrite('impulsedata.xlsx',vv,7)%outputs linear momentum of centre of
mass
xlswrite('impulsedata.xlsx',vref,9)%outputs a vector parallel to the
shoulder/hips
xlswrite('Icomp.xlsx',Hb,'D1:F1560')%outputs angular momentum of the
body
xlswrite('I.xlsx',Hb,'D1:F1560')%outputs angular momentum of the body
xlswrite('I.xlsx',icctotal,'A1:C1560')%outputs inertia tensor of the
body
xlswrite('segmenttotalangularmomentum.xlsx',h,'B1:AT1560')%outputs
angular momentum of each segment
xlswrite('segmentmomentofmomentum.xlsx',h1,'B1:AT1560')%outputs the r x
mv component of angular momentum for each segment
xlswrite('segmentIw.xlsx',h2,'B1:AT1560')%outputs the I omega component
of angular momentum for each segment
xlswrite('angularacc.xlsx',Hd,'B1:D1560')%outputs the time derivative of
angular momentum, i.e., sum of moments
```

```
xlswrite('angularacc.xlsx',time')%output the time vector
```

balancemoments.m

```
clear all
close all

% To determine equilibrating forces on body centre of mass (model)
% insight into balance?

nn = 1569;%number of frames
time = [0:0.005:0.005*(nn-1)]; %[seconds]
m = fiona(1); %mass [kg]
g = 9.81; %gravitational acceleration[m/s^2]

bcg=littledog(8); %coordinates of the body's centre of mass
cop=bigdog(3);
gr=cop(:,1:3);

vertical=[zeros(1569,2) ones(1569,1)];
for n=1:nn;
    if gr(n,1:3)==[0 0 0]
        nothing=1;
    else
        long(n,1:3)=bcg(n,1:3)-gr(n,1:3); %longitudinal axis/body lean
        lgaxis(n,1:3)=long(n,1:3)./[mag(long(n,1:3)) mag(long(n,1:3))
mag(long(n,1:3))]; %longitudinal axis unit vector
        maxdev(n,1:2)=bcg(n,1:2)-gr(n,1:2);
        maxdevscalar(n,1)=sqrt(maxdev(n,1).^2 + maxdev(n,2).^2);
        gamma(n,1)=asin(maxdevscalar(n,1)./mag(long(n,1:3)));
        gammadegrees(n,1)=asind(maxdevscalar(n,1)./mag(long(n,1:3)));
    end
end

anklepivot=cross(long,vertical,2);
pivotaxis=anklepivot./[mag(anklepivot) mag(anklepivot) mag(anklepivot)];
proxtorque=bigdog(2);
ankletorque=proxtorque(:,7:9);
pivottorque=dot(ankletorque,pivotaxis,2);

alpha=pug(1);%pug is the same program as littledog.m
omega=pug(2);
bodyvel=pug(4);
bodyacc=pug(5);

cfi=m*(bodyvel(:,1).^2 + bodyvel(:,2).^2)./maxdevscalar;%centripetal
force
fo=m*g;


fallingmoment=-fo.*maxdevscalar;
restoringmoment=cfi.*bcg(:,3);


plot(time,fallingmoment,time,restoringmoment)
legend('falling moment','restoring moment')

xlswrite('balancemoments.xlsx',time','A1:A1569')
```

```
xlswrite('balancemoments.xlsx',fallingmoment,'B1:B1569')
xlswrite('balancemoments.xlsx',restoringmoment,'C1:C1569')
```

bodyplotter.m

```
clear all
close all

%this file is specific to fiona's data
time = [0:0.005:7.8]; %[seconds]
CGPn=littledog(3); %[m]

%first revolution
hold on
plot3(CGPn(704:900,1),CGPn(704:900,2),CGPn(704:900,3),'r')
plot3(CGPn(704:900,4),CGPn(704:900,5),CGPn(704:900,6),'r')
plot3(CGPn(704:900,10),CGPn(704:900,11),CGPn(704:900,12),'r')

plot3(CGPn(704:900,7),CGPn(704:900,8),CGPn(704:900,9),'g')
plot3(CGPn(704:900,13),CGPn(704:900,14),CGPn(704:900,15),'g')
plot3(CGPn(704:900,16),CGPn(704:900,17),CGPn(704:900,18),'g')

plot3(CGPn(704:900,19),CGPn(704:900,20),CGPn(704:900,21),'b')
plot3(CGPn(704:900,22),CGPn(704:900,23),CGPn(704:900,24),'b')
plot3(CGPn(704:900,28),CGPn(704:900,29),CGPn(704:900,30),'b')

plot3(CGPn(704:900,25),CGPn(704:900,26),CGPn(704:900,27),'c')
plot3(CGPn(704:900,37),CGPn(704:900,38),CGPn(704:900,39),'c')
plot3(CGPn(704:900,43),CGPn(704:900,44),CGPn(704:900,45),'c')

plot3(CGPn(704:900,31),CGPn(704:900,32),CGPn(704:900,33),'k')
plot3(CGPn(704:900,34),CGPn(704:900,35),CGPn(704:900,36),'k')
plot3(CGPn(704:900,40),CGPn(704:900,41),CGPn(704:900,42),'k')
figure

%second revolution
hold on
plot3(CGPn(900:1099,1),CGPn(900:1099,2),CGPn(900:1099,3),'r')
plot3(CGPn(900:1099,4),CGPn(900:1099,5),CGPn(900:1099,6),'r')
plot3(CGPn(900:1099,10),CGPn(900:1099,11),CGPn(900:1099,12),'r')

plot3(CGPn(900:1099,7),CGPn(900:1099,8),CGPn(900:1099,9),'g')
plot3(CGPn(900:1099,13),CGPn(900:1099,14),CGPn(900:1099,15),'g')
plot3(CGPn(900:1099,16),CGPn(900:1099,17),CGPn(900:1099,18),'g')

plot3(CGPn(900:1099,19),CGPn(900:1099,20),CGPn(900:1099,21),'b')
plot3(CGPn(900:1099,22),CGPn(900:1099,23),CGPn(900:1099,24),'b')
plot3(CGPn(900:1099,28),CGPn(900:1099,29),CGPn(900:1099,30),'b')

plot3(CGPn(900:1099,25),CGPn(900:1099,26),CGPn(900:1099,27),'c')
plot3(CGPn(900:1099,37),CGPn(900:1099,38),CGPn(900:1099,39),'c')
plot3(CGPn(900:1099,43),CGPn(900:1099,44),CGPn(900:1099,45),'c')

plot3(CGPn(900:1099,31),CGPn(900:1099,32),CGPn(900:1099,33),'k')
plot3(CGPn(900:1099,34),CGPn(900:1099,35),CGPn(900:1099,36),'k')
plot3(CGPn(900:1099,40),CGPn(900:1099,41),CGPn(900:1099,42),'k')
figure


%third revolution
```

```
hold on
plot3(CGPn(1099:1304,1),CGPn(1099:1304,2),CGPn(1099:1304,3),'r')
plot3(CGPn(1099:1304,4),CGPn(1099:1304,5),CGPn(1099:1304,6),'r')
plot3(CGPn(1099:1304,10),CGPn(1099:1304,11),CGPn(1099:1304,12),'r')

plot3(CGPn(1099:1304,7),CGPn(1099:1304,8),CGPn(1099:1304,9),'g')
plot3(CGPn(1099:1304,13),CGPn(1099:1304,14),CGPn(1099:1304,15),'g')
plot3(CGPn(1099:1304,16),CGPn(1099:1304,17),CGPn(1099:1304,18),'g')

plot3(CGPn(1099:1304,19),CGPn(1099:1304,20),CGPn(1099:1304,21),'b')
plot3(CGPn(1099:1304,22),CGPn(1099:1304,23),CGPn(1099:1304,24),'b')
plot3(CGPn(1099:1304,28),CGPn(1099:1304,29),CGPn(1099:1304,30),'b')

plot3(CGPn(1099:1304,25),CGPn(1099:1304,26),CGPn(1099:1304,27),'c')
plot3(CGPn(1099:1304,37),CGPn(1099:1304,38),CGPn(1099:1304,39),'c')
plot3(CGPn(1099:1304,43),CGPn(1099:1304,44),CGPn(1099:1304,45),'c')

plot3(CGPn(1099:1304,31),CGPn(1099:1304,32),CGPn(1099:1304,33),'k')
plot3(CGPn(1099:1304,34),CGPn(1099:1304,35),CGPn(1099:1304,36),'k')
plot3(CGPn(1099:1304,40),CGPn(1099:1304,41),CGPn(1099:1304,42),'k')
figure

%fourth revolution
hold on
plot3(CGPn(1304:1529,1),CGPn(1304:1529,2),CGPn(1304:1529,3),'r')
plot3(CGPn(1304:1529,4),CGPn(1304:1529,5),CGPn(1304:1529,6),'r')
plot3(CGPn(1304:1529,10),CGPn(1304:1529,11),CGPn(1304:1529,12),'r')

plot3(CGPn(1304:1529,7),CGPn(1304:1529,8),CGPn(1304:1529,9),'g')
plot3(CGPn(1304:1529,13),CGPn(1304:1529,14),CGPn(1304:1529,15),'g')
plot3(CGPn(1304:1529,16),CGPn(1304:1529,17),CGPn(1304:1529,18),'g')

plot3(CGPn(1304:1529,19),CGPn(1304:1529,20),CGPn(1304:1529,21),'b')
plot3(CGPn(1304:1529,22),CGPn(1304:1529,23),CGPn(1304:1529,24),'b')
plot3(CGPn(1304:1529,28),CGPn(1304:1529,29),CGPn(1304:1529,30),'b')

plot3(CGPn(1304:1529,25),CGPn(1304:1529,26),CGPn(1304:1529,27),'c')
plot3(CGPn(1304:1529,37),CGPn(1304:1529,38),CGPn(1304:1529,39),'c')
plot3(CGPn(1304:1529,43),CGPn(1304:1529,44),CGPn(1304:1529,45),'c')

plot3(CGPn(1304:1529,31),CGPn(1304:1529,32),CGPn(1304:1529,33),'k')
plot3(CGPn(1304:1529,34),CGPn(1304:1529,35),CGPn(1304:1529,36),'k')
plot3(CGPn(1304:1529,40),CGPn(1304:1529,41),CGPn(1304:1529,42),'k')
```

bigdog.m

```
function [output_a] = bigdog(stick)
%bigdog...This function retrieves the data in a useful form
%  pulls original data stored from exported visual 3d program,

%  force, torque, and pressure

load datalab.txt
data = datalab;


LAR_PEF = [data(:,22) data(:,23) data(:,24)];
LFA_PEF = [data(:,56) data(:,57) data(:,58)];
LFT_PEF = [data(:,99) data(:,100) data(:,101)];
LHA_PEF = [data(:,133) data(:,134) data(:,135)];
LSK_PEF = [data(:,167) data(:,168) data(:,169)];
LTH_PEF = [data(:,182) data(:,183) data(:,184)];
RAR_PEF = [data(:,235) data(:,236) data(:,237)];
RFA_PEF = [data(:,269) data(:,270) data(:,271)];
RFT_PEF = [data(:,312) data(:,313) data(:,314)];
RHA_PEF = [data(:,346) data(:,347) data(:,348)];
RHE_PEF = [data(:,380) data(:,381) data(:,382)];
RPV_PEF = [data(:,414) data(:,415) data(:,416)];
RSK_PEF = [data(:,448) data(:,449) data(:,450)];
RTA_PEF = [data(:,482) data(:,483) data(:,484)];
RTH_PEF= [data(:,516) data(:,517) data(:,518)];

PEFmatrix=[LAR_PEF LFA_PEF LFT_PEF LHA_PEF LSK_PEF LTH_PEF RAR_PEF
RFA_PEF RFT_PEF RHA_PEF RHE_PEF RPV_PEF RSK_PEF RTA_PEF RTH_PEF];

LAR_PET = [data(:,28) data(:,29) data(:,30)];
LFA_PET = [data(:,62) data(:,63) data(:,64)];
LFT_PET = [data(:,105) data(:,106) data(:,107)];
LHA_PET = [data(:,139) data(:,140) data(:,141)];
LSK_PET = [data(:,173) data(:,174) data(:,175)];
LTH_PET = [data(:,188) data(:,189) data(:,190)];
RAR_PET = [data(:,241) data(:,242) data(:,243)];
RFA_PET = [data(:,275) data(:,276) data(:,277)];
RFT_PET = [data(:,318) data(:,319) data(:,320)];
RHA_PET = [data(:,352) data(:,353) data(:,354)];
RHE_PET = [data(:,386) data(:,387) data(:,388)];
RPV_PET = [data(:,420) data(:,421) data(:,422)];
RSK_PET = [data(:,454) data(:,455) data(:,456)];
RTA_PET = [data(:,488) data(:,489) data(:,490)];
RTH_PET = [data(:,522) data(:,523) data(:,524)];

PETmatrix=[LAR_PET LFA_PET LFT_PET LHA_PET LSK_PET LTH_PET RAR_PET
RFA_PET RFT_PET RHA_PET RHE_PET RPV_PET RSK_PET RTA_PET RTH_PET];

LFT_COP = [data(:,84) data(:,85) data(:,86)];
RFT_COP = [data(:,297) data(:,298) data(:,299)];

LFT_FORCE = [data(:,93) data(:,94) data(:,95)];
RFT_FORCE = [data(:,306) data(:,307) data(:,308)];

LFT_FM = [data(:,96) data(:,97) data(:,98)];
```

```
RFT_FM = [data(:,309) data(:,310) data(:,311)];

CFMmatrix = [LFT_COP RFT_COP LFT_FORCE RFT_FORCE LFT_FM RFT_FM];

if stick==1
    output_a=PEFmatrix;
elseif stick==2
    output_a=PETmatrix;
elseif stick==3
    output_a=CFMmatrix;
else

end
```

energyandIcalc.m

```
clear all
close all

%subject specific data
nn=1568;
time = [0:0.005:nn*0.005]; %[seconds]
m = fiona(1); %[kg]
w = fiona(3);
inertia=fiona(4);

bcgp=littledog(8); %[m] body centre of mass
g = 9.81; %[m/s^2]

%omega, alpha,etc.
og=littledog(1); %omega [radians/s] angular velocity
al=littledog(2); %alpha [radians/s^2] angular acceleration
CGPn=littledog(3); %[m] segment centre of mass
CGVn=littledog(4); %[m] segment velocity
CGAn=littledog(5); %[m] segment acceleration

c=1;
k=1;
T=0;

for c=1:15
       Im = inertia;
Ic=Im(c,:);
Is=[Ic(1) 0 0;
    0 Ic(2) 0;
    0 0 Ic(3)];

ogs = og(k:k+2,:);
als = al(k:k+2,:);

Ts1 = CGVn(:,k:k+2).^2;
Ts2 = (Ic*ogs.^2)';
Ts = 0.5*w(c)*m*sum(Ts1,2) + 0.5*sum(Ts2,2);%segment kinetic energy [J]

q=1;

for q = 1:(nn+1)
    Hg(:,q) = Is*ogs(:,q);
    %HDOT(:,nn+1) = Is*als(:,q);
    q=q+1;
end

Hgmatrix(:,k:k+2)= Hg';
%HDOTmatrix(:,k:k+2)= HDOT';

T=T+Ts;%kinetic energy [J]

c=c+1;
k=k+3;
end
```

```
%angular momentum
Hb=0;

for v=1:3:43
    L=cross(CGPn(1:nn-9,v:v+2),m*w((v+2)/3)*CGVn(1:nn-9,v:v+2));
    H = L + Hgmatrix(1:nn-9,v:v+2);
    Hb=Hb+H;
    Lmatrix(:,v:v+2)=L;
end

xlswrite('Icomp.xlsx',Hb,'A1:C1560')

%gravitational potential energy of the centre of mass
bpe = m*g*bcgp(1:nn-8,3);
xlswrite('impulsedata.xlsx',bpe,4)

%position plots in new coordinate system
for o=1:3:43
    x=CGPn(1:nn-8,o);
    y=CGPn(1:nn-8,o+1);
    z=CGPn(1:nn-8,o+2);

    %polar coordinates
    height=z; rho=sqrt(x.^2+y.^2); theta=atan2(y,x);


    plotdata(:,o)=height;
    plotdata(:,o+1)=rho;
    plotdata(:,o+2)=unwrap(theta);

end

xlswrite('plotdata.xlsx',time','A1:A1560')
xlswrite('plotdata.xlsx',plotdata,'B1:AT1560')
```

fminteraction.m

```
%this function calculates the force and moment interactions at the foot
ground
%interface

clear all
close all

%subject specific data
m=fiona(1);%[kg]
nn=1569; %number of frames

a=bigdog(3); %centre of pressure data
b=littledog(6); %distal end position data
d=littledog(8); %body centre of mass data

clft=a(1:nn,1:3)-d; %distance from lft centre of pressure to centre of
mass
crft=a(1:nn,4:6)-d; %distance from rft centre of pressure to centre of
mass
forceleft=a(1:nn,7:9); %reaction force
forceright=a(1:nn,10:12); %reaction force

fmleft=a(1:nn,13:15); %free moment left
fmright=a(1:nn,16:18); %free moment right

momenta=cross(clft,forceleft,2)+cross(crft,forceright,2); %moment caused
by the reaction force
momentb=fmleft+fmright;
moment= momenta +momentb; %total moment

%numerical integration
for k=2:(nn-1)
    imp(1,:)=0.005*moment(1,:);
    imp(k+1,:)=0.005*((moment(k+1,:)+moment(k-1,:))/2);
end

xlswrite('impulsedata.xlsx',imp) %impulse as calculated from the
numerical integration of the moments, equation no.--
xlswrite('impulsedata.xlsx',d,5) %body centre of mass
xlswrite('impulsedata.xlsx',moment,8) %moment equation no.--
```

horizontalforce.m

```
clear all
close all

%subject specific data
nn=1568;
time = [0:0.005:nn*0.005]; %[seconds]
m = fiona(1); %[kg]
w = fiona(3);
inertia=fiona(4);
g=9.81;

segtorque=bigdog(2);
cfm=bigdog(3);
cga=littledog(9);
cg=littledog(8);

%horizontal direction
lefthforce=cfm(:,7:8);
righthforce=cfm(:,10:11);

position=[cg(:,1:2) zeros(length(cg),1)];
hposition=mag(position);
deltahp=hposition-hposition(1,1)*ones(length(hposition),1);
totalhorizontalforceacc=(1/m)*[lefthforce+righthforce
zeros(length(lefthforce),1)];
hcga=[cga(:,1:2) zeros(length(cga),1)];
visceralhcga=totalhorizontalforceacc-hcga;
combinedhacc=mag(visceralhcga);

force1=m*mag(visceralhcga);
force2=m*mag(totalhorizontalforceacc);

plot(time,force1,time,force2)
figure
```

littledog.m

```
function [output] = littledog(tennisball)
%  littledog...This function retrieves the data in a useful form
%  pulls original data stored from exported visual 3d program, then
changes
%  the coordinate system with an origin located at the body's centre of
mass

% position, velocity, acceleration, angular vel., angular acc.


load datalab.txt
data = datalab;
%--eq. 11--(lines 12 through 26)
LAR_CGP = [data(:,10) data(:,11) data(:,12)];
LFA_CGP = [data(:,44) data(:,45) data(:,46)];
LFT_CGP = [data(:,78) data(:,79) data(:,80)];
LHA_CGP = [data(:,121) data(:,122) data(:,123)];
LSK_CGP = [data(:,155) data(:,156) data(:,157)];
LTH_CGP = [data(:,189) data(:,190) data(:,191)];
RAR_CGP = [data(:,223) data(:,224) data(:,225)];
RFA_CGP = [data(:,257) data(:,258) data(:,259)];
RFT_CGP = [data(:,291) data(:,292) data(:,293)];
RHA_CGP = [data(:,334) data(:,335) data(:,336)];
RHE_CGP = [data(:,368) data(:,369) data(:,370)];
RPV_CGP = [data(:,402) data(:,403) data(:,404)];
RSK_CGP = [data(:,436) data(:,437) data(:,438)];
RTA_CGP = [data(:,470) data(:,471) data(:,472)];
RTH_CGP = [data(:,504) data(:,505) data(:,506)];

%--eq. 13--
BodyCGP = 0.028*LAR_CGP + 0.028*RAR_CGP + 0.016*LFA_CGP + 0.016*RFA_CGP
+ 0.0145*LFT_CGP + 0.0145*RFT_CGP + 0.006*LHA_CGP + 0.006*RHA_CGP +
0.1*LTH_CGP + 0.1*RTH_CGP + 0.0465*LSK_CGP + 0.0465*RSK_CGP +
0.081*RHE_CGP + 0.142*RPV_CGP  + 0.355*RTA_CGP ;

%--eq 14--
LAR_CGV = [data(:,13) data(:,14) data(:,15)];
LFA_CGV = [data(:,47) data(:,48) data(:,49)];
LFT_CGV = [data(:,81) data(:,82) data(:,83)];
LHA_CGV = [data(:,124) data(:,125) data(:,126)];
LSK_CGV = [data(:,158) data(:,159) data(:,160)];
LTH_CGV = [data(:,192) data(:,193) data(:,194)];
RAR_CGV = [data(:,226) data(:,227) data(:,228)];
RFA_CGV = [data(:,260) data(:,261) data(:,262)];
RFT_CGV = [data(:,294) data(:,295) data(:,296)];
RHA_CGV = [data(:,337) data(:,338) data(:,339)];
RHE_CGV = [data(:,371) data(:,372) data(:,373)];
RPV_CGV = [data(:,405) data(:,406) data(:,407)];
RSK_CGV = [data(:,439) data(:,440) data(:,441)];
RTA_CGV = [data(:,473) data(:,474) data(:,475)];
RTH_CGV= [data(:,507) data(:,508) data(:,509)];

%--eq. 16--
BodyCGV = 0.028*LAR_CGV + 0.028*RAR_CGV + 0.016*LFA_CGV + 0.016*RFA_CGV
+ 0.0145*LFT_CGV + 0.0145*RFT_CGV + 0.006*LHA_CGV + 0.006*RHA_CGV +
```

```
0.1*LTH_CGV + 0.1*RTH_CGV + 0.0465*LSK_CGV + 0.0465*RSK_CGV +
0.081*RHE_CGV + 0.142*RPV_CGV  + 0.355*RTA_CGV ;
xlswrite('bodydata.xlsx',BodyCGV)

%--eq. 15--
LAR_CGA = [data(:,7) data(:,8) data(:,9)];
LFA_CGA = [data(:,41) data(:,42) data(:,43)];
LFT_CGA = [data(:,75) data(:,76) data(:,77)];
LHA_CGA = [data(:,118) data(:,119) data(:,120)];
LSK_CGA = [data(:,152) data(:,153) data(:,154)];
LTH_CGA = [data(:,186) data(:,187) data(:,189)];
RAR_CGA = [data(:,220) data(:,221) data(:,222)];
RFA_CGA = [data(:,254) data(:,255) data(:,256)];
RFT_CGA = [data(:,288) data(:,289) data(:,290)];
RHA_CGA = [data(:,331) data(:,332) data(:,333)];
RHE_CGA = [data(:,365) data(:,366) data(:,367)];
RPV_CGA = [data(:,399) data(:,400) data(:,401)];
RSK_CGA = [data(:,433) data(:,434) data(:,435)];
RTA_CGA = [data(:,467) data(:,468) data(:,469)];
RTH_CGA= [data(:,501) data(:,502) data(:,503)];

%--eq. 17--
BodyCGA = 0.028*LAR_CGA + 0.028*RAR_CGA + 0.016*LFA_CGA + 0.016*RFA_CGA
+ 0.0145*LFT_CGA + 0.0145*RFT_CGA + 0.006*LHA_CGA + 0.006*RHA_CGA +
0.1*LTH_CGA + 0.1*RTH_CGA + 0.0465*LSK_CGA + 0.0465*RSK_CGA +
0.081*RHE_CGA + 0.142*RPV_CGA  + 0.355*RTA_CGA ;


LAR_AV = [data(:,4) data(:,5) data(:,6)];
LFA_AV = [data(:,38) data(:,39) data(:,40)];
LFT_AV = [data(:,72) data(:,73) data(:,74)];
LHA_AV = [data(:,115) data(:,116) data(:,117)];
LSK_AV = [data(:,149) data(:,150) data(:,151)];
LTH_AV = [data(:,183) data(:,184) data(:,185)];
RAR_AV = [data(:,217) data(:,218) data(:,219)];
RFA_AV = [data(:,251) data(:,252) data(:,253)];
RFT_AV = [data(:,285) data(:,286) data(:,287)];
RHA_AV = [data(:,328) data(:,329) data(:,330)];
RHE_AV = [data(:,362) data(:,363) data(:,364)];
RPV_AV = [data(:,396) data(:,397) data(:,398)];
RSK_AV = [data(:,430) data(:,431) data(:,432)];
RTA_AV = [data(:,464) data(:,465) data(:,466)];
RTH_AV = [data(:,498) data(:,499) data(:,500)];
BodyAV = 0.028*LAR_AV + 0.028*RAR_AV + 0.016*LFA_AV + 0.016*RFA_AV +
0.0145*LFT_AV + 0.0145*RFT_AV + 0.006*LHA_AV + 0.006*RHA_AV + 0.1*LTH_AV
+ 0.1*RTH_AV + 0.0465*LSK_AV + 0.0465*RSK_AV + 0.081*RHE_AV +
0.142*RPV_AV  + 0.355*RTA_AV ;

LAR_AA = [data(:,1) data(:,2) data(:,3)];
LFA_AA = [data(:,35) data(:,36) data(:,37)];
LFT_AA = [data(:,69) data(:,70) data(:,71)];
LHA_AA = [data(:,112) data(:,113) data(:,114)];
LSK_AA = [data(:,146) data(:,147) data(:,148)];
LTH_AA = [data(:,180) data(:,181) data(:,182)];
RAR_AA = [data(:,214) data(:,215) data(:,216)];
RFA_AA = [data(:,248) data(:,249) data(:,250)];
RFT_AA = [data(:,282) data(:,283) data(:,284)];
RHA_AA = [data(:,325) data(:,326) data(:,327)];
```

```
RHE_AA = [data(:,359) data(:,360) data(:,361)];
RPV_AA = [data(:,393) data(:,394) data(:,395)];
RSK_AA = [data(:,427) data(:,428) data(:,429)];
RTA_AA = [data(:,461) data(:,462) data(:,463)];
RTH_AA = [data(:,495) data(:,496) data(:,497)];
BodyAA = 0.028*LAR_AA + 0.028*RAR_AA + 0.016*LFA_AA + 0.016*RFA_AA +
0.0145*LFT_AA + 0.0145*RFT_AA + 0.006*LHA_AA + 0.006*RHA_AA + 0.1*LTH_AA
+ 0.1*RTH_AA + 0.0465*LSK_AA + 0.0465*RSK_AA + 0.081*RHE_AA +
0.142*RPV_AA  + 0.355*RTA_AA ;


BAV=[BodyAV BodyAV BodyAV BodyAV BodyAV BodyAV BodyAV BodyAV BodyAV
BodyAV BodyAV BodyAV BodyAV BodyAV BodyAV]';
ogAV = [LAR_AV LFA_AV LFT_AV LHA_AV LSK_AV LTH_AV RAR_AV RFA_AV RFT_AV
RHA_AV RHE_AV RPV_AV RSK_AV RTA_AV RTH_AV]';
og = ogAV - BAV;%--eq. 20--

BAA=[BodyAA BodyAA BodyAA BodyAA BodyAA BodyAA BodyAA BodyAA BodyAA
BodyAA BodyAA BodyAA BodyAA BodyAA BodyAA]';
alAA = [LAR_AA LFA_AA LFT_AA LHA_AA LSK_AA LTH_AA RAR_AA RFA_AA RFT_AA
RHA_AA RHE_AA RPV_AA RSK_AA RTA_AA RTH_AA]';
al=alAA - BAA;%--eq. 21--

LAR_DEP = [data(:,16) data(:,17) data(:,18)];
LFA_DEP = [data(:,50) data(:,51) data(:,52)];
LFT_DEP = [data(:,87) data(:,88) data(:,89)];
LHA_DEP = [data(:,127) data(:,128) data(:,129)];
LSK_DEP = [data(:,161) data(:,162) data(:,163)];
LTH_DEP = [data(:,195) data(:,196) data(:,197)];
RAR_DEP = [data(:,229) data(:,230) data(:,231)];
RFA_DEP = [data(:,263) data(:,264) data(:,265)];
RFT_DEP = [data(:,300) data(:,301) data(:,302)];
RHA_DEP = [data(:,340) data(:,341) data(:,342)];
RHE_DEP = [data(:,374) data(:,375) data(:,376)];
RPV_DEP = [data(:,408) data(:,409) data(:,410)];
RSK_DEP = [data(:,442) data(:,443) data(:,444)];
RTA_DEP = [data(:,476) data(:,477) data(:,478)];
RTH_DEP = [data(:,510) data(:,511) data(:,512)];

LAR_PEP = [data(:,25) data(:,26) data(:,27)];
LFA_PEP = [data(:,59) data(:,60) data(:,61)];
LFT_PEP = [data(:,102) data(:,103) data(:,104)];
LHA_PEP = [data(:,136) data(:,137) data(:,138)];
LSK_PEP = [data(:,170) data(:,171) data(:,172)];
LTH_PEP = [data(:,204) data(:,205) data(:,206)];
RAR_PEP = [data(:,238) data(:,239) data(:,240)];
RFA_PEP = [data(:,272) data(:,273) data(:,274)];
RFT_PEP = [data(:,315) data(:,316) data(:,317)];
RHA_PEP = [data(:,349) data(:,350) data(:,351)];
RHE_PEP = [data(:,383) data(:,384) data(:,385)];
RPV_PEP = [data(:,417) data(:,418) data(:,419)];
RSK_PEP = [data(:,451) data(:,452) data(:,453)];
RTA_PEP = [data(:,485) data(:,486) data(:,487)];
RTH_PEP= [data(:,519) data(:,520) data(:,521)];

%wrt global coordinate sys
CGPmatrix=[LAR_CGP LFA_CGP LFT_CGP LHA_CGP LSK_CGP LTH_CGP RAR_CGP
RFA_CGP RFT_CGP RHA_CGP RHE_CGP RPV_CGP RSK_CGP RTA_CGP RTH_CGP];
```

```
%origin of new coordinate sys
CGPB=[BodyCGP BodyCGP BodyCGP BodyCGP BodyCGP BodyCGP BodyCGP BodyCGP
BodyCGP BodyCGP BodyCGP BodyCGP BodyCGP BodyCGP BodyCGP];
%segment cg wrt new coordinate sys
CGPn=CGPmatrix - CGPB; %--eq. 3,4--

%wrt global coordinate sys
CGVmatrix=[LAR_CGV LFA_CGV LFT_CGV LHA_CGV LSK_CGV LTH_CGV RAR_CGV
RFA_CGV RFT_CGV RHA_CGV RHE_CGV RPV_CGV RSK_CGV RTA_CGV RTH_CGV];
%origin of new coordinate sys
CGVB=[BodyCGV BodyCGV BodyCGV BodyCGV BodyCGV BodyCGV BodyCGV BodyCGV
BodyCGV BodyCGV BodyCGV BodyCGV BodyCGV BodyCGV BodyCGV];
%segment cg wrt new coordinate sys
CGVn=CGVmatrix - CGVB; %--eq. 18--

%wrt global coordinate sys
CGAmatrix=[LAR_CGA LFA_CGA LFT_CGA LHA_CGA LSK_CGA LTH_CGA RAR_CGA
RFA_CGA RFT_CGA RHA_CGA RHE_CGA RPV_CGA RSK_CGA RTA_CGA RTH_CGA];
%origin of new coordinate sys
CGAB=[BodyCGA BodyCGA BodyCGA BodyCGA BodyCGA BodyCGA BodyCGA BodyCGA
BodyCGA BodyCGA BodyCGA BodyCGA BodyCGA BodyCGA BodyCGA];
%segment cg wrt new coordinate sys
CGAn=CGAmatrix - CGAB; %--eq. 19--

%wrt global coordinate sys
DEPmatrix=[LAR_DEP LFA_DEP LFT_DEP LHA_DEP LSK_DEP LTH_DEP RAR_DEP
RFA_DEP RFT_DEP RHA_DEP RHE_DEP RPV_DEP RSK_DEP RTA_DEP RTH_DEP];

DEP = DEPmatrix;

%wrt global coordinate sys
PEPmatrix=[LAR_PEP LFA_PEP LFT_PEP LHA_PEP LSK_PEP LTH_PEP RAR_PEP
RFA_PEP RFT_PEP RHA_PEP RHE_PEP RPV_PEP RSK_PEP RTA_PEP RTH_PEP];

PEP=PEPmatrix;

if tennisball==1
    output=og;
elseif tennisball==2
    output=al;
elseif tennisball==3
    output=CGPn;
elseif tennisball==4
    output=CGVn;
elseif tennisball==5
    output=CGAn;
elseif tennisball==6
    output=DEP;
elseif tennisball==7
    output=PEP;
elseif tennisball==8
    output=BodyCGP;
else
    output=BodyCGA;
end


end
```

verticalforce.m

```
clear all
close all

%subject specific data
nn=1569;
time = [0:0.005:(nn-1)*0.005]; %[seconds]
m = fiona(1); %[kg]
w = fiona(3);
inertia=fiona(4);
g=9.81;
a=bigdog(3);

segtorque=bigdog(2);
cfm=bigdog(3);
cga=littledog(9);
cg=littledog(8);

leftankletorque=segtorque(:,7:9);
rightankletorque=segtorque(:,25:27);

%vertical direction
leftverticalforce=cfm(:,9);
rightverticalforce=cfm(:,12);

verticalposition=cg(:,3);
deltavp=verticalposition-
verticalposition(1,1)*ones(length(verticalposition),1);
totalverticalforce=leftverticalforce+rightverticalforce-
m*g*ones(length(cfm),1);
combinedverticalacc=totalverticalforce/m;
verticalcga=cga(:,3);
visceralcga=combinedverticalacc-verticalcga;

force1v=m*combinedverticalacc;
force2v=.86*m*verticalcga;
force3v=.14*m*visceralcga;


copdistance=a(1:nn,1:3)-a(1:nn,4:6);

work1=m*combinedverticalacc.*deltavp;
work2=.86*m*verticalcga.*deltavp;
work3=.14*m*visceralcga.*deltavp;

%gravitational potential energy of the centre of mass
bpe = m*g*deltavp;



%plot(time,force1)
%figure
%plot(time,force2,'gr--')
%figure
%plot(time,force3,'r-.')
```

```
%figure
plot(time,work1,time,work2,'--',time, work3,'-.')
figure
plot(time,force1v,time,force2v,'--',time, force3v,'-.')

%numerical integration
for k=2:(nn-1)
    imp2(1,:)=0.005*moment2(1,:);
    imp2(k+1,:)=0.005*((moment2(k+1,:)+moment2(k-1,:))/2);
end

%numerical integration
for k=2:(nn-1)
    imp3(1,:)=0.005*moment3(1,:);
    imp3(k+1,:)=0.005*((moment3(k+1,:)+moment3(k-1,:))/2);
end

xlswrite('imp2vertical.xlsx',imp2)
xlswrite('imp3visceral.xlsx',imp3)

plot(time,imp2)
figure
plot(time,imp3)
```

Appendix B

Additional theoretical notes—program notation

The program bigdog.m retrieves the data and outputs vectors in the original coordinate system. The force and torque vectors output from the program are used in the calculation of forces and impulses at the ground. The reaction forces occur at the centre of pressure (COP) $\vec{F}_L = \{F_x, F_y, F_z\}$ at $\vec{r}_L = \{x_{COP}, y_{COP}, 0\}_L$ and $\vec{F}_R = \{F_x, F_y, F_z\}$ acting at $\vec{r}_R = \{x_{COP}, y_{COP}, 0\}_R$, where the subscripts L and R denote the left and right foot, respectively.

The diagram in Figure B-1 depicts the variables and vectors used in the calculation of the moment about a vertical axis that runs through the centre of mass. The moment created about this axis will create the principal motion of the turn. Equation 36 shows that the moment created about the vertical axis is composed of the force of the one or both feet acting at a distance from the vertical axis. At the start of the series of turns, this moment may come from both feet. During the series, only the support leg will generate a moment.

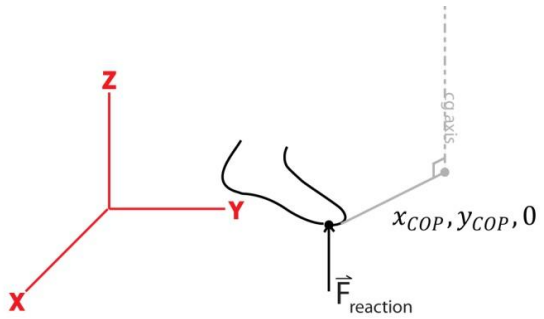

Figure B-1. Moments about the centre of mass's vertical axis

35

$$\vec{M} = \vec{p}_L \times \vec{F}_L + \vec{p}_R \times \vec{F}_R + \text{ free moment}$$

The angular impulse is calculated numerically as the integral of the moment. Equation 36 is implemented using a two-point Riemann sum in the program fminteraction.m (see Appendix A).

36

$$\int_{t_1}^{t_2} \vec{M} dt$$

Appendix C

C.1 *Proof of Equation*

$$\vec{q} = \vec{r} - \vec{r}_{CG_b}$$
$$\frac{d\vec{q}}{dt} = \frac{d}{dt}\left(\vec{r} - \vec{r}_{CG_b}\right)$$
$$\frac{d\vec{q}}{dt} = \frac{d\vec{r}}{dt} - \frac{d\vec{r}_{CG_b}}{dt}$$
$$\therefore \vec{v}_q = \vec{v} - \vec{v}_{CG_b}$$

C.2 *Proof of Equation*

$$\vec{v}_q = \vec{v} - \vec{v}_{CG_b}$$
$$\frac{d\vec{v}_q}{dt} = \frac{d}{dt}\left(\vec{v} - \vec{v}_{CG_b}\right)$$
$$\frac{d\vec{v}_q}{dt} = \frac{d\vec{v}}{dt} - \frac{d\vec{v}_{CG_b}}{dt}$$
$$\therefore \vec{a}_q = \vec{a} - \vec{a}_{CG_b}$$

C.3

For each segment about its own centre of mass,

$$\vec{L}_{G_k}(t) = \bar{\bar{I}}_k \omega_k(t)$$

for k=1,2,…,15.

For each segment about the body's centre of mass (moment of momentum),

$$\vec{L}_{O_k}(t) = \vec{q}_{CG_k}(t) \times m_k v_k + \vec{L}_{G_k}(t)$$

Where,

$$m_k = m n_k$$

is the mass of the segment.

$$\vec{L}_{O_b}(t) = \sum_{k=1}^{15} \vec{L}_{O_k}(t)$$

C.5

$$\vec{L}_{O_b}(t_1) + \int_{t_1}^{t_2} \vec{M}\, dt = \vec{L}_{O_b}(t_2)$$
$$\int_{t_1}^{t_2} \vec{M}\, dt = \vec{L}_{O_b}(t_2) - \vec{L}_{O_b}(t_1)$$

Appendix D

Polar plots of each limb

left upper arm 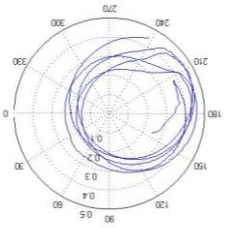	left forearm 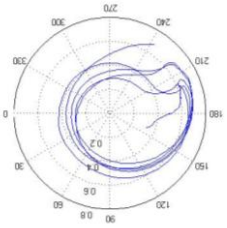	left hand 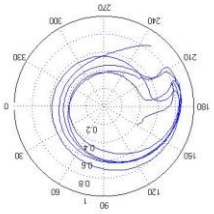
Left foot 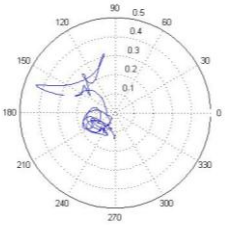	Left lower leg 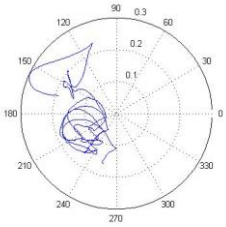	Left thigh 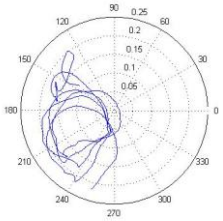
Right upper arm 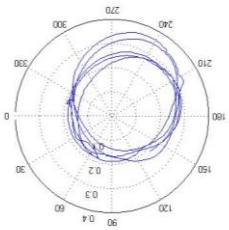	Right forearm 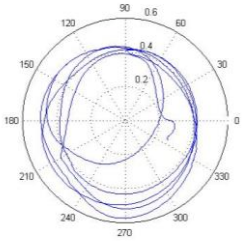	Right hand 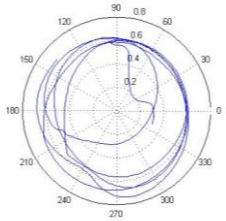
Right foot 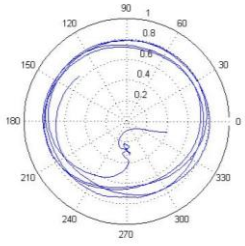	Right lower leg 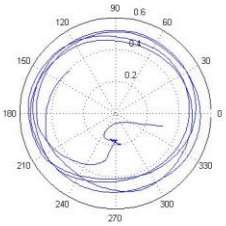	Right thigh 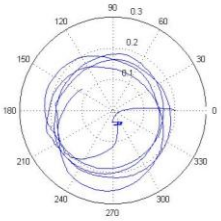
Head 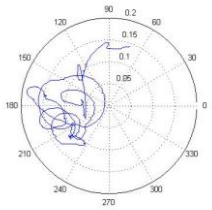	Pelvis 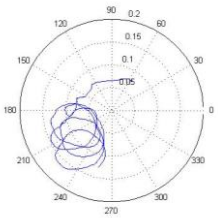	Thorax 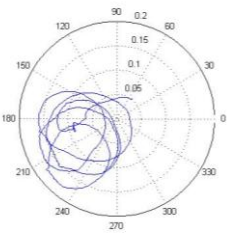

Appendix E

Visual 3D's calculation of angular momentum

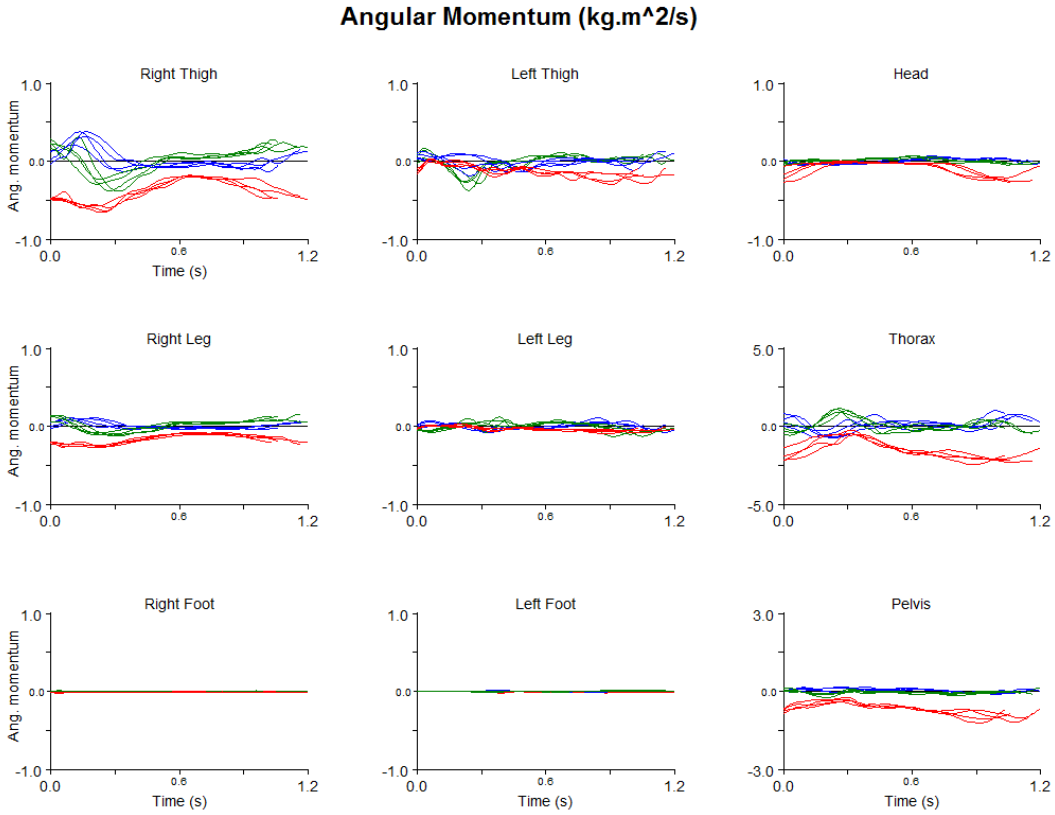

Case 1

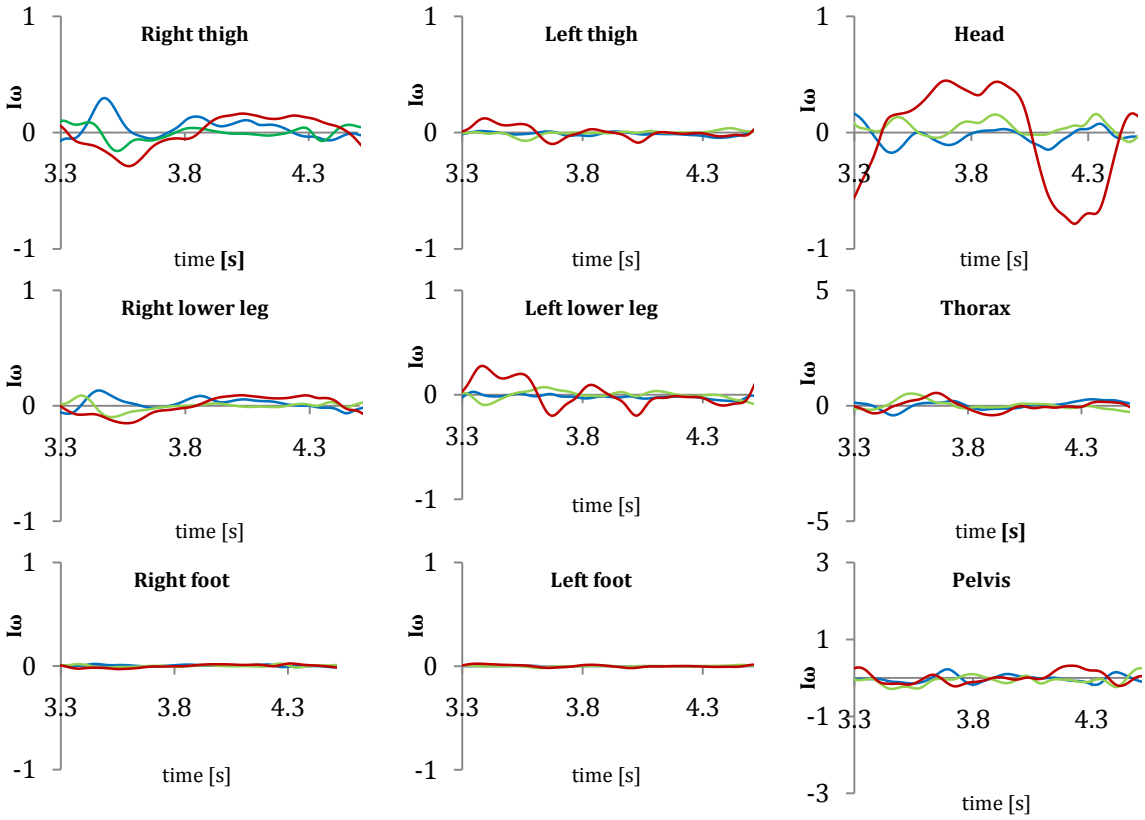
Right thigh
Left thigh
Head
Right lower leg
Left lower leg
Thorax
Right foot
Left foot
Pelvis
Iω
time [s]
time **[s]**
3.3
3.8
4.3

Case 2

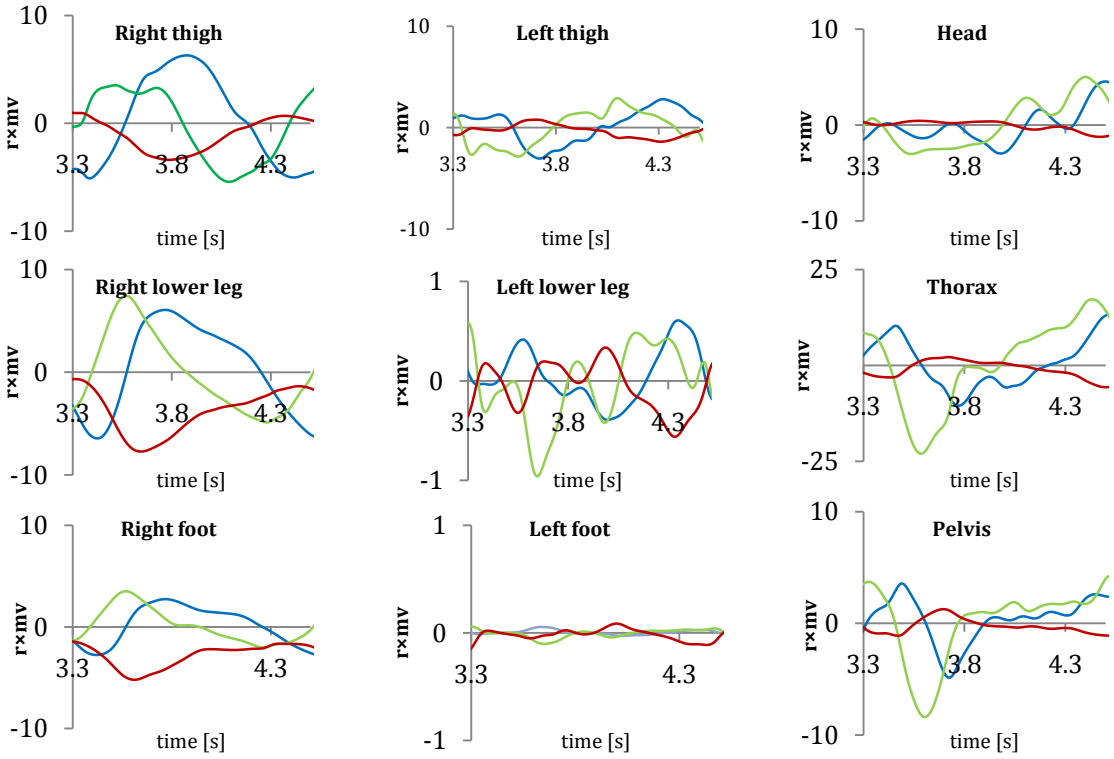
Right thigh
Left thigh
Head
Right lower leg
Left lower leg
Thorax
Right foot
Left foot
Pelvis
r×mv
time [s]
3.3
3.8
4.3

Case 3

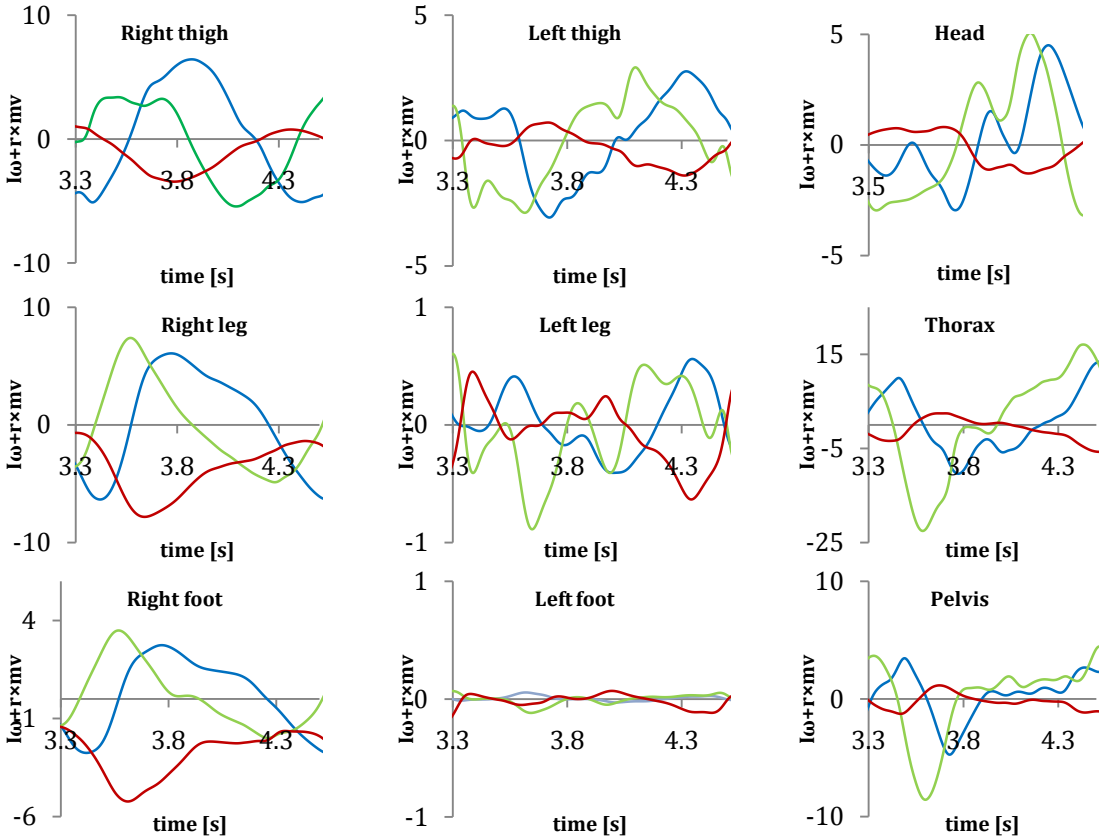
Right thigh
Left thigh
Head
Right leg
Left leg
Thorax
Right foot
Left foot
Pelvis
Iω+r×mv
time [s]
3.3
3.8
4.3
3.5